

UNCLASSIFIED

AD NUMBER

AD813868

LIMITATION CHANGES

TO:

Approved for public release; distribution is unlimited. Document partially illegible.

FROM:

Distribution authorized to U.S. Gov't. agencies and their contractors;
Administrative/Operational Use; MAY 1967. Other requests shall be referred to NASA Manned Spacecraft Center, Houston, TX. Document partially illegible.

AUTHORITY

AEDC ltr 27 Jun 1974

THIS PAGE IS UNCLASSIFIED

AEDC-TR-67-63

**ARCHIVE COPY
DO NOT LOAN**

Cy1



**QUALIFICATION TESTS OF THE APOLLO
BLOCK II SERVICE MODULE ENGINE
(AJ10-137)**

E. S. Gall, M. W. McIlveen, and A. L. Berg

ARO, Inc.

May 1967

This document has been approved for public release
its distribution is unlimited.

*Per A. F. Letter
dated 27 June 1973*

~~This document is subject to special export controls
and each transmittal to foreign governments or foreign
nationals may be made only with prior approval of
National Aeronautic and Space Administration (EP-2),
Manned Spacecraft Center, Houston, Texas.~~

**ROCKET TEST FACILITY
ARNOLD ENGINEERING DEVELOPMENT CENTER
AIR FORCE SYSTEMS COMMAND
ARNOLD AIR FORCE STATION, TENNESSEE**

AEDC TECHNICAL LIBRARY



PROPERTY OF U. S. AIR FORCE
AEDC LIBRARY
AF 40(600)1200

NOTICES

When U. S. Government drawings, specifications, or other data are used for any purpose other than a definitely related Government procurement operation, the Government thereby incurs no responsibility nor any obligation whatsoever, and the fact that the Government may have formulated, furnished, or in any way supplied the said drawings, specifications, or other data, is not to be regarded by implication or otherwise, or in any manner licensing the holder or any other person or corporation, or conveying any rights or permission to manufacture, use, or sell any patented invention that may in any way be related thereto.

Qualified users may obtain copies of this report from the Defense Documentation Center.

References to named commercial products in this report are not to be considered in any sense as an endorsement of the product by the United States Air Force or the Government.

QUALIFICATION TESTS OF THE APOLLO
BLOCK II SERVICE MODULE ENGINE
(AJ10-137)

E. S. Gall, M. W. McIlveen, and A. L. Berg
ARO, Inc.

This document has been approved for public release
and its distribution is unlimited.

*Per A.F. Letter
dated 27 June 1973*

~~This document is subject to special export controls
and each transmittal to foreign governments or foreign
nationals may be made only with prior approval of
National Aeronautic and Space Administration (EP-2),
Manned Spacecraft Center, Houston, Texas.~~

FOREWORD

The contents of this report are the results of an altitude qualification testing program of the Aerojet-General Corporation (AGC), Block II, AJ10-137, liquid-propellant rocket engine and the North American Aviation (NAA) F-3 propellant tankage fixture. This program was sponsored by the National Aeronautics and Space Administration-Manned Spacecraft Center (NASA-MSC) under System 921E/9158. Technical liaison was provided by AGC, which is a subcontractor of North American Aviation-Space and Information Division (NAA-S&ID) for the development of the Apollo Service Module (SM) engine. North American Aviation is the prime contractor to NASA for the complete SM vehicle. Quality control surveillance was provided by AGC and ARO, Inc.

The test program was requested to support the Apollo project under MIPR-T-298446 subgroup I. Testing was conducted by ARO, Inc. (a subsidiary of Sverdrup & Parcel and Associates, Inc.), contract operator of the Arnold Engineering Development Center (AEDC), Air Force Systems Command (AFSC), Arnold Air Force Station, Tennessee, under Contract AF40(600)-1200. The results of these tests were obtained in the Propulsion Engine Test Cell (J-3) of the Rocket Test Facility (RTF) during the period between November 18, 1966, and February 1, 1967, under ARO Project No. RM1630. This manuscript was submitted for publication on March 14, 1967.

The authors wish to acknowledge the invaluable collaboration in the preparation of this report by C. E. Robinson, an associate in the J-3 Projects Section.

Information in this report is embargoed under the Department of State International Traffic in Arms Regulations. This report may be released to foreign governments by departments or agencies of the U. S. Government subject to approval of NASA (EP-2), or higher authority. Private individuals or firms require a Department of State export license.

This technical report has been reviewed and is approved.

Joseph R. Henry
Lt Col, USAF
AF Representative, RTF
Directorate of Test

Leonard T. Glaser
Colonel, USAF
Director of Test

ABSTRACT

High altitude qualification tests of an Apollo Block II Service Module engine were conducted to establish the performance characteristics and engine durability. Test hardware consisted of an Aerojet-General Corporation liquid-propellant rocket engine (AJ10-137) and a North American Aviation ground test replica of the Apollo Service Module propellant system. Seventy-two firings with an accumulated duration of 4524 sec were conducted on six engine assemblies at pressure altitudes of approximately 115,000 ft. Engine performance characteristics and engine durability were determined at various chamber pressures, mixture ratios, and propellant temperatures. The vacuum specific impulse obtained from the engine assemblies tested was dependent on the injector used, although all injectors were of identical design within limits of quality control. The average repeatability of I_{sp_v} data for a particular injector was ± 0.07 percent (1σ); however, the deviation from the average I_{sp_v} (313.2 $\text{lb}_f\text{-sec}/\text{lb}_m$) for all injectors was ± 0.57 percent (1σ). The estimated error in the measurement of I_{sp_v} is 0.19 percent (1σ). Chamber durability was excellent except during one test series when the fiber glass overwrap separated from the chamber-nozzle flange. The thrust chamber valve had excessive leakage past the ball seals on several occasions during these tests.

CONTENTS

	<u>Page</u>
ABSTRACT	iii
NOMENCLATURE	viii
I. INTRODUCTION	1
II. APPARATUS	1
III. PROCEDURE	11
IV. RESULTS AND DISCUSSION	18
V. SUMMARY OF RESULTS	29
REFERENCES	31

APPENDIXES

I. ILLUSTRATIONS

Figure

1. AJ10-137 Rocket Engine Assembly S/N 54B	35
2. AJ10-137 Rocket Engine S/N 55 without Nozzle	36
3. Injector S/N 104	
a. View of Injector Face	37
b. Close-up Showing Baffle Configuration and Orifice Counterboring	38
4. Ablative Thrust Chamber and Flange Details	39
5. Ablative Thrust Chamber S/N 313	
a. Side View	40
b. View from Injector Mounting Flange	40
6. Nozzle Extension S/N 54	41
7. Schematic of Thrust Chamber Valve	42
8. Schematic of F-3 Fixture	43
9. Facility and NAA Heat Shields	
a. Photograph of Installation	44
b. Artist's Sketch of Installation	45
10. Test Cell J-3	
a. Complex	46
b. Schematic	47

<u>Figure</u>	<u>Page</u>
27. Nozzle Extension S/N 54 after 2250 sec of Firing Time	65
28. Combustion Chamber Temperature History.	66
29. Nozzle Extension Temperature History.	67
30. Nozzle Extension Temperature Profile.	68
31. Thrust Vector Excursion of Engine S/N 54	
a. Variation of Thrust Vector Intercept Components in the Gimbal Plane	69
b. Angular Variation of Thrust Vector Components	69
32. Thrust Vector Excursion of Engine S/N 54B	
a. Variation of Thrust Vector Intercept Components in the Gimbal Plane	70
b. Angular Variation of Thrust Vector Components	70
33. Thrust Vector Excursion of Engine S/N 55	
a. Variation of Thrust Vector Intercept Components in the Gimbal Plane	71
b. Angular Variation of Thrust Vector Components	71
 II. TABLES	
I. Engine Configurations Tested.	72
II. Propellant Contamination Particle Counts	73
III. Summary of Test Firings.	74
IV. Summary of Engine Performance	77
V. Summary of Ignition Transient Impulse Data	80
VI. Summary of Shutdown Transient Impulse Data	81
VII. Minimum Impulse Bit Summary.	82
 III. PROPELLANT FLOWMETER AND WEIGH SCALE CALIBRATIONS	
	86

NOMENCLATURE

A	Area at particular nozzle station, in. ²
A/A_t	Area ratio
A_e	Nozzle exit area, in. ²
A_t	Nozzle throat area, in. ²
$A_{t_{calc}}$	Calculated chamber throat area, in. ²
C_{F_v}	Vacuum thrust coefficient
$c_{i,j}$	Calibration constants
c^*	Characteristic velocity, ft/sec
c^*_i	Characteristic velocity calculated at the beginning of each new test series, ft/sec
F_a	Axial thrust, lb _f
$F_{a_{cal}}$	Axial thrust calibrate, lb _f
$F_{O_{wt}}$	Oxidizer weight, lb _f
$F_{f_{wt}}$	Fuel weight, lb _f
$F_{P1_{cal}}$	Upper pitch force calibrate, lb _f
$F_{P1_{data}}$	Upper Pitch force data, lb _f
$F_{P2_{cal}}$	Lower pitch force calibrate, lb _f
$F_{P2_{data}}$	Lower pitch force data, lb _f
$F_{R_{cal}}$	Roll force calibrate, lb _f
$F_{R_{data}}$	Roll force data, lb _f
FS-1	Electrical signal to fire engine
FS-2	Electrical signal to terminate engine firing
F_v	Vacuum thrust, lb _f
$F_{Y1_{cal}}$	Upper yaw force calibrate, lb _f

F_{Y1data}	Upper yaw force data, lb_f
F_{Y2cal}	Lower yaw force calibrate, lb_f
F_{Y2data}	Lower yaw force data, lb_f
g	Dimensional constant, $32.174 \text{ lb}_m\text{-ft/lb}_f\text{-sec}^2$
I_{sp_v}	Vacuum specific impulse, $\frac{lb_f\text{-sec}}{lb_m}$
K	Flowmeter constant, $lb\text{-H}_2\text{O/cycle}$
$K_{j,i}$	Force balance constants
L_j	Applied load
MR	Mixture ratio, oxidizer-to-fuel
P_a	Test cell pressure, psia
P_c	Combustion chamber pressure, psia
P_{fl}	Fuel interface pressure, psia
P_{ol}	Oxidizer interface pressure, psia
R_i	Data load cell output, lb_f
SG	Specific gravity
\dot{W}_f	Fuel weight flow, lb_m/sec
\dot{W}_o	Oxidizer weight flow, lb_m/sec
\dot{W}_t	Total propellant weight flow, lb_m/sec
X	Distance of the thrust vector from the balance centerline in the balance pitch plane and engine gimbal plane, in.
Y	Distance of the thrust vector from the balance centerline in the balance yaw plane and engine gimbal plane, in.
θ	Pitch angle, deg
ϕ	Yaw angle, deg

SECTION I INTRODUCTION

The Apollo spacecraft consists of a Command Module (CM) (three-man capsule), Service Module (SM) which contains the propellant tanks and main propulsion system, and the Lunar Module (LM). The Block II engine (AGC AJ10-137) is installed in the SM as the main propulsion system. This engine will be utilized on all later Apollo spacecraft flights including manned flights to the moon.

The Apollo SM tests have periodically occupied the J-3 test cell from May 1963 to February 1967. During this period of time, a total of 787 engine firings with a total firing time of 24,060 sec on 42 engines have been accomplished. Phase I was an engine development phase completed in April 1964 (Refs. 1 through 6). Phase II was an extended engine development program utilizing a heavy-duty version of the spacecraft propellant tankage and lines (F-3 fixture) and was completed in October 1965 (Refs. 7 and 8). Phase III was the altitude qualification test program for the Block I engine (completed in April 1966, Ref. 9) and Phase IV was a Block II engine development test (completed in October 1966, Refs. 10 and 11). Phase V, reported herein, was the altitude qualification test program for the Block II engine. The F-3 fixture was used for all tests during Phases II through V.

The results presented in this report were obtained during six test series with six engine assemblies. Seventy-two firing tests were conducted for an accumulated firing duration of 4524 sec. The primary objective of the Phase V testing was to establish the performance characteristics and durability of the Apollo SM engine at pressure altitudes of approximately 115,000 ft. Performance characteristics and engine durability were determined at various propellant temperatures, chamber pressures, and mixture ratios.

SECTION II APPARATUS

2.1 TEST ARTICLE

The Aerojet AJ10-137 rocket engine and an Apollo SM propellant system (plumbing and heavy-duty tankage, designated the F-3 fixture and supplied by NAA-S&ID) constituted the test article for these qualification tests. Six engine assemblies with three different injectors of the same

design were utilized during these tests. The gimbal actuators used on the first engine were not final qualification design, and a new thrust chamber valve ball seal material was used on the last two engines. These were the only configuration changes made.

The F-3 fixture is a heavy-duty version of the Apollo SM spacecraft propellant tankage. The propellant tanks on this fixture are of the same size, shape, and volume as on the spacecraft, and the propellant lines duplicate the size, hydrodynamic characteristics, and routing of the spacecraft. A facility propellant tank helium pressurization system was used because a large portion of the testing was conducted at off-design mixture ratios and chamber pressures. The engine mounting in this fixture did not duplicate the spacecraft mounting because six-component forces were measured.

2.2 ENGINE

The AJ10-137 engine is a pressure-fed, liquid-propellant rocket engine consisting of an injector, a combustion chamber, a bipropellant valve assembly, a gimbal actuator-mount assembly, and a nozzle extension. The overall height of the complete engine assembly (Fig. 1, Appendix I) is approximately 13 ft, and the diameter of the nozzle extension exit is approximately 8 ft.

This engine is designed to operate at nominal conditions of 1.60 mixture ratio (MR) at a chamber pressure of 97 psia, with a minimum of 50 restarts over an operating life of 750 sec. Storable hypergolic propellants with nitrogen tetroxide (N_2O_4) as the oxidizer and Aerozine-50 (AZ-50) as the fuel are burned by this engine. The N_2O_4 had a nominal 0.6 percent by weight nitric oxide additive.

The thrust chamber assembly consists of an injector and an ablatively cooled combustion chamber. A bipropellant valve is mounted on top of the injector dome. The thrust chamber assembly is mounted in a ring mount assembly and is gimballed in two orthogonal planes by two electrically driven gimbal actuators. The radiation-cooled nozzle extension is attached to the bottom of the combustion chamber at the 6:1 area ratio.

A tabulation of all components used in each engine assembly is presented in Table I (Appendix II), and a photograph of an engine assembly without the nozzle extension is shown in Fig. 2.

2.2.1 Propellant Injector

The injectors used on all engines were designated by AGC as Modification No. 4 injectors. This injector is a doublet orifice type with a center hub and five equally spaced radial baffles of approximately 4-in. constant chord for improved combustion stability (Fig. 3). All oxidizer and selected fuel orifices were counterbored to prevent spontaneous engine pops. The injector baffles were regeneratively cooled with fuel, which was routed through the baffles and back to the injection ring passages. A small portion of the fuel was discharged from each baffle extremity. Film cooling of the combustion chamber was provided by fuel flow from orifices in the extreme outer fuel ring of the injector adjacent to the injector mounting flange. Approximately 5 percent of the engine fuel flow was injected for film cooling.

Combustion stability was demonstrated during the first firing of each engine assembly by a pulse charge fastened to the center of the injector. This charge consisted of a No. 8 blasting cap and 150 grains of C-4 explosive in a Teflon® holder. The charge was detonated by combustion heat and resulted in a sudden pressure pulse in the chamber.

2.2.2 Combustion Chamber

The combustion chamber was constructed with an ablative liner, an asbestos insulating liner, and an external wrap (Fig. 4). The ablative liner consisted of a silica glass fabric tape impregnated with a phenolic resin compound. The chambers were constructed so that the maximum ablative thickness was obtained at the throat section. Several layers of resin-impregnated fiber glass wrap (glass fabric and glass filament) were bonded over the asbestos insulation. The mounting flange for the injector and nozzle extension was attached to the chamber by bonding the flange lips to the ablative material and overwrapping with fiber glass. Figure 5 shows pre-fire views of the combustion chamber.

2.2.3 Exhaust Nozzle Extension

The radiation-cooled nozzle extension was bolted to the ablative chamber at the 6:1 area ratio and extended to the 62.5:1 area ratio. The extension was constructed of 0.030-in. -thick columbium to the 20:1 area ratio, 0.020-in. -thick columbium to the 40:1 area ratio, and 0.025-in. -thick titanium to the exit. Two circumferential I-beam stiffeners were utilized to reinforce the extension at the exit and at the 40:1 area ratio section. The columbium surfaces were coated to prevent oxidation, and the titanium surfaces were coated with a high emissivity coating to reduce surface temperatures. A photograph of an unfired nozzle extension is shown in Fig. 6.

2.2.4 Thrust Chamber Propellant Valve (TCV)

A pneumatic, pressure-operated, bipropellant valve was used on all engines. Gaseous nitrogen stored in two spheres at pressures up to 2500 psia and regulated to approximately 220 psia provided actuation pressure. Electrical command signals were required for opening and closing the valve.

The propellant valving system consisted of eight ball valves: two in each of two parallel fuel passages and two each in the two parallel oxidizer passages (Fig. 7). One fuel passage and one oxidizer passage constituted an independent valve bank; thus the TCV had two valve banks, designated valve banks A and B. Complete redundancy in the TCV was provided since each of four TCV actuators operates one fuel and one oxidizer ball valve, and one nitrogen sphere and regulator provided pressure for operation. Each of two solenoid pilot valves operated a pair of actuators; thus, valve bank A, bank B, or both, could be utilized to fire the engine.

Orifices were installed at the TCV inlets to balance the parallel passages so that engine operation using either valve bank would produce nearly the same engine ballistic performance for given propellant interface pressures. Orifice sizes for all test series are listed in Table I.

2.3 NAA F-3 FIXTURE

The F-3 fixture was designed to reproduce the propellant system hydrodynamics of the SM spacecraft with necessary modifications incorporated to facilitate ground test operations. The fixture structural frame, tanks, and plumbing had overall dimensions of 100 by 153 in. laterally and was 15 ft high. The fixture weighed approximately 27,500 lb. A schematic diagram of the fixture is presented in Fig. 8.

2.3.1 Propellant System

The propellant tanks were of the same size, shape, and volume as the spacecraft tanks but were designed and fabricated to meet the specification of the ASME pressure vessel code. Both fuel and oxidizer systems had identical volumes of 2360 gal each. Each system consisted of two tanks: one 1310 and one 1050-gal tank. The two tanks were connected in series with a crossover line from the bottom of the smaller storage tank to the top of the larger sump tank. The engine propellant feed line was connected to the bottom of the sump tank. Tank pressurization was accomplished at the top of the storage tank. With this line

arrangement, feed pressure was constant, but variations in engine feed pressure occurred with changes in propellant level.

The only changes from the spacecraft configuration were made in the propellant feed lines. These lines were modified to accommodate AEDC flowmeters and bypass connections for in-place flowmeter calibrations.

2.3.2 Propellant Feed Pressurization System

Since a large number of test firings were conducted at various mixture ratios and chamber pressures, and AEDC facility helium pressurization system was used. Automatically controlled valves limited pressure fluctuations to less than 5 psia during the firings. This pressurization system was connected to the F-3 fixture upstream of the array of doubly redundant check valves.

2.3.3 Heat Shield

A permanent facility-type heat shield (Fig. 9) was used to protect instrumentation, plumbing, and the F-3 fixture from the thermal radiation of the nozzle extension. This shield consisted of two layers of stainless steel with high temperature silica insulation between. The conical area facing the nozzle extension was covered with carbon impregnated Teflon held in place with a wire mesh.

For test periods EA, EB, EC, and EF, an NAA heat shield made of stainless steel was attached to the combustion chamber-nozzle extension attachment flange. This heat shield is also shown in Fig. 9 and was utilized in addition to the facility heat shield.

2.4 INSTALLATION

The F-3 flxture and AJ10-137 engine were installed in the Propulsion Engine Test Cell (J-3), a vertical test cell for testing rocket engines at pressure altitudes of approximately 115,000 ft (Fig. 10 and Ref. 12). A 40-ft-high by 18-ft-diam aluminum test cell capsule lined with thermopanel to permit temperature conditioning was installed over the test article to form the pressure-sealed test chamber.

A rigid cage structure was installed inside the F-3 fixture, and another inner cage was installed inside the rigid cage. The inner cage was attached to the rigid cage by means of six flexure-mounted load cells for six-component force measurements (Fig. 11). The engine was

mounted inside the inner cage. Force system measurements consisting of axial, pitch, and yaw forces together with pitching, yawing, and rolling moment were determined using the mathematical procedures explained in Ref. 13. These forces and moments were then combined to determine thrust vector.

Pressure altitudes were maintained, prior to and following test engine firings, with a steam-driven ejector in the test cell exhaust duct in series with the facility exhaust compressors. During the steady-state portion of the firing, pressure altitude was maintained with a supersonic engine exhaust diffuser (Fig. 10b). Ejector steam was supplied by the AEDC boiler plant and supplemented by steam from the J-3 steam accumulators.

Additional test facility systems required to conduct these tests include ground level propellant tanks; helium storage and regulation for F-3 propellant tank pressurization; gaseous nitrogen for test article purging, leak checking, and valve operation; heat exchangers for temperature conditioning propellants and capsule; and necessary electrical power. Equipment for test article operation located in the J-3 control room included the AGC gimbal system control console, firing console, and combustion stability monitor (CSM).

2.5 QUALITY CONTROL

Quality control was exercised throughout this program to ensure that proper procedures were used and documentation of all activities was accomplished. Surveillance of this program was provided by AGC and ARO, Inc.

2.5.1 AJ10-137 Engine

All engines shipped to AEDC for testing had propellant systems in Level 1 (Ref. 14) clean condition. To maintain Level 1 cleanliness, engines were assembled whenever possible in the RTF Class 10000 (Ref. 15) clean room. To expedite testing, engine S/N 54A, 54C, and 55A used for test series EB, ED, and EF, respectively, had thrust chambers replaced in the test cell. This change would not affect Level 1 cleanliness. However, in addition to the chamber change, it was necessary to replace the propellant valve in the test cell on engine S/N 54C. Large leakages in the pneumatic package of this valve required replacement of this system. With all of these changes in the test cell, this engine could not be certified Level 1 clean prior to test.

All engine assembly was the responsibility of AGC. The buildup of each engine was conducted by ARO, Inc., under supervision of AGC quality control personnel. After engine assembly and documentation were completed, the engine was inspected and accepted by ARO, Inc. This engine was then the responsibility of ARO, Inc., until completion of testing.

2.5.2 Propellants

Propellant cleanliness requirements for this test (Ref. 14) state that no particles in excess of 500 microns or fibers in excess of 1500 by 50 microns shall be present in the propellants. Table II shows that these requirements were met only for test series EB and ED. However, prior to each test period, the propellant sample cleanliness requirements were waived, when necessary, by both AGC and NAA in order to prevent delay of the test firing.

Prior to test series EF, it was not possible to temperature condition the oxidizer to the required temperature (30 to 35°F) because of facility propellant filter contamination. The cleanliness requirements for this test were waived, since engine performance was desired at low propellant temperatures. The oxidizer filter was removed from the line, and this accounts for the large number (56) of particles greater than 500 microns present in the oxidizer sample (Table II) prior to test series EF.

2.5.3 Installation and Testing

All test hardware was installed, and all testing activities were conducted using written procedures. ARO, Inc., quality control verification points were incorporated in all applicable procedures, and all procedures were approved by AGC prior to initiation of this test program.

2.6 INSTRUMENTATION

Instrumentation was provided to measure engine axial and side forces; chamber pressure; propellant system pressures, temperatures, and flow rates; engine temperatures; test cell pressures; capsule wall temperatures; and various accelerations. Visual coverage was also provided by television and motion-picture cameras.

2.6.1 Force Measuring System

2.6.1.1 Axial Force

The axial thrust force (F_a) was measured with a dual-bridge, strain-gage-type load cell with a rated capacity of 50,000 lbf. In-place calibration was accomplished with a hydraulically actuated, axial loading system containing a calibration load cell (Fig. 10b). The calibration load cell was periodically laboratory calibrated with traceability to the National Bureau of Standards (NBS).

2.6.1.2 Side Forces

Two forces in the yaw plane, two forces in the pitch plane, and one roll force were measured with strain-gage-type load cells with a rated capacity of 500 lbf each. These five forces together with axial force are required for engine thrust vector determination. The five side forces were calibrated in place against calibration load cells (Fig. 11) traceable to NBS. Side loads were measured only during test series EA, EC, and EE.

2.6.2 Pressures

2.6.2.1 Combustion Chamber Pressure

Combustion chamber pressure was measured with two strain-gage-type transducers. One transducer was close coupled for high response to pressure transients, and the other transducer was calibrated in place using applied pressure and a precision variable reluctance-type transducer as a secondary standard. The secondary standard was periodically laboratory calibrated with NBS traceability.

Output of the close-coupled transducer was recorded on two different magnetic tape channels to provide optimum transient impulse data. One channel was full-range spanned to provide data over the complete range of chamber pressure (0 to 115 psia) and the other channel was full-range spanned to provide improved data resolution from 0 to 15 psia.

2.6.2.2 Test Cell Pressure

Test cell pressure was measured with two capacitance-type precision pressure transducers located outside the test cell capsule in a controlled-temperature environment and by two strain-gage-type transducers located inside the test cell behind shields to minimize thermal radiation effects. The precision transducers were laboratory calibrated

periodically with a precision mercury manometer and in-place calibrated by electrical voltage substitution. These transducers were used to correct engine data to vacuum thrust conditions during steady-state engine operation. The strain-gage transducers were used to obtain the transient impulse critical ratio because of their higher frequency response.

2.6.2.3 Propellant Pressures

Pressures in the F-3 fixture tanks and lines, engine lines, injector header, and TCV were measured with strain-gage-type pressure transducers (Figs. 8 and 12). These transducers were laboratory calibrated prior to installation and were resistance calibrated prior to and during each test series.

2.6.3 Temperatures

2.6.3.1 Engine Assembly Temperatures

Nozzle extension, combustion chamber, injector surface, TCV, and injector header temperatures were measured with Chromel®-Alumel® (CA) thermocouples (Fig. 12). Thermocouples were installed on the various components by welding, peening, bonding, or taping. In addition, five injector and two combustion chamber throat temperatures were measured with resistance temperature transducers (RTT). These RTT's were calibrated at AGC prior to installation on the engine.

2.6.3.2 Propellant Temperatures

Propellant temperatures in the F-3 fixture tanks and lines were measured with copper-constantan thermocouple immersion probes. Propellant temperatures near the flowmeters, which were used for flow calculations, were measured with RTT immersion probes. Propellant temperatures between the balls of the TCV were measured with CA thermocouple probes.

2.6.3.3 Test Cell Wall Temperatures

The interior temperatures of the test cell capsule walls were sensed by copper-constantan thermocouples welded to the wall surface.

2.6.4 Propellant Flow Rates

Propellant flow rates were measured with one flowmeter in each F-3 fixture propellant feed line, upstream of the engine interface. The flowmeters are rotating permanent-magnet, turbine-type, axial-flow, volumetric flow sensors with two induction coil signal generators. The flowmeters were calibrated in place with propellants. The calibration techniques and data are presented in Appendix III.

2.6.5 Engine Acceleration

Engine injector accelerations were measured in three mutually perpendicular planes with piezoelectric-type accelerometers (Fig. 12). One accelerometer had its output connected to the AGC combustion stability monitor (CSM) unit during test series EC and EE. This unit was set so that engine shutdown would be automatically initiated if peak-to-peak acceleration of 180 g's over a frequency range from 600 to 7000 cps for a time of 0.080 sec was exceeded.

During test series EA, EB, ED, and EF, an NAA flight-type CSM unit was used. This unit consisted of three accelerometers mounted at 120-deg intervals around the rim of the injector. The accelerometers were connected to a signal conditioner and then a logic box. This logic box was set so that if any two accelerometers exceeded 180 g's peak-to-peak amplitude over a range from 600 to 5000 cps for a time of 0.070 ± 0.020 sec, the engine would shut down. No CSM shutdowns were experienced with this unit or the AGC unit at any time during these tests.

2.6.6 Gimbal Parameters

Electrical voltage and current signals from the gimbal control console were used to obtain gimbal actuator position, actuator position change rate, actuator drive motor voltage and current, and actuator clutch currents.

2.6.7 Data Conditioning and Recording

A continuous recording of data on magnetic tape was obtained from analog instrument signals by (1) analog-to-frequency converters, (2) frequency modulated (FM) recording, and (3) digital recordings. Instrument signals produced in a proportionate frequency form were amplified for continuous FM recording on magnetic tape. The cyclic outputs of the propellant flowmeters were conditioned and recorded on magnetic tape in the pulse duration modulation (PDM) mode. Magnetic tape recordings in digital form were obtained using a recorder system that both produces and records an analog signal in binary-coded decimal form.

Light-beam oscillographs were used for continuous graphic recordings of analog and proportionate frequency signals. Frequency signals from the propellant flowmeters were recorded on an oscillograph with a divided frequency to improve record readability. The higher frequency parameters were recorded on magazine-type oscillographs, and the lower frequency parameters and parameters necessary immediately after a firing were recorded on direct-writing oscillographs.

Direct-inking, strip-chart recorders were used for immediate access, continuous, graphic recordings. Analog signals produced pen deflections with a null-balance potentiometer mechanism. These charts were used only to observe and obtain necessary engine and facility parameters during and immediately after test firings.

2.6.8 Visual Coverage

Two closed-circuit television systems permitted visual monitoring of the engine during testing operations. Permanent visual documentation of test firings was obtained with three 16-mm, motion-picture cameras. Each camera provided coverage of different portions of the test article. Various test article parameters were displayed on visual indicators to provide control room information on test article and facility operations and performance.

SECTION III PROCEDURE

3.1 TEST CELL OPERATION

3.1.1 Pre-Test Operations at Ambient Pressures

Prior to each test period, the following functions were performed at ambient pressure conditions:

1. The six-component thrust system was calibrated with the propellant lines pressurized to 185 psia. After completion of calibration, the propellant lines were depressurized to ambient conditions. This step was eliminated for test series EB, ED, and EF because side forces were not measured.
2. Instrumentation parameters necessary for engine qualification data were checked for operation. Any inoperative parameters were either repaired or deleted by AGC and NAA.
3. A functional check of all systems and operation of all equipment by the firing sequencer were performed. Gimbal system calibrations, TCV checks for operation of valve instrumentation, and valve operational times were also conducted at this time.
4. The F-3 fixture was loaded with propellants, and in-place flowmeter calibrations were conducted (see Appendix III). For test series EC and EF, propellants were recirculated through

the heat exchanger to temperature condition the propellants to nominal temperatures of 110°F for test series EC and 35°F for test series EF prior to loading the F-3 fixture.

5. The F-3 fixture was reloaded, after flowmeter calibrations, with propellants (temperature conditioned for test series EC and EF) for each test firing, and propellant samples were obtained for chemical analysis and particle contamination count. Results of propellant samples were reviewed and waived, when necessary, by AGC and NAA prior to the first test firing of a test series.
6. All transducers were resistance calibrated, and all temperature recording equipment was calibrated by millivolt substitution.
7. The test cell was closed, and all preparations for altitude conditions were completed.

3.1.2 Operation with Test Cell at Altitude

The test cell was evacuated to approximately 0.4 psia with the facility exhaust compressors, and the following operations were performed:

1. All strain-gage transducers were resistance calibrated.
2. The propellant lines were pressurized to 185 psia, and axial force, chamber pressure, and test cell pressure transducers were calibrated in place.

For each test firing, the following operations were conducted:

1. The propellant lines were pressurized to the required pressure.
2. The steam ejector driven with plant steam was used to further reduce cell pressure to approximately 0.15 psia.
3. Approximately 3 min before firing time, the steam accumulators were used to augment plant steam to further reduce cell pressure to approximately 0.05 psia. Steam accumulators were not used for firings of 1 sec duration or less.
4. Sixty seconds prior to firing, the firing sequencer was initiated, and operations including instrumentation and camera starts, engine firing, engine shutdown, and instrumentation and camera stops were automatically accomplished. For firing durations of 1 sec or less, engine firing and shutdown were accomplished with timers on the AGC firing console rather than the firing sequencer.

5. Immediately after a test firing, the steam accumulators were shut down, and pressure altitude was maintained during coast periods up to 1 hr using the plant steam-driven ejector and facility exhausters (test cell pressure approximately 0.15 psia). Pressure altitude for coast periods after the first hour was maintained with only facility exhausters (test cell pressure approximately 0.4 psia).

After the first test firing of a new engine assembly, the data obtained were corrected to standard inlet conditions using an AGC method of calculation. This calculation determined if the engine propellant lines were correctly orificed, and these data were approved by AGC before continuing the test firing schedule.

After the last firing of a test series, the following operations were accomplished:

1. Axial thrust, chamber pressure, and test cell pressure transducers were in-place calibrated with propellant lines pressurized to 185 psia. Lines were depressurized after completion of calibration.
2. Resistance calibrations of all transducers were accomplished.
3. F-3 fixture tanks were drained into the J-3 storage tanks.
4. The propellant lines downstream of the main F-3 shutoff valves were drained and aspirated by venting the lines to test cell pressure for approximately 1 hr. After test series EA, EC, and EE, the engine TCV and injector were also purged with nitrogen after aspiration was completed. The purge was necessary since engine rebuild in the test cell was accomplished after these test series.
5. The test cell pressure was raised to ambient atmospheric conditions.

3.1.3 Post-Test Operations at Ambient Pressures

After completion of a test series with the test cell at ambient pressure, all transducers were resistance calibrated, and all thermocouple instrumentation was calibrated by millivolt substitution.

3.2 NOZZLE EXTENSION-CHAMBER FLANGE LEAK CHECK

The nozzle extension-chamber flange joint was leak checked several times during these tests. The first leak check was conducted outside the

test cell prior to test series EC, using nozzle extension S/N 54 and chamber S/N 313 (Table I). The nozzle extension shipping container includes leak checking hardware, and the engine and nozzle extension mounted on this hardware are shown in Fig. 1.

Prior to and immediately following test series ED, the nozzle extension-chamber flange joint was leak checked with the engine installed in the test cell. This check was made using the equipment shown in Fig. 13 and mounted in the test cell as shown in Fig. 14. Figure 14 also shows details of the leak checking ring fitted against the flange joint. After the in-cell leak checking equipment was installed, the ring was forced against the inside of the chamber and nozzle extension at the flange joint by means of the jack post. Air pressure at 3 to 5 psia was introduced into the leak check ring, and any leaks at the flange joint were detected with leak check solution. This same procedure was also followed after test series EF.

3.3 PERFORMANCE DATA ACQUISITION AND REDUCTION

All primary engine operational parameters were recorded on magnetic tape. Digital computers were used to recover data from the magnetic tape records, produce data printouts in engineering units, and perform computations to produce engine performance information as follows:

1. Rocket engine ballistic performance (specific impulse and characteristic velocity),
2. Total impulse of ignition and shutdown transients,
3. Total impulse of minimum impulse bit operation, and
4. Thrust vector determination.

The equations used for engine performance calculations were according to general standard practice modified slightly to account for area changes of the ablative nozzle throat. Performance calculations were based on combustion chamber pressure measured at the injector face. No corrections were applied for total pressure loss from the injector to the nozzle throat. Steady-state performance calculations were made from measured data, which were recorded continuously and averaged over 4-sec time intervals for firings greater than 10 sec and over 2-sec time intervals for firings of 10 sec. Performance calculations were not made for firings less than 7 sec.

The estimated error (one standard deviation, 1σ) of the measured parameters required for engine performance are as follows:

<u>Parameter</u>	<u>1σ Error, percent</u>
F_a	0.15
P_c	0.25
\dot{W}_f	0.17
\dot{W}_o	0.14
P_a	1.85

The one-sigma errors in calculated parameters are estimated to be:

<u>Parameter</u>	<u>1σ Error, percent</u>
\dot{W}_t	0.11
F_v	0.16
I_{spv}	0.19

3.3.1 Ballistic Performance

Because of the nonuniform variations of the effective nozzle throat area during a firing and the physical impossibility of measuring the throat area between firings during a particular test series, characteristic velocity was calculated using the following assumptions:

1. Characteristic velocity, corrected to a mixture ratio of 1.6, is constant for a particular test series,
2. Characteristic velocity is a function of mixture ratio only, and
3. The slope of the c^* versus MR curve conforms to previous experimental data.

The c_i^* for a given injector chamber combination was calculated using (1) the measured data between 2 and 6 sec of the initial firing with a new chamber, (2) the pretest measured nozzle throat area, and (3) the relationship:

$$c_i^* = P_c A_t g / \dot{W}_t$$

The c^* for an MR = 1.6 was derived using the following curve slope factor supplied by AGC:

$$MR_{corr} = 5771.35/[5424.914 + 594.293 (MR) - 236.080 (MR)^2]$$

then $c^* (MR = 1.6) = (c^*_i) (MR_{corr})$

This $c^* (MR = 1.6)$ was retained as the standard for the given injector-chamber assembly and was used for data reduction during the remainder of the test series. The c^* for any other MR during subsequent firings was derived by reversing the process and applying the MR slope factor (MR_{corr}) to the standard $c^* (MR = 1.6)$.

The throat area of the nozzle for subsequent firings was calculated using the c^* derived above, the measured chamber pressure, and measured propellant flow rates in the relationship:

$$A_{t_{calc}} = c^* \dot{W}_t / P_c g$$

The measured axial thrust was corrected to vacuum conditions using measured test cell pressure as follows:

$$F_v = F_a + P_a A_e$$

This vacuum thrust was used with calculated nozzle throat area and measured chamber pressure to determine vacuum thrust coefficient as follows:

$$C_{F_v} = F_v / P_c A_{t_{calc}}$$

Substituting the equation for $A_{t_{calc}}$ in the above equation results in

$$C_{F_v} = I_{sp_v} g / c^*$$

Thus C_{F_v} is no longer a direct function of the ratio F_v / P_c and is not considered a meaningful measurement of nozzle performance.

3.3.2 Total Impulse of Ignition and Shutdown Transients

The total impulse (lb_f-sec) of the start transient covered the time period from ignition (initial chamber pressure rise) to 100 percent of steady-state thrust. The impulse was derived using calculated thrust based on chamber pressure:

$$I_t = C_{F_v} A_t \int_0^t P_c dt$$

Intermediate impulse values were also derived for levels of chamber pressure at intervals of 10 percent up to the steady-state value.

The total impulse of the shutdown transient was calculated by a similar equation except that the integral covered the time period from 100 to 0 percent of steady-state thrust. The 0-percent level was defined as the thrust level at which the exhaust flow in the nozzle throat becomes

unchoked. This point of unchoking has been determined experimentally at RTF to be the ratio of P_c/P_a equal to 1.2 (called the critical ratio). Vacuum thrust computed from measured thrust was not used because force system dynamics invalidate thrust data during the ignition and shutdown transients.

Measured combustion chamber pressure was reduced at 0.005-sec intervals (200 intervals/sec) during ignition transients and at 0.020-sec intervals (50 intervals/sec) during shutdown transients from the continuous magnetic tape recording of close-coupled transducer data. During the ignition transient, the P_c tape channel spanned from 0 to 15 psia was used for calculations up to 15 psia, and the tape channel spanned for the full range of chamber pressure was used for calculations of 15 psia and greater. During the shutdown transient, the reverse was true with the full-range channel being utilized down to 15 psia and the other tape channel used from 15 to 0 psia. The combustion chamber pressure was used with calculated nozzle throat area to compute vacuum thrust. The values of C_{F_v} and A_t , obtained from the steady-state firing nearest the transient of interest, were assumed to be constant throughout the transient.

A digital computer program determined the time of occurrence, the thrust rise rate, and the integrated total impulse at the specific percentage levels of chamber transients.

3.3.3 Total Impulse Bit

The method of calculating the total impulse (lbf-sec) of the impulse bit firings was identical to the method used for the ignition and shutdown transients except that impulse was totalized for the entire firing from chamber pressure rise to the critical ratio. Since the impulse bit firings were too short to establish steady-state engine performance levels, the vacuum thrust coefficient (C_{F_v}) and nozzle throat area (A_t) used were obtained from the nearest previous engine firing which produced steady-state data at the same operating conditions. The same assumptions of constant C_{F_v} and A_t throughout the impulse bit firings were retained.

3.3.4 Thrust Vector Determination

The multicomponent force measurement system (Fig. 11) measured the six components of force; forward and aft pitch, forward and aft yaw, roll, and axial force. This system employed the premise of a linear repeatable mechanical interaction for a given force application; that is, for a given force application (L), the force (R) measured in any load cell can be obtained by

$$R_i = C_{i,j} L_j$$

where $C_{i,j}$ represents the calibration constants based on the slope of the interaction. Because there were six data and six calibrate load cells, both i (which represented the data load cell being observed) and j (which represented the load applicator being used) varied from one to six, and $C_{i,j}$ was a six-by-six matrix.

To obtain true forces from the thrust system, an equation of the following form was used:

$$L_j = K_{j,i} R_i$$

where $K_{j,i}$ represents the balance constants and was the inverse of the calibration constant matrix ($C_{i,j}$). The true forces were obtained by multiplying the force measured by the inversion of the calibration constants. A complete explanation of the force system and the method of determining balance constants are given in Ref. 13.

Once the forces were determined at the six load cells, the equations of static equilibrium were used to resolve these forces into a thrust vector at the engine gimbal plane (plane of engine throat). This thrust vector is presented in the form of an angle, from vertical, in the pitch and yaw planes and the distance from the centerline of the inner thrust cage to the point of intersection of the thrust vector with the gimbal plane.

SECTION IV RESULTS AND DISCUSSION

Ballistic qualification performance data for the Apollo Block II Service Module engine were obtained during 72 test firings, utilizing six engine assemblies with three different Modification No. 4 injectors. Each injector was tested for two complete test series. Data were obtained at mixture ratios ranging from 1.4 to 1.8 and chamber pressures from 79 to 115 psia. Propellant temperatures during these tests were varied from extremes of 35°F to 110°F with the majority of testing at normal temperatures (60°F). A summary of all test firings is presented in Table III. The ballistic performance data obtained during these tests were not compared with specification values because the specification values were not furnished by AGC.

Two basic parameters (vacuum specific impulse, I_{sp_v} , and characteristic velocity, c^*) were used to determine engine ballistic performance. Vacuum specific impulse was calculated using engine thrust corrected to vacuum conditions, and this parameter described the overall engine

performance. Characteristic velocity was calculated using the chamber pressure measured at the injector face and is a measure of the injector-combustion chamber performance.

An indication of nozzle performance (C_{F_v}) was obtained using the assumptions stated in Section 3.3.1. Since the nozzle throat area varies in an unknown manner during a firing, the calculation of C_{F_v} depends on the value of c^* and I_{sp_v} and is not a true indication of nozzle performance. This parameter will not be discussed in the text but is presented for academic reasons in Table IV, which is a summary of performance data obtained during the various firings.

Since I_{sp_v} was calculated from measured data only, this parameter is considered the most accurate indication of performance during all firings. Characteristic velocity incorporates the assumptions stated in Section 3.3.1 and, therefore, is not as accurate an indication of performance as I_{sp_v} .

4.1 ENGINE PERFORMANCE

4.1.1 Vacuum Specific Impulse

Vacuum specific impulse data obtained between 7 and 40 sec after engine ignition at the nominal engine chamber pressure of 97 psia were grouped together and used to construct (by digital computer) second-order least-squares curves as a function of mixture ratio. Three groups of data corresponding to the three different injectors were analyzed, and these data are summarized as follows:

Engine S/N	54	54A	54B	54C	55	55A
Test Series	EA	EB	EC	ED	EE	EF
Injector S/N	104		115		103	
Number of Test Firings ($P_c = 97$ psia)	7		6		10	
Number of Data Samples	29		15		43	
I_{sp_v} at MR = 1.60, lb _f -sec/lb _m	313.5		311.3		314.8	
One Standard Deviation of I_{sp_v} about Second- Order, Least-Squares Curve, percent	±0.066		±0.083		±0.060	

The results of this analysis provided not only a mathematical expression for the overall engine performance, but also an indication of the precision of data acquisition and engine repeatability. The best fit second-order equations for calculating I_{sp_v} for the three injectors are:

$$\text{Injector S/N 104: } I_{sp_v} = 214.084 + 123.292 (MR) - 38.215 (MR)^2$$

$$\text{Injector S/N 115: } I_{sp_v} = 214.863 + 120.019 (MR) - 37.347 (MR)^2$$

$$\text{Injector S/N 103: } I_{sp_v} = 245.951 + 85.059 (MR) - 26.253 (MR)^2$$

These equations are plotted in Fig. 15, and the slopes are nearly the same for all injectors. The peak I_{sp_v} values (at $\partial I_{sp_v} / \partial MR = 0$) occurred at mixture ratio values of 1.613, 1.607, and 1.620 for injectors S/N 104, 115, and 103, respectively.

Propellant temperature had little effect on engine performance. Tests with injector S/N 115 were conducted at propellant temperatures of 110 and 70°F during test series EC and ED, respectively. When these data were grouped together as shown in Fig. 15, the repeatability of data was within ± 0.083 percent (1σ). Injector S/N 103 was tested at temperatures of 70 and 30°F during test series EE and EF, respectively. The I_{sp_v} data from this injector were repeatable within ± 0.060 percent (1σ). The large difference in I_{sp_v} level between these two injectors was caused by the injectors and not by propellant temperatures.

Although all three injectors tested were of an identical design, a discrete level of engine performance (I_{sp_v}) was obtained from each injector. A comparison of the I_{sp_v} levels of the three injectors (Fig. 15) indicates that there is a significant variation of engine performance. The average repeatability of data for a particular injector was ± 0.070 percent (1σ). However, when grouping the I_{sp_v} values for all injectors, the deviation from the average I_{sp_v} at $MR = 1.60$ (313.2 lbf-sec/lb_m) was ± 0.57 percent (1σ) (± 1.8 lbf-sec/lb_m).

Thirty-two of the qualification test firings were conducted at off-design chamber pressures ranging from 79 to 115 psia (Fig. 16). The extrapolated data from Fig. 16 are cross-plotted in Fig. 17 at a mixture ratio of 1.60. These data indicate that engine performance increased almost linearly with chamber pressure. The slope of the I_{sp_v} versus P_c curve is approximately 0.5 lbf-sec/lb_m/psi. The extrapolated values of I_{sp_v} at a 1.60 mixture ratio and a chamber pressure of 115 psia for the three injectors tested are:

1. Injector S/N 104: 314.3 lbf-sec/lb_m

2. Injector S/N 115: 312.3 lbf-sec/lb_m
3. Injector S/N 103: 315.6 lbf-sec/lb_m

The data from test firing EC-01 were not included in the least-squares program. Although no abnormalities could be found in the data acquisition systems or data reduction procedures, the performance data are not believed to be representative of injector S/N 115 because:

1. The values of I_{sp_v} obtained during EC-01 were 1.7 lbf-sec/lb_m higher than the mean of other I_{sp_v} data for this group. This deviation from the mean value is greater than 6σ , and statistically there is less than 1 chance out of 2×10^6 of this value being true.
2. The characteristic velocity obtained during EC-01 was 0.6 percent higher than obtained during ED-01 using the same injector. Although the c^* obtained during EC-01 (injector S/N 115) compared with the c^* obtained during the EA and EB test series (injector S/N 104), data obtained from Aerojet indicate that injector S/N 115 should have a c^* approximately 1 percent lower than injector S/N 104.

These differences in performance are listed in Table IV. Characteristic velocity for all of test series EC was high because this parameter was calculated during the first firing as explained in Section 3.3.1.

4.1.2 Characteristic Velocity

Characteristic velocity (c^*) is used as an indication of the injector-combustion chamber performance. A detailed method of calculation of c^* is described in Section 3.3.1. The initial c^* was calculated early in the first firing of a new chamber (2 to 6 sec) by the relationship $P_c A_t \cdot g/W_t$ using the measured pre-fire nozzle throat area. This value of c^* was then empirically adjusted to a mixture ratio of 1.60. The initial values of c^* for five engine assemblies (data from test series EC were excluded) are shown in Fig. 18, and these values adjusted to 1.60 are summarized as follows:

Engine S/N	54	54A	54C	55	55A
Injector S/N	104	104	115	103	103
c^* Adjusted to MR = 1.60, ft/sec	5915.2	5930.3	5886.3	5943.2	5938.7

The c^* values in the above table were obtained at a chamber pressure of 97 psia. The values of c^* are based on the chamber pressure as measured at the injector face, and no attempt has been made to correct for the total pressure loss in the chamber.

Each injector had its own discrete level of performance. The values of c^* obtained with a different chamber using the same injector were repeatable within 0.255 and 0.076 percent for injectors S/N 104 and 103, respectively. The variation in magnitude of c^* at $MR = 1.60$ between the three injectors is significant. Grouping all values of c^* obtained from the three injectors shows the deviation from the mean c^* at $MR = 1.60$ (5916.7 ft/sec) to be ± 0.47 percent (1σ) (± 27.9 ft/sec).

4.1.3 Thrust Data

All ballistic performance data were calculated from measurements obtained between 7 and 40 sec of the engine firing time. During firings of greater than 40 sec duration, a thrust system shift occurred that was proportional to firing time, with the largest shift occurring during the longest firing. A summary of the thrust system zero shift after the longest firing in each test series (550 sec) is present below:

Test Number	Thrust System Zero Shift, lb
EA-06	155
EB-06	110
EC-06	630
ED-06	65
EE-06	550
EF-06	132

The thrust system zero shift is believed to be caused by shifts in tare loads due to heating of the various force balance components and propellant lines during firings of greater than 40 sec.

Figure 19 shows the variation of thrust, chamber pressure, flow rate, and vacuum specific impulse during firing EC-06. The thrust system anomaly can best be seen after tank crossover between 300 and 550 sec after FS-1. During this period of time, chamber pressure and flow rate varied 2 percent, and thrust remained essentially constant. Figure 19 also shows the I_{sp_v} to be 321.3 sec at the end of the firing. By subtracting the amount of thrust system zero shift at the end of the firing from the measured thrust at the last performance calculation and recalculating I_{sp_v} , this parameter reduces to a value of 312.6 sec. The recalculated I_{sp_v} is then in agreement with the average I_{sp_v} value

of 312.8 during the first 40 sec of firing time. For this reason all firing data of less than 40 sec firing duration is considered valid and not affected by thrust data difficulties.

4.1.4 Effect of Propellant Valve Bank Selection

During engine operation, flow through the propellant valve assembly may be routed through TCV bank A only, TCV bank B only, or through both banks simultaneously, as discussed in Section 2.2.4. The operating parameters changed significantly when both valve banks were used (Fig. 20) because of the change in flow resistance through the thrust chamber valve. However, a review of the performance data (I_{sp_v}) indicated that, within the precision of the data (< 0.1 percent), engine ballistic performance remained the same regardless of valve bank selection. The ratio of P_c/W_t or F_v/P_c remained essentially constant for a given mixture ratio for any TCV bank selection.

4.1.5 Engine Transient Characteristics

4.1.5.1 Engine Ignition Transient Impulse

The total impulse (lb_f -sec) developed during the engine ignition or shutdown transients was determined for each test firing (duration > 1.0 sec) during Phase V by the method discussed in Section 3.3.3. A tabulation of the impulse developed from ignition to 90-percent steady-state thrust appears in Table V. The transient specifications (Ref. 16) presented in the table below are valid only if the interface specifications ($P_{01} = 160 \pm 4$ psia, $P_{f1} = 166 \pm 4$ psia) are met. There were only nine firings that met these interface pressure specifications. All nine were at a combustion chamber pressure of 97 psia and using TCV bank A during ignition. A summary of the average impulse from ignition to 90-percent steady-state thrust for these nine firings is presented in the table below:

	Time from FS-1 to 90 percent of Steady-State Thrust, sec	Run-to-Run Deviation, sec	Total Impulse from Ignition to 90 percent of Steady-State Thrust, lb_f -sec	Run-to-Run Deviation, lb_f -sec
Specification	0.350 to 0.550	---	100 to 400	± 100
Data	0.559	+ 0.026 - 0.032	568	+ 140 - 231

The average ignition impulse from FS-1 to 90-percent of steady-state thrust was 568 lbf-sec with a standard deviation of ± 119 lbf-sec. This value is 30 percent higher than the upper specification limit. The average time required to develop this impulse was 0.559 sec (1.6 percent higher than the highest specification limit) with a standard deviation of ± 0.016 sec. The above table shows that neither the impulse nor the time were within limits and that the run-to-run deviation of the impulse also exceeded the specified repeatability limits. A typical ignition transient is shown in Fig. 21.

4.1.5.2 Engine Shutdown Transient Impulse

A tabulation of the shutdown impulse developed during each test firing appears in Table VI. A summary of the average shutdown impulse based on the nine firings that met the interface pressure specifications is as follows:

Condition	Time from FS-2 to 10 percent Steady-State Thrust, sec	Impulse from FS-2 to 10 percent Steady-State Thrust, lbf-sec		Impulse from 10 to 1 percent of Steady-State Thrust, lbf-sec	Impulse from 1 percent to Critical Ratio, lbf-sec
		Magnitude	Run-to-Run Deviation		
Specification	0.650-0.900	7,000 to 12,000	± 300	375-700	260
Data*	1.008 $\begin{smallmatrix} +0.047 \\ -0.044 \end{smallmatrix}$	10,190	$\begin{smallmatrix} +633 \\ -631 \end{smallmatrix}$	964 $\begin{smallmatrix} +407 \\ -437 \end{smallmatrix}$	126 $\begin{smallmatrix} +53 \\ -58 \end{smallmatrix}$

*Valve bank B was used during the shutdown of three firings included here.

NOTE: The \pm values in the above table are run-to-run deviations.

The table above shows that the time from FS-2 to 10 percent of the steady-state thrust exceeded the specification range by 12 percent; however, the corresponding average impulse was within limits although the run-to-run deviation exceeded specified repeatability limits. The average impulse from 10 to 1 percent of steady-state thrust exceeded the specification range by 38 percent. A typical shutdown transient is shown in Fig. 22.

4.1.6 Minimum Impulse Operations

The impulse data for the minimum impulse test firings (firings of duration less than 1 sec) were totalized from the time of ignition until the flow in the nozzle throat became unchoked after FS-2. Unchoked flow in the nozzle throat is defined as the time when the ratio of $P_c/P_a = 1.2$. These data are tabulated in Table VII.

The total impulse developed during the impulse bit operations was almost a linear function of the firing duration as shown in Fig. 23. The data also indicate that the firing duration would have to be greater than 0.3 sec for any impulse to be developed (Fig. 24).

The total impulse developed using valve bank B was higher (approximately 0.5 percent for firing duration of 0.980 sec) than the impulse developed using valve bank A (Fig. 23). This was due to differences in timing of the valve banks, which affected the chamber pressure transients (Fig. 24).

4.2 ENGINE DURABILITY

4.2.1 Combustion Chamber

Combustion chamber durability was satisfactory for all chambers tested during these tests. Post-fire photographs of a typical chamber are shown in Fig. 25. Very little ablation is evident when compared with the unfired chamber shown in Fig. 5b. The only difficulty experienced with a chamber was the separation of the fiber glass overwrap from the chamber-nozzle flange during the last engine test. This separation is discussed in the next section and shown in Fig. 26.

4.2.2 Nozzle Extension-Chamber Flange Joint Leak Check

The nozzle extension-chamber flange joint was leak checked several times during these tests. In the following table, the leak checks and the results are listed:

Test Number	Engine Installed in Test Cell	Nozzle Extension Bolt Torque, in. -lb	Nozzle Extension-Chamber Flange Leakage, percent of Circumference
Pre-EC	No	44	40
Pre-ED	Yes	44	25
Pre-ED*	Yes	55	40
Post-ED	Yes	55	75
Post-EF	Yes	44	0

*Test series ED was conducted with a nozzle extension bolt torque of 55 in. -lb.

An anti-foaming silica rubber was applied to the joint between the nozzle extension-chamber flange prior to test series EF. The post-test leak check of this joint in the test cell revealed no leakage at this joint. However, large leakage around approximately 50 percent of the circumference of the chamber-nozzle flange was evident. The fiber glass overwrap separated from the chamber-nozzle flange (Fig. 26) which caused this large leakage.

4.2.3 Nozzle Extension

Excellent durability of both nozzle extensions used during this test was evident. Both extensions were fired for durations of approximately 2250 sec each, and no discrepancies were noted. A photograph of nozzle extension S/N 54 after 2250 sec of operation is shown in Fig. 27.

4.2.4 Thrust Chamber Valve

Difficulties were experienced with the thrust chamber valves throughout these tests. The main problem was leakage past the valve ball seals that was greater than the maximum specifications (Ref. 16) value of 400 cc/hr. The TCV S/N 122 used during test series EA and EB had leakages in excess of specification values following test series EB, and TCV S/N 126 was installed for test series EC. Excessive ball seal leakages of this valve following test series EC necessitated TCV change to S/N 128 for test series ED. All ball seals through test series ED were of white Teflon (TFE) material. After test series EB, TCV S/N 122 was shipped back to AGC, and new ball seals of Teflon Flourea Blue (BF-1) were installed. This valve was shipped back to AEDC and used for test series EE and EF. Leakages of this valve were within specification limits prior to test series EE but outside specification values following the test. Test series EF was made with this leaking propellant valve, and post-fire leak checks showed that leakages did not increase during this test series although leakages were in excess of specification values.

4.3 ENGINE TEMPERATURE CHARACTERISTICS

4.3.1 Combustion Chamber Temperature

The temperature of the combustion chamber was measured by thermocouples attached to the external skin of the chamber; therefore, it was difficult to derive any but gross conclusions from the temperature data. The chamber temperature measurements were influenced not only by the heat capacity of the chamber, but also by reradiation from the test cell installation components.

Thermal equilibrium was not attained during actual test firings because of the low thermal conductivity of the chamber ablative material. The chamber temperature history of a typical maximum duration firing (550 sec) is shown in Fig. 28. The peak temperatures were experienced during the post-fire coast period approximately 30 min after engine shut-down. The rapid temperature rise and fall of the nozzle extension mounting flange was the result of (1) thermal radiation from the nozzle extension and (2) conduction through the metallic mounting flange.

The maximum temperature reached on the outer surface of the chamber during the various long-duration firings and subsequent coast periods are presented below. As expected, the maximum temperature occurred at the chamber/nozzle throat.

Test Series	Engine S/N	Test Duration, sec	Chamber Pre-Fire Temperature, °F	Peak Temperature, °F	Peak Temperature Time after FS-2, min
EA	54	550	190	461	30
EB	54A	550	200	458	31
EC	54B	550	220	465	28
ED	54C	550	200	434	29
EE	55	550	200	441	27
EF	55A	550	200	453	24

The high and low (approximately 110°F test series EC and 30°F test series EF) test cell wall and propellant temperatures had little effect on the temperature experienced by the combustion chamber because the peak temperatures shown above are all within 40°F of each other.

4.3.2 Nozzle Extension Temperature

Nozzle extension temperatures were measured by thermocouples attached to the external skin of the columbium-titanium nozzle. The acquisition of nozzle temperature data was of secondary importance during this testing phase, and only limited data were obtained. The output of numerous thermocouples became invalid during the test firings because of detachment from the nozzle extension skin or shorting of the thermocouple lead wire upstream of the attachment point. Therefore, no attempt was made to distinguish between the temperature history of the two nozzle extensions. A typical nozzle temperature history (Fig. 29) indicates that near equilibrium temperatures were reached after about 50 sec of engine operation.

The measured equilibrium temperature profile of the nozzle extension and the AGC design curve are shown in Fig. 30. An individual temperature profile is not presented for a particular test firing, but the data from both nozzle extensions are grouped to form an "envelope" of data. No measured temperature data were available beyond the area ratio of 42:1.

A discontinuity of the temperature profile occurred across the columbium-titanium joint of the nozzle extension. The decrease in the measured temperature on the titanium skin was apparently caused by the high emissivity coating, which was not on the columbium portion of the extension.

4.4 GIMBAL SYSTEM OPERATION

The engine was gimballed during all test series for a total of 36 of the 72 test firings (Table III). Gimbal operation was omitted during several firings in order to obtain steady-state thrust vector data acquisition or because firing duration was not long enough to accommodate a satisfactory gimbal program. The gimbal amplitude was limited to 1.5 deg during these operations to preclude spilling the nozzle exhaust gases over the inlet edge of the exhaust diffuser and into the test cell (see Fig. 10b). The gimbal operations included ramp, step, and sine function command signals of various frequencies in both the pitch and yaw planes to evaluate gimbal system mechanical and electrical dynamics. All analysis of the gimbal data was done by AGC.

4.5 THRUST VECTOR EXCURSION

Six-component force data were measured for three of the six engine assemblies tested during Apollo Block II qualification testing. Data reduction techniques and a detailed description of the force balance are presented in Ref. 13.

The thrust vector excursion for engine assemblies S/N 54, 54B, and 55 are presented in Figs. 31, 32, and 33, respectively. The format of presentation is a history in both the pitch and yaw planes of the angular excursion and the excursion of the point of intersection of the thrust vector with the gimbal plane. Thrust vector excursion data are presented only during periods of nongimbaling (engine null) since the force balance was designed and functions only as a static system. Data reduction techniques present the vector referenced to the centerline of the force balance. At present, there is no definitive method of determining the relationship between the engine geometric centerline and the force balance centerline. Angular excursion was small for each engine

assembly presented. The following table presents the total vector excursion for each engine tested.

S/N 54 EA Series		S/N 54B EC Series		S/N 55 EE Series	
θ , deg	θ , deg	θ , deg	θ , deg	θ , deg	θ , deg
-0.24	+0.12	-0.14	-0.28	-0.10	-0.18

The excursion of the point of intersection of the thrust vector with the gimbal plane as presented in Figs. 31a, 32a, and 33a is tabulated below:

S/N 54 EA Series		S/N 54B EC Series		S/N 55 EE Series	
X, in.	Y, in.	X, in.	Y, in.	X, in.	Y, in.
+0.055	+0.050	0	0	-0.01	+0.04

The small excursions tabulated indicate uniform ablation of the chamber throat.

During testing of the Apollo Block II engine, a progressive change in the relationship between the balance and the engine geometric centerline was observed as a function of firing time. This force system anomaly is discussed in Section 4.1.3. Because of this temperature effect, data from firings EA-10, EC-06, and EE-06 are not included in the vector position excursion tabulation. These data are presented in Figs. 31a, 32a, and 33a for the latter portion of the above firings to show this temperature effect.

SECTION V SUMMARY OF RESULTS

The significant results obtained during the Apollo Service Module Block II Engine Qualification Test are summarized as follows:

1. The I_{spv} of the engine assemblies tested was dependent on the injector used although all three injectors were of identical

design within limits of quality control. The values of I_{sp_v} at $MR = 1.60$ were 313.5, 311.3, and 314.8 $lb_f\text{-sec}/lb_m$ for the engine assemblies using injectors S/N 104, 115, and 103, respectively. The average repeatability of I_{sp_v} data for a particular injector was ± 0.07 percent (1σ); however, the deviation from the average I_{sp_v} (313.2 $lb_f\text{-sec}/lb_m$) for all injectors was ± 0.57 percent (1σ). The estimated error in the measurement of I_{sp_v} is ± 0.19 percent (1σ).

2. The peak I_{sp_v} value as determined from second-order, least-squares curves occurred at mixture ratio values of 1.613, 1.607, and 1.620 for the three different injectors tested.
3. I_{sp_v} increased linearly with chamber pressure over the P_c range tested (79 to 115 psia). This increase was approximately 0.5 $lb_f\text{-sec}/lb_m/\text{psi}$.
4. The thrust chamber valve had excessive leakages past the ball seal valves on several occasions during these tests.
5. Very little chamber ablation occurred during any of the test firings. The only difficulty experienced with a chamber was the separation of the fiber glass overwrap from the chamber-nozzle flange during the last test series.
6. Nozzle extension durability was excellent for these tests.
7. Variation of propellant temperatures between 30 and 110°F had little effect on engine performance.
8. Engine ballistic performance was independent of TCV bank selection.
9. During ignition transients, the engine did not meet specification limits for either the time to develop 90-percent thrust or the total impulse to this level. The time to 90 percent of steady-state thrust exceeded the upper specification limit by 1.60 percent, and total impulse to this level exceeded specification limits by 30 percent.
10. During the shutdown transient impulse, the time from shutdown to 10 percent of steady-state thrust exceeded specification limits by 1.2 percent, and corresponding impulse was within limits. From 10 to 1 percent of steady-state thrust, the engine exceeded specification limits on impulse by 38 percent.
11. Engine firing duration must be greater than 0.3 sec for any impulse to be developed.

REFERENCES

1. DeFord, J. F. "Simulated Altitude Testing of the Aerojet-General Corporation AJ10-137 Rocket Engine (Report I - Phase I Development Test)." AEDC-TDR-64-81 (AD350408), May 1964.
2. McIlveen, M. W. "Simulated Altitude Testing of the Aerojet-General Corporation AJ10-137 Rocket Engine (Report II - Phase I Development Test)." AEDC-TDR-64-82 (AD350407), May 1964.
3. Vetter, N. R. and DeFord, J. F. "Simulated Altitude Testing of the Aerojet-General Corporation AJ10-137 Rocket Engine (Report III - Phase I Development Test)." AEDC-TDR-64-146. (AD352141), July 1964.
4. McIlveen, M. W. "Simulated Altitude Testing of the Aerojet-General Corporation AJ10-137 Rocket Engine (Report IV - Phase I Development Test)." AEDC-TDR-64-147 (AD352327), August 1964.
5. Vetter, N. R. and DeFord, J. F. "Simulated Altitude Testing of the Aerojet-General Corporation AJ10-137 Rocket Engine (Report V - Phase I Development Test)." AEDC-TDR-64-158 (AD352700), August 1964.
6. Vetter, N. R. and McIlveen, M. W. "Simulated Altitude Testing of the Aerojet-General Corporation AJ10-137 Rocket Engine (Report VI - Phase I Development Test)." AEDC-TDR-64-171, September 1964.
7. Schulz, G. H. and DeFord, J. F. "Simulated Altitude Testing of the Apollo Service Module Propulsion System (Report I - Phase II Development Test)." AEDC-TR-65-233 (AD368743), January 1966.
8. Schulz, G. H. and DeFord, J. F. "Simulated Altitude Testing of the Apollo Service Module Propulsion System (Report II - Phase II Development Test)." AEDC-TR-66-17 (AD369807), February 1966.
9. Gall, E. S., McIlveen, M. W., and Berg, A. L. "Qualification Testing of the Block I Apollo AJ10-137 Service Module Engine." AEDC-TR-66-129, August 1966.
10. Pelton, J. M. and McIlveen, M. W. "Block II AJ10-137 Apollo Service Module Engine Testing at Simulated High Altitude (Report I - Phase IV Development)." AEDC-TR-66-169, November 1966.

11. DeFord, J. F., McIlveen, M. W., and Berg, A. L. "Block II AJ10-137 Apollo Service Module Engine Testing at Simulated High Altitude (Report II - Phase IV Development)." AEDC-TR-67-47, April 1967.
12. Test Facilities Handbook (6th Edition). "Rocket Test Facility, Volume 2." Arnold Engineering Development Center, November 1966.
13. Robinson, C. E. and Runyan, R. B. "Thrust Vector Determination for the Apollo Service Module Propulsion Engine using a Six-Component Force Balance." AEDC-TR-65-250 (AD475564), December 1965.
14. AGC Specification 46652. "Cleanliness Requirements for the Apollo Service Module Engine." June 30, 1964.
15. Federal Standard No. 209. "Clean Room and Work Station Requirements, Controlled Environment." December 16, 1963.
16. AGC Specification 46848. "Altitude Qualification Test Procedure for Engine AJ10-137 (Apollo)." September 14, 1966.

APPENDIXES

- I. ILLUSTRATIONS**
- II. TABLES**
- III. PROPELLANT FLOWMETER AND WEIGH SCALE CALIBRATION**



Fig. 1 AJ10-137 Rocket Engine Assembly S/N 54B

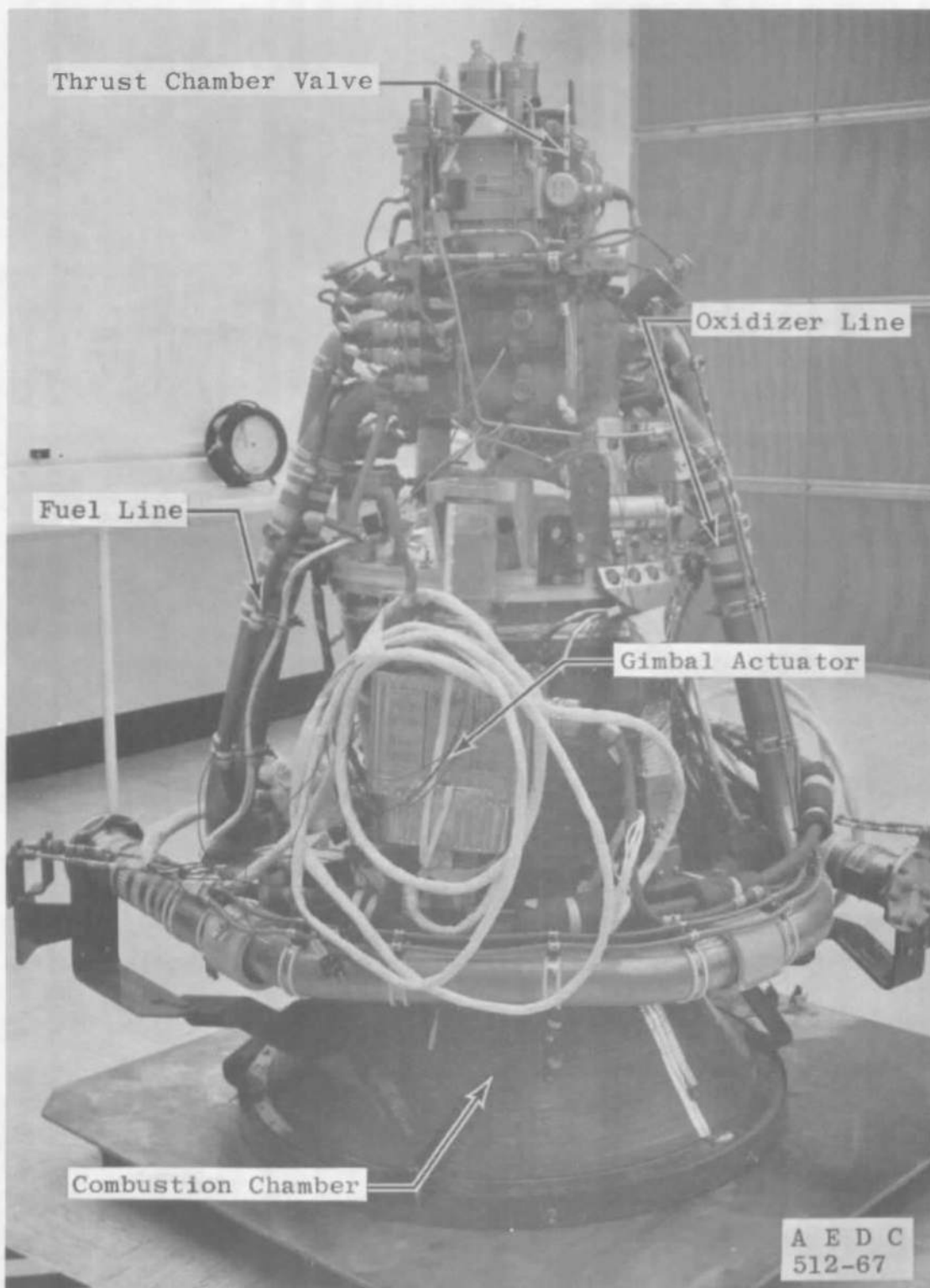
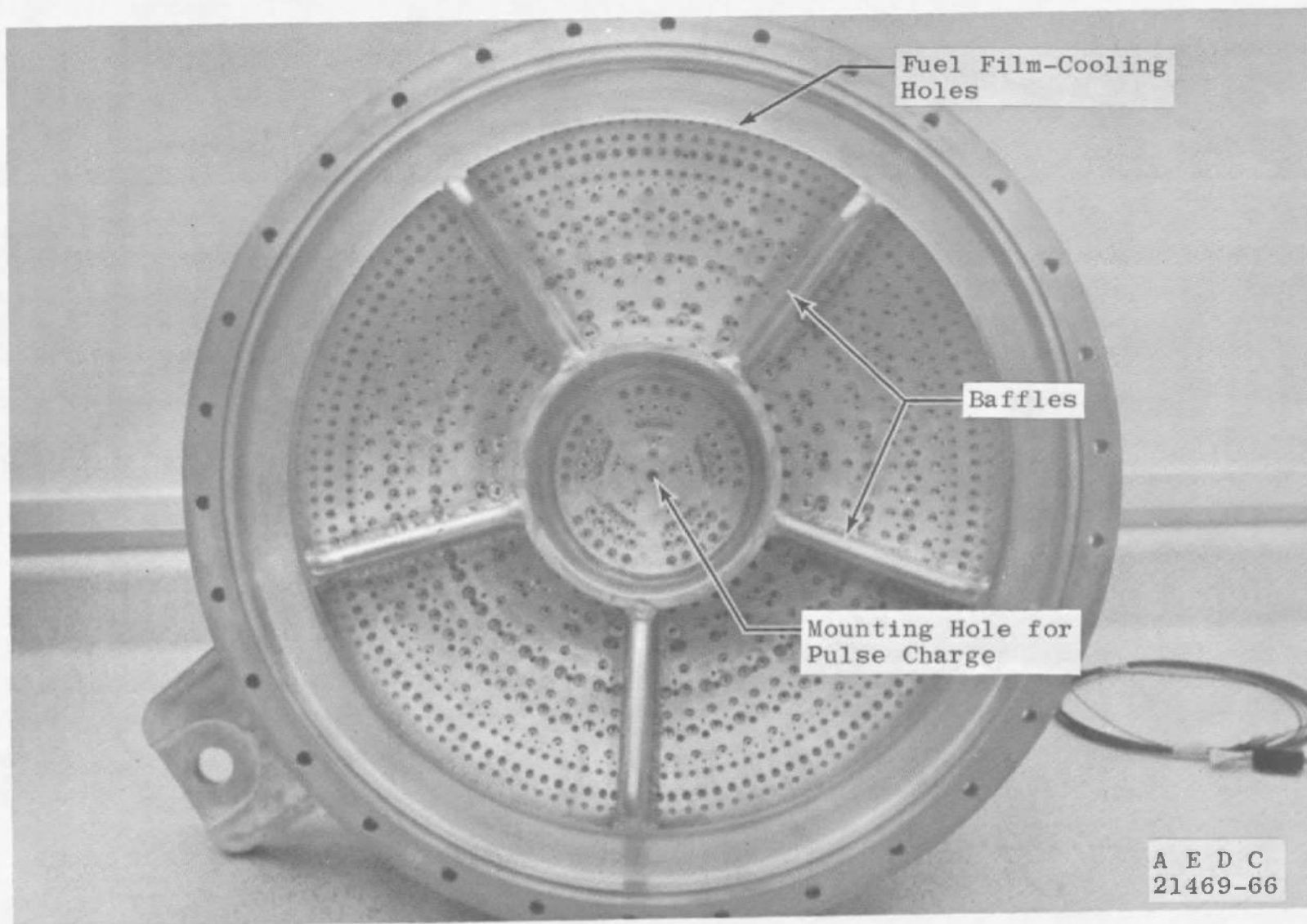


Fig. 2 AJ10-137 Rocket Engine S/N 55 without Nozzle



a. View of Injector Face

Fig. 3 Injector S/N 104



b. Close-up Showing Baffle Configuration and Orifice Counterboring

Fig. 3 Concluded

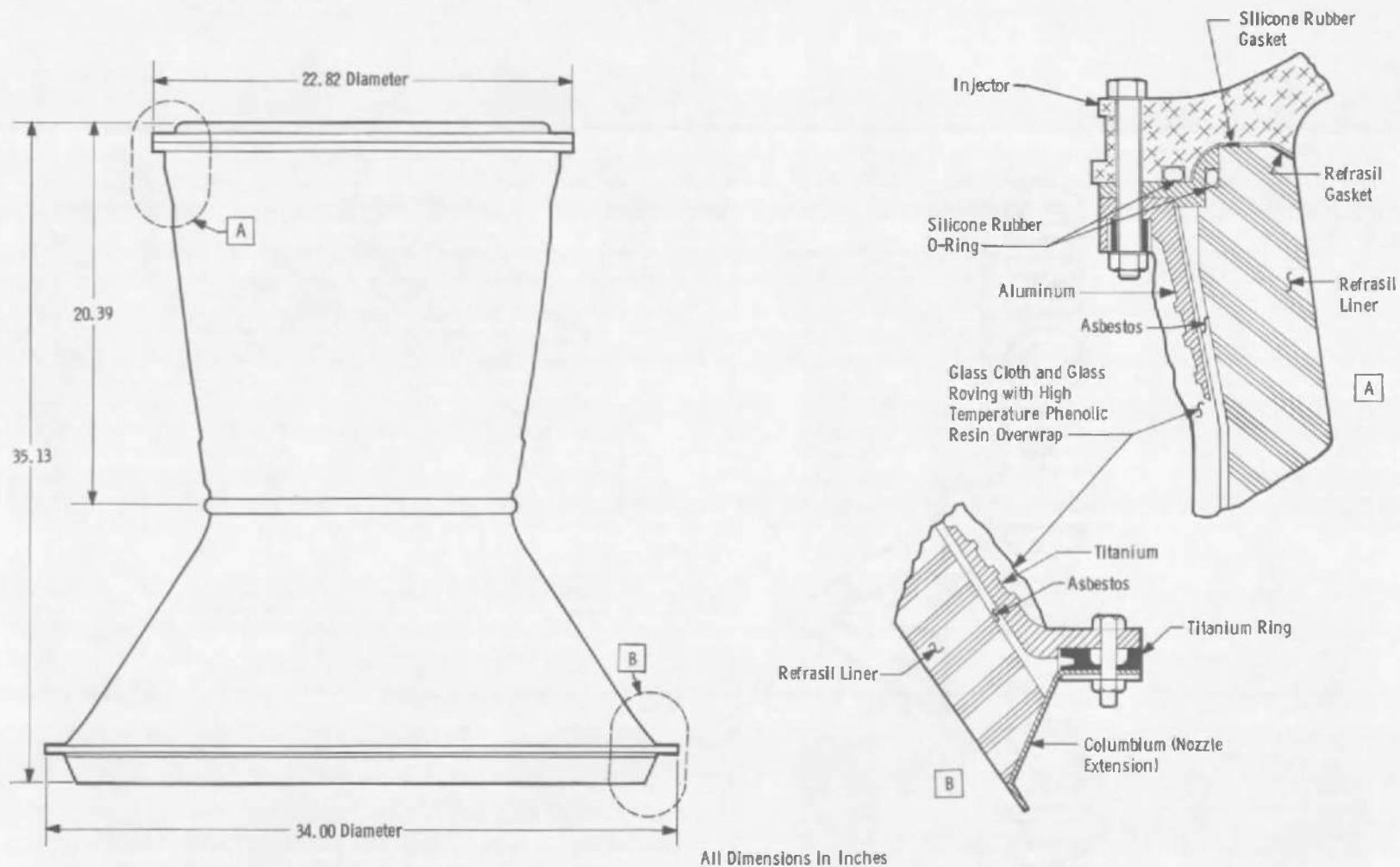
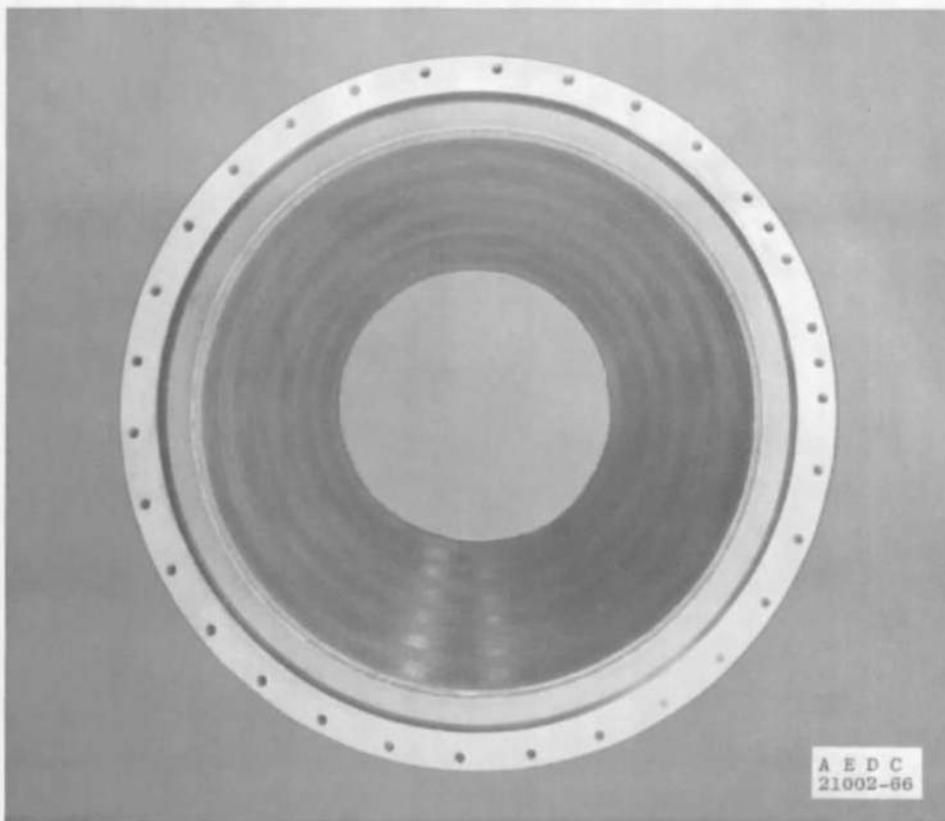


Fig. 4 Ablative Thrust Chamber and Flange Details



a. Side View



b. View from Injector Mounting Flange
Fig. 5 Ablative Thrust Chamber S/N 313

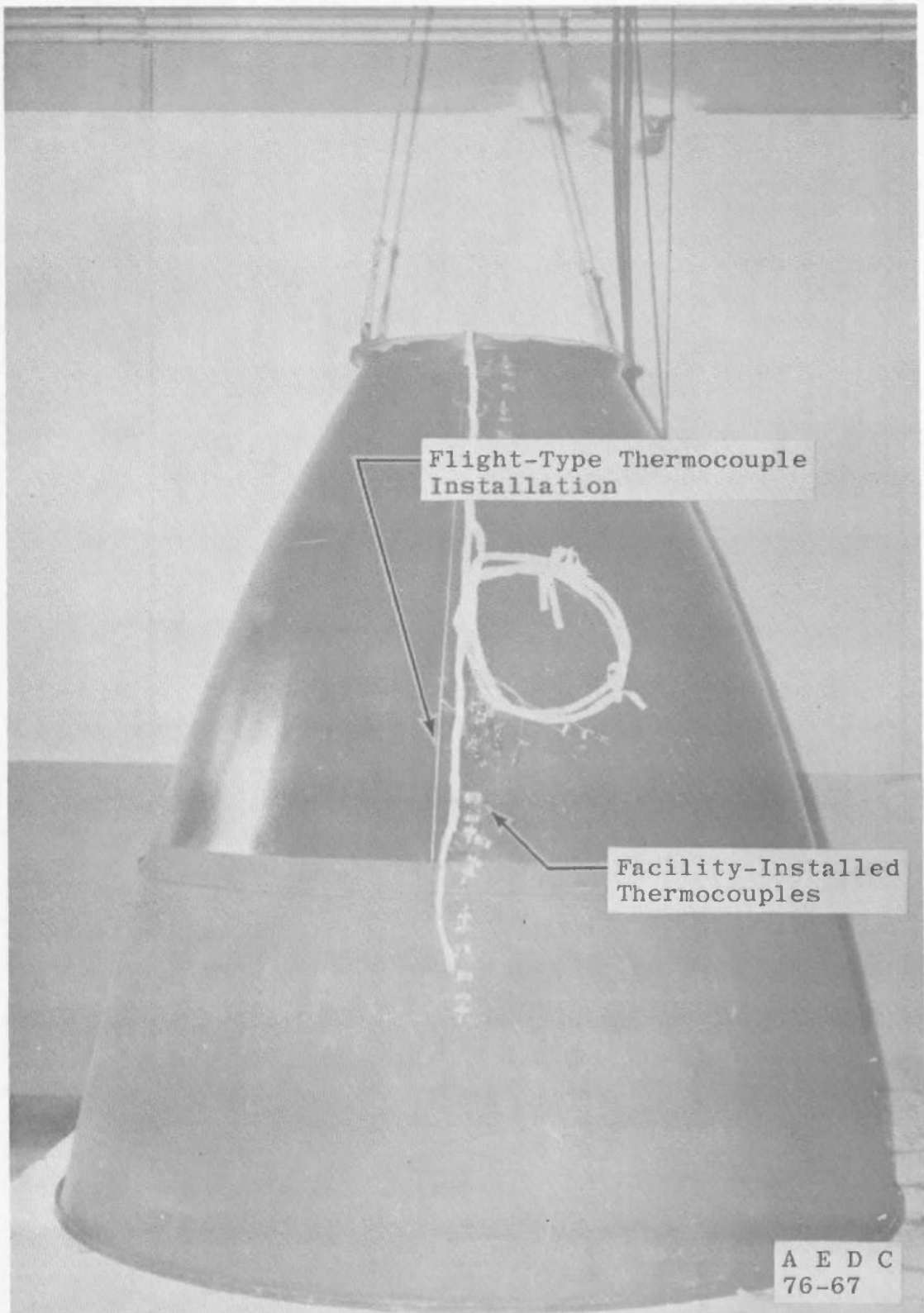


Fig. 6 Nozzle Extension S/N 54

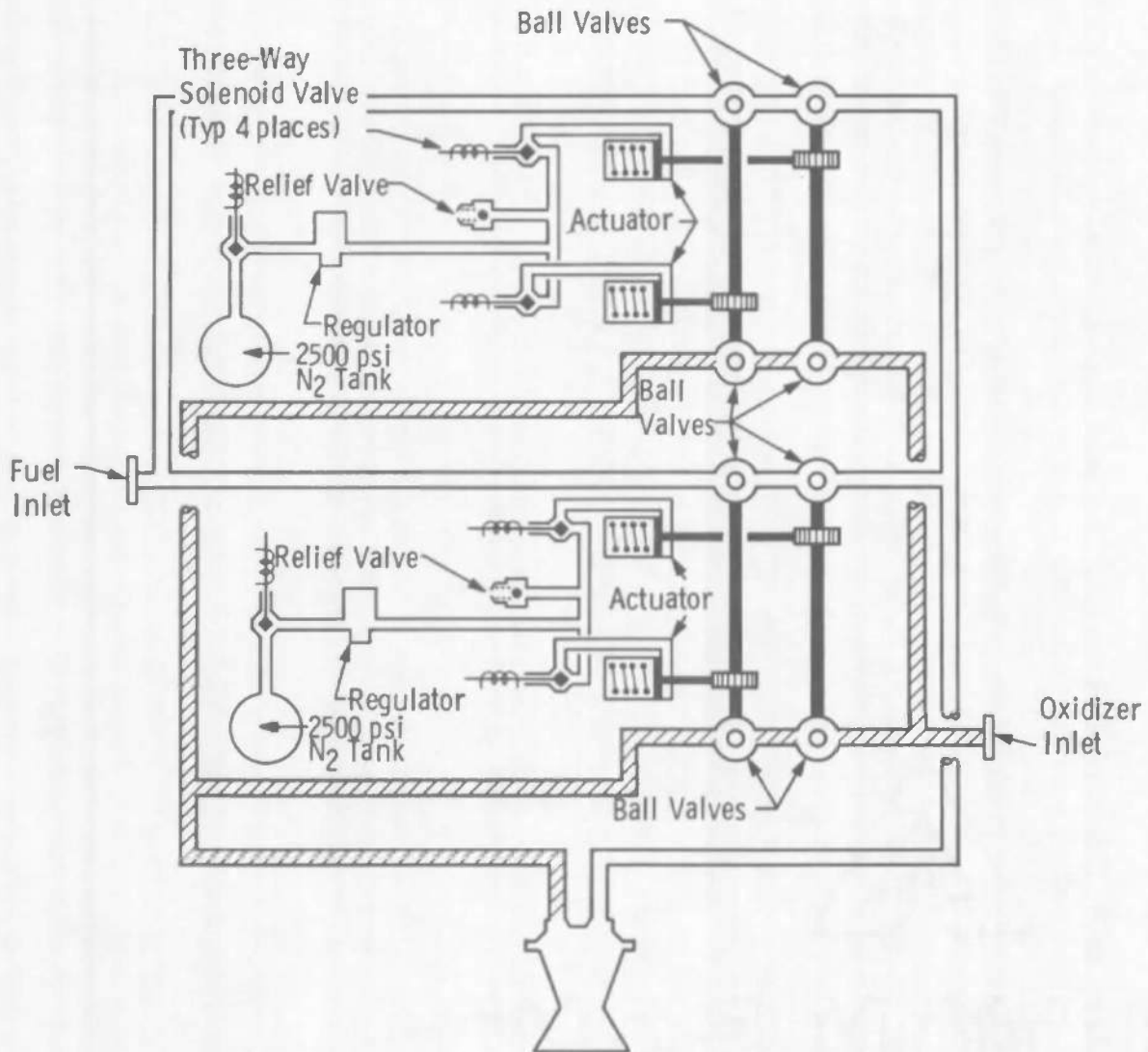


Fig. 7 Schematic of Thrust Chamber Valve

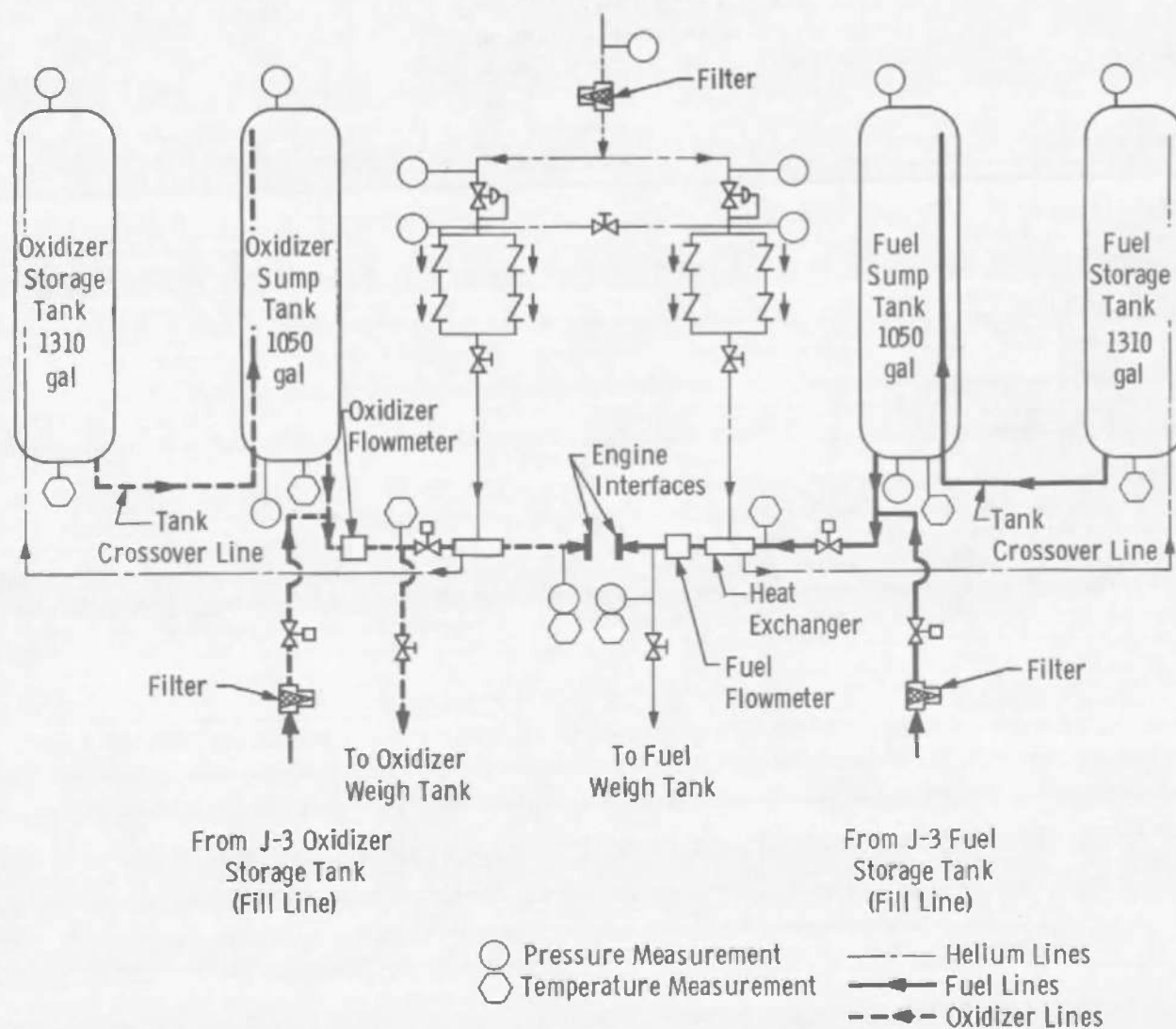
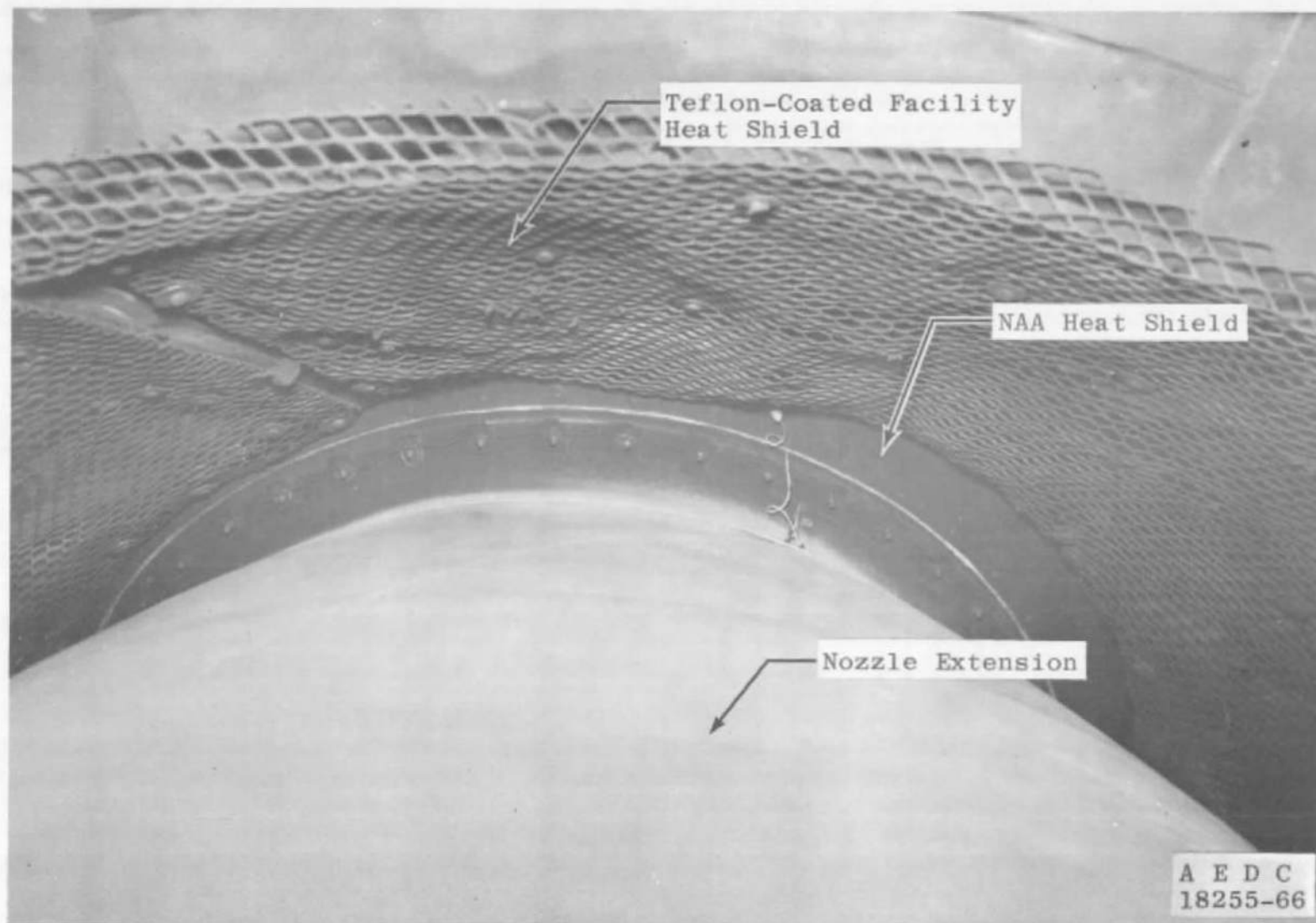
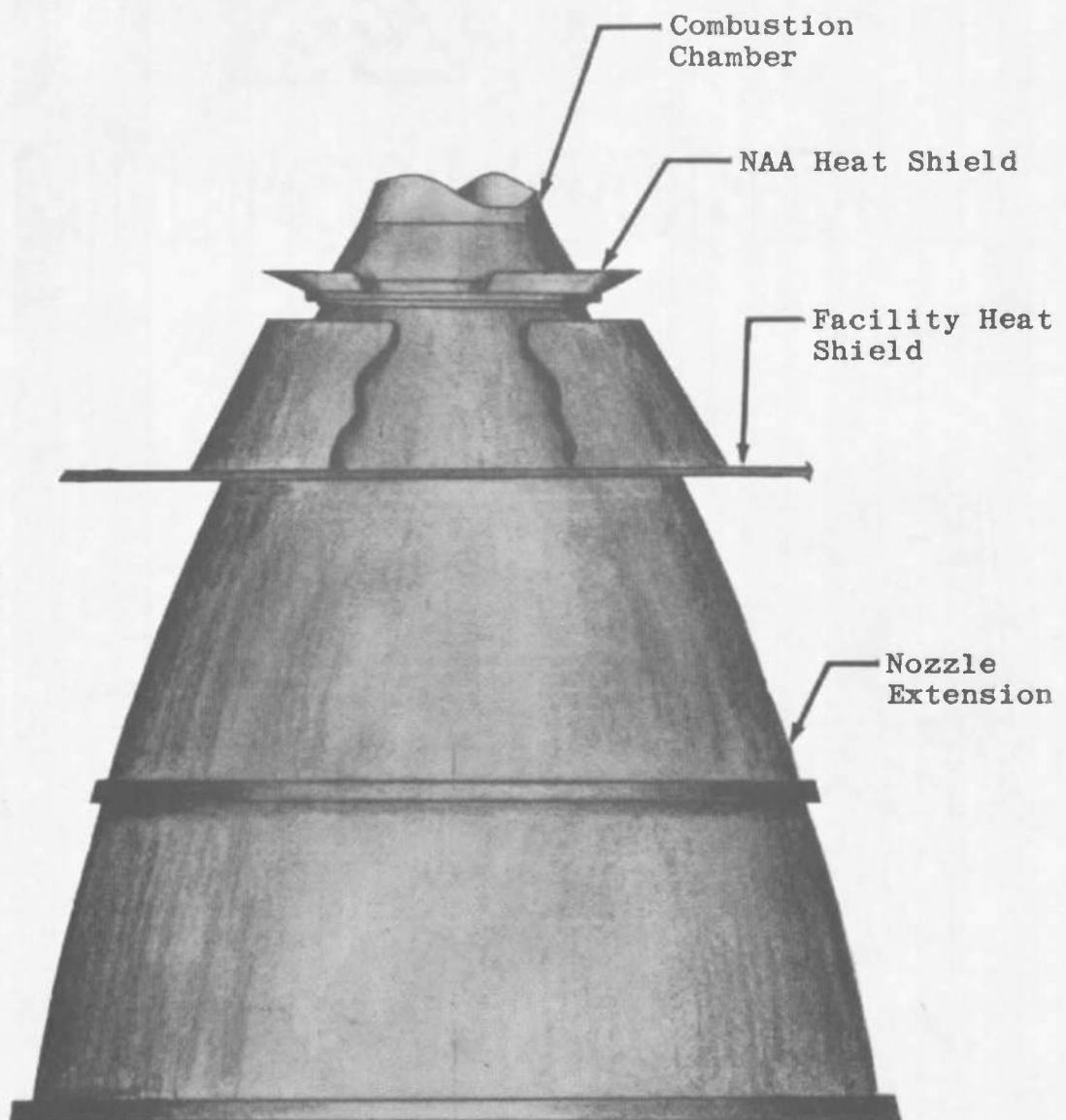


Fig. 8 Schematic of F-3 Fixture



a. Photograph of Installation
Fig. 9 Facility and NAA Heat Shields



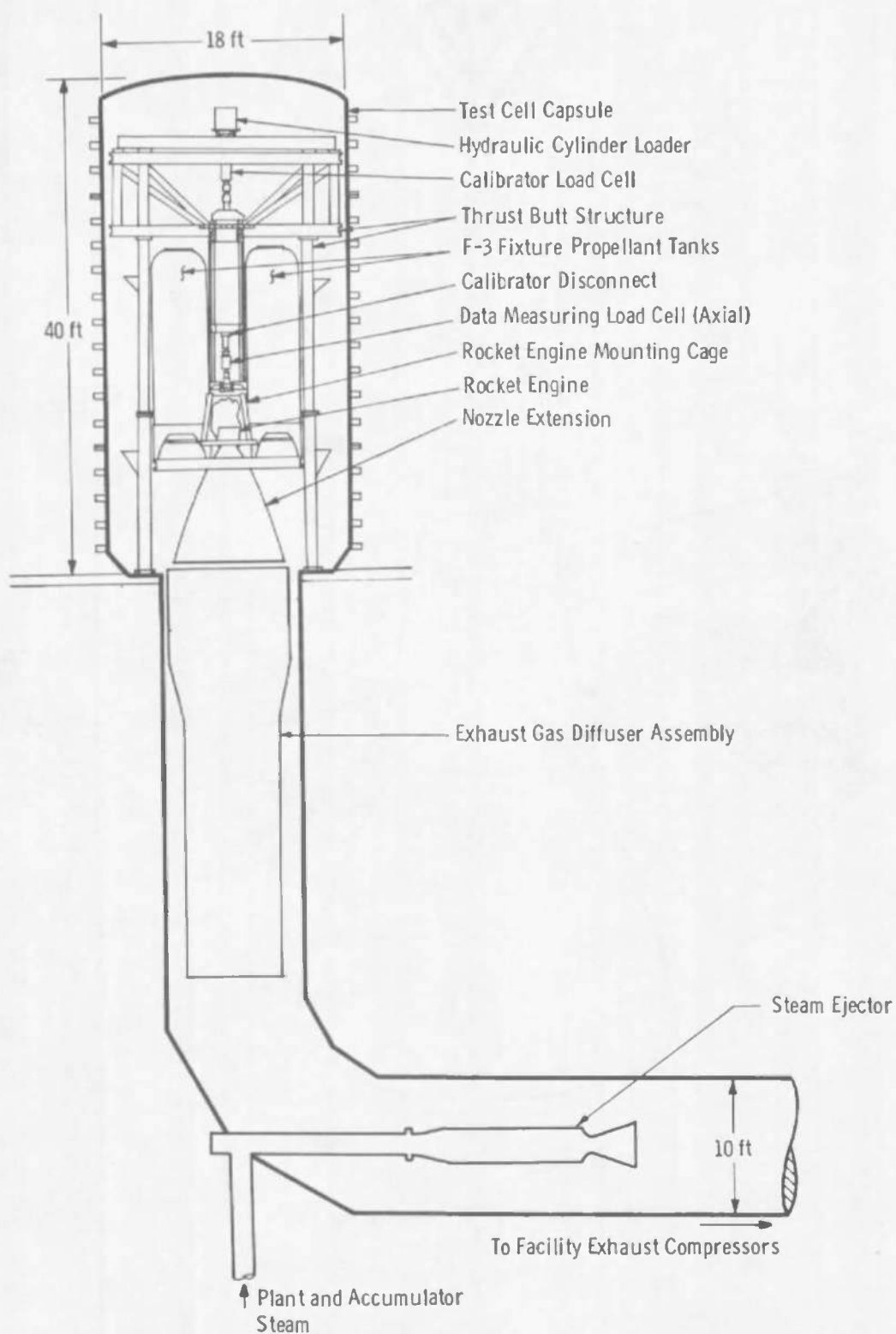
b. Artist's Sketch of Installation

Fig. 9 Concluded



a. Complex

Fig. 10 Test Cell J-3



b. Schematic

Fig. 10 Concluded

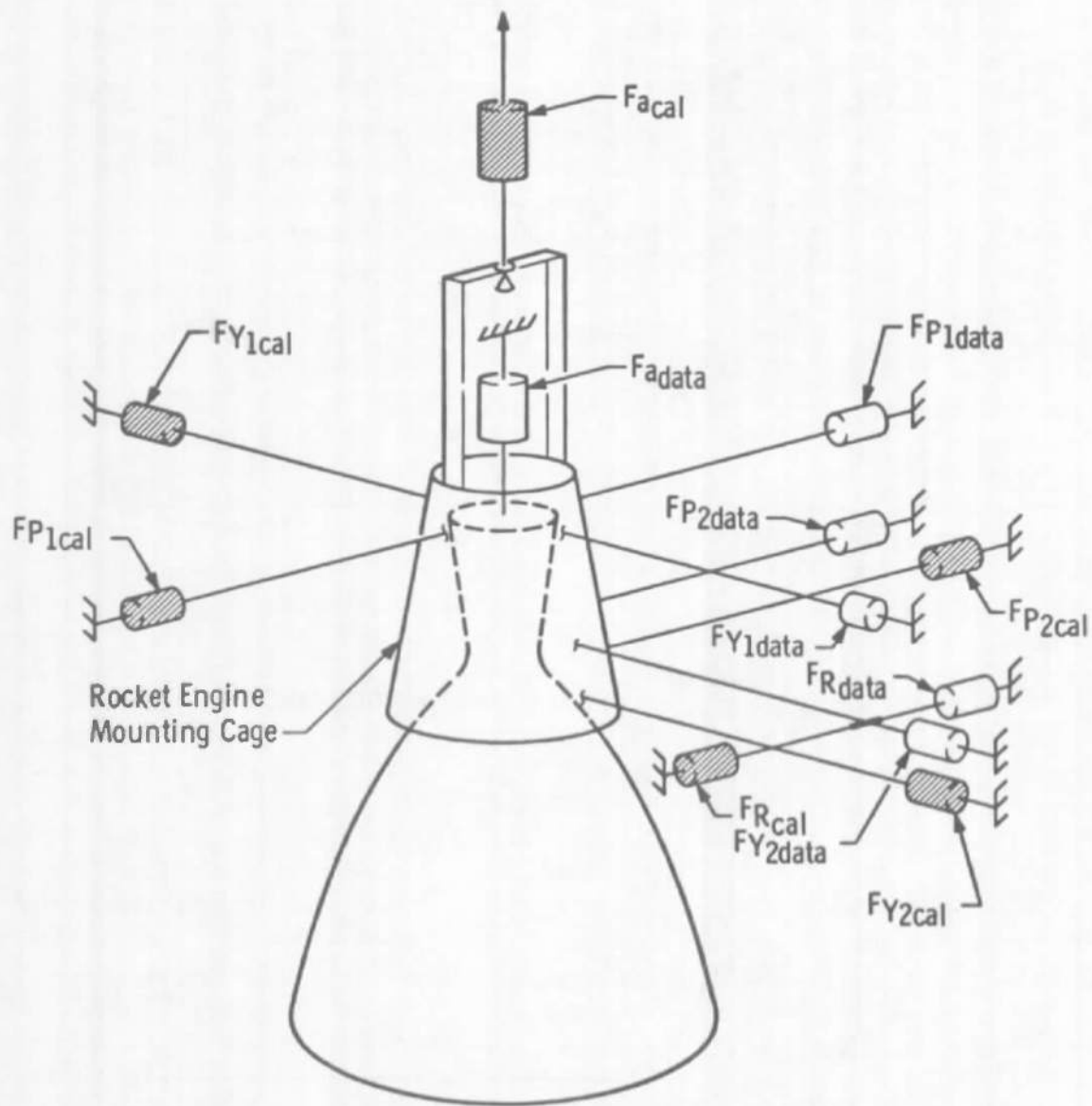


Fig. 11 Schematic of Six-Component Force System

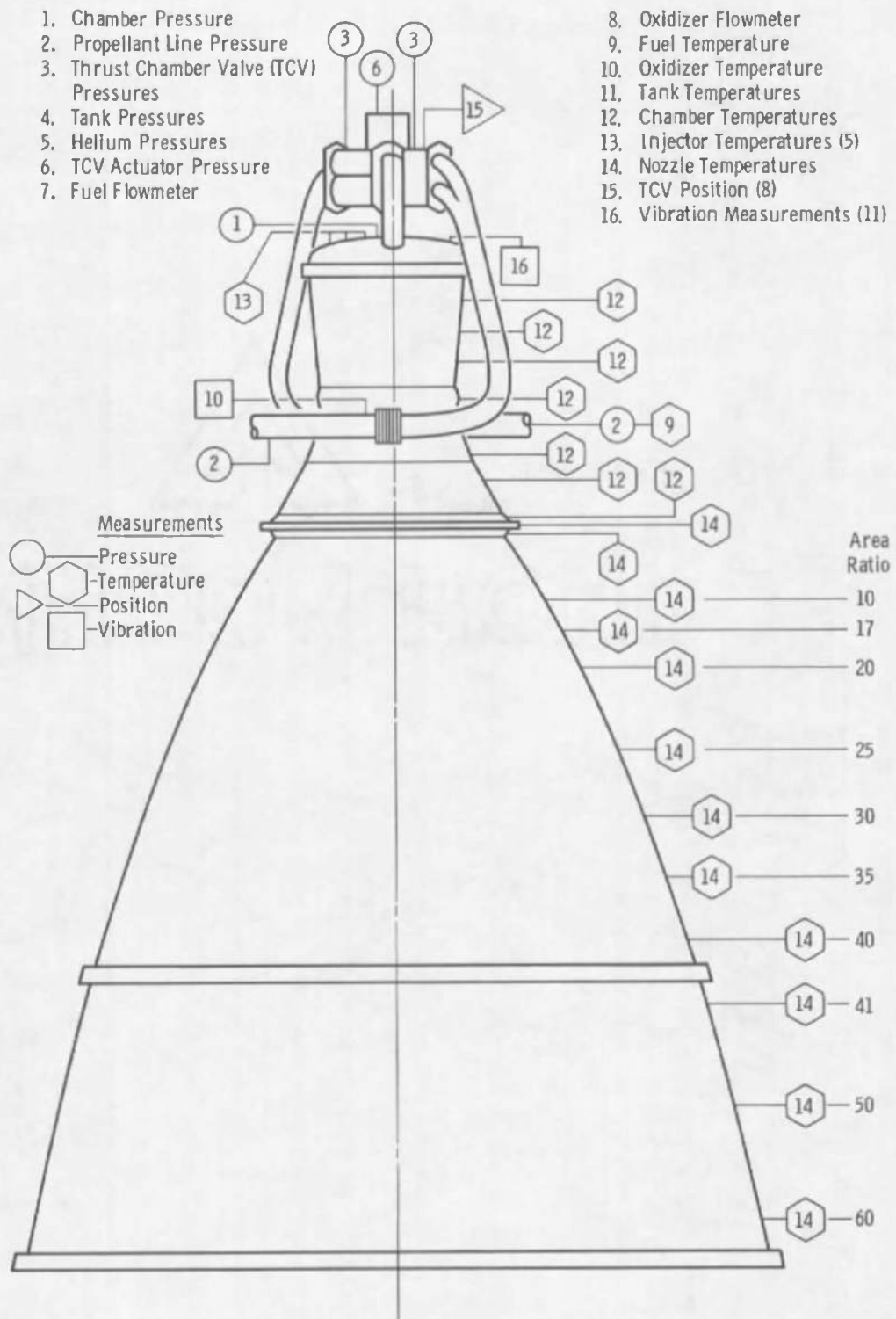


Fig. 12 Engine and Nozzle Extension Instrumentation Location

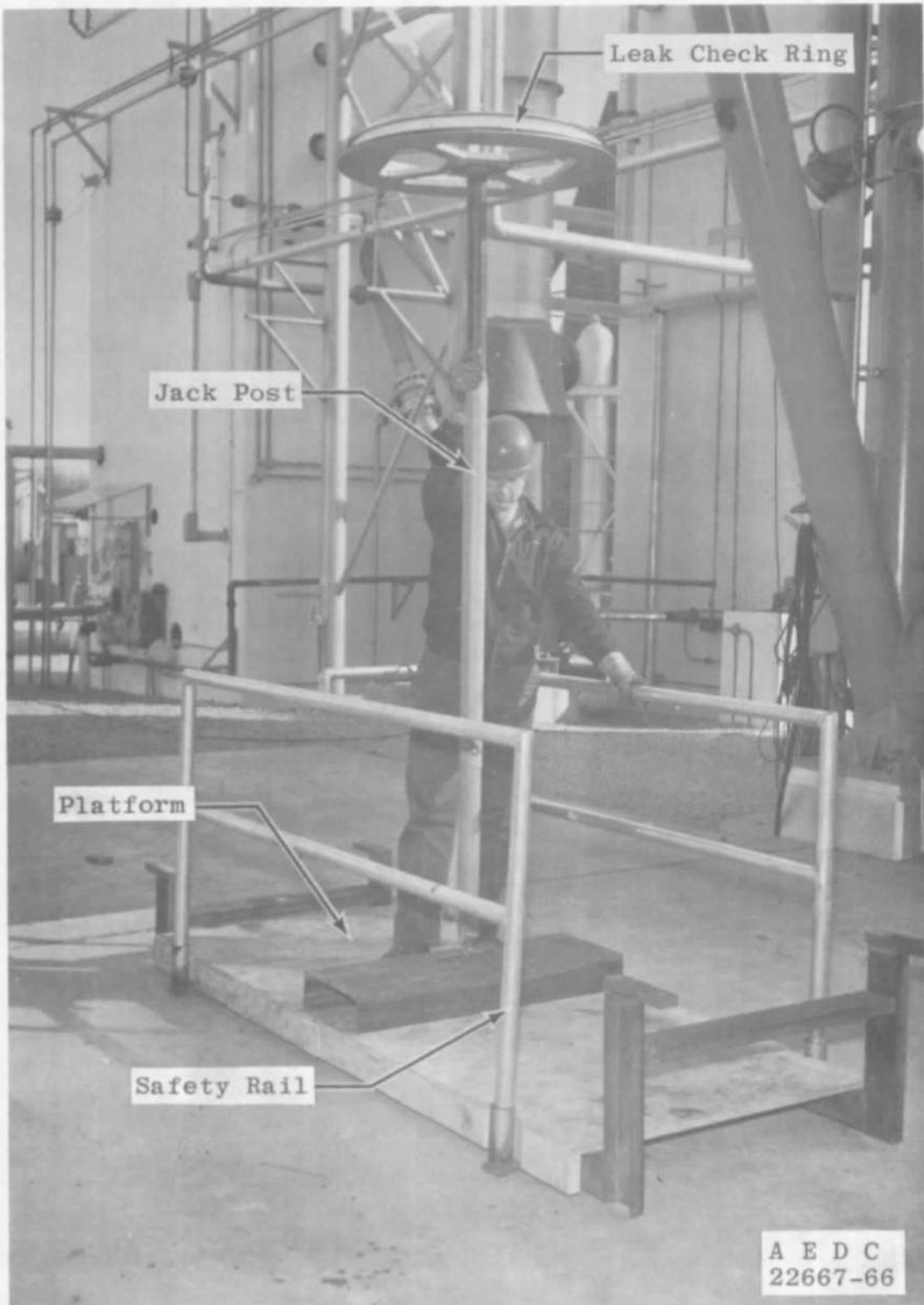


Fig. 13 In-Cell Nozzle Extension-Chamber Flange Joint Leak Check Fixture

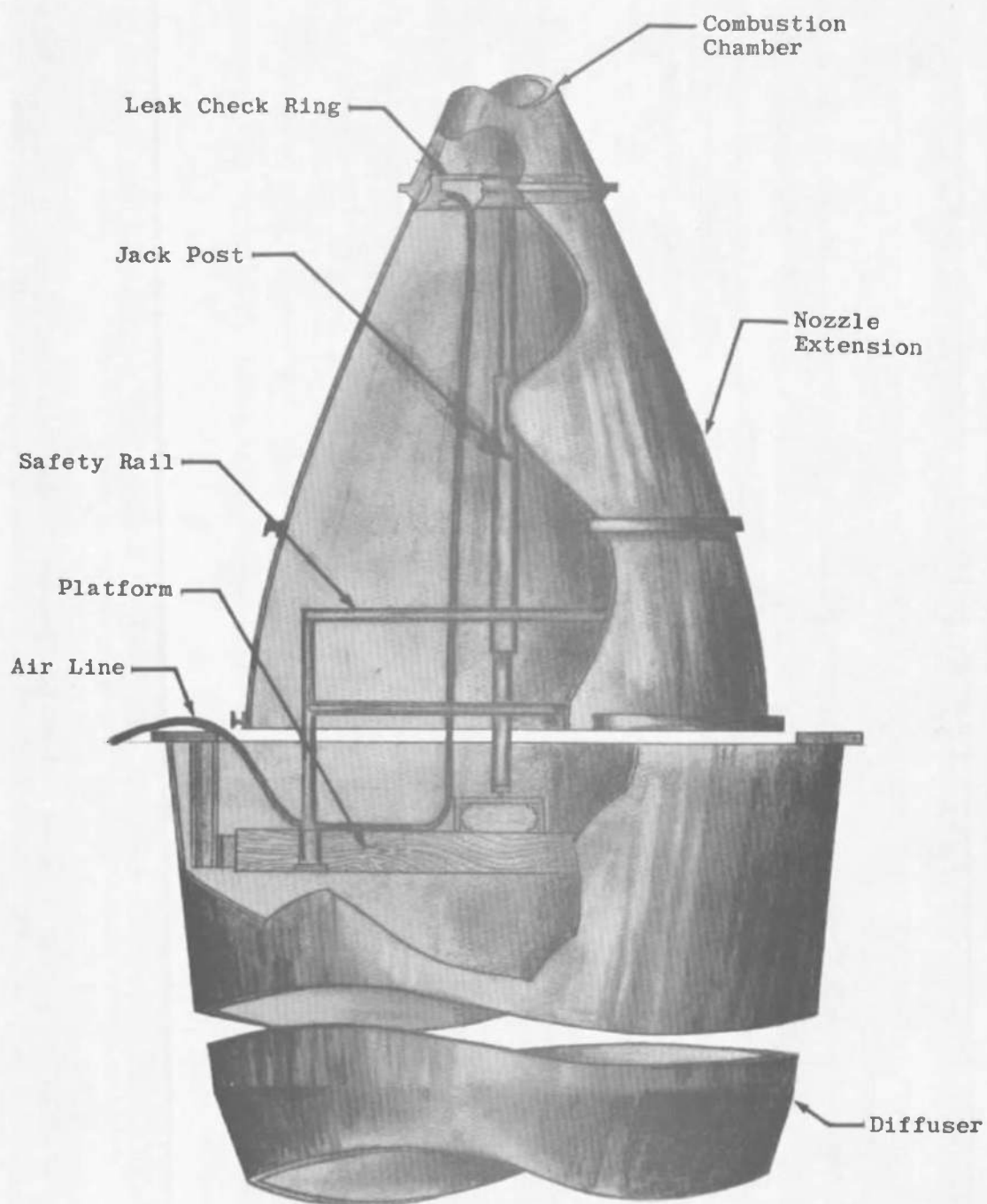


Fig. 14 Artist's Sketch of Leak Check Fixture Installed in Test Cell

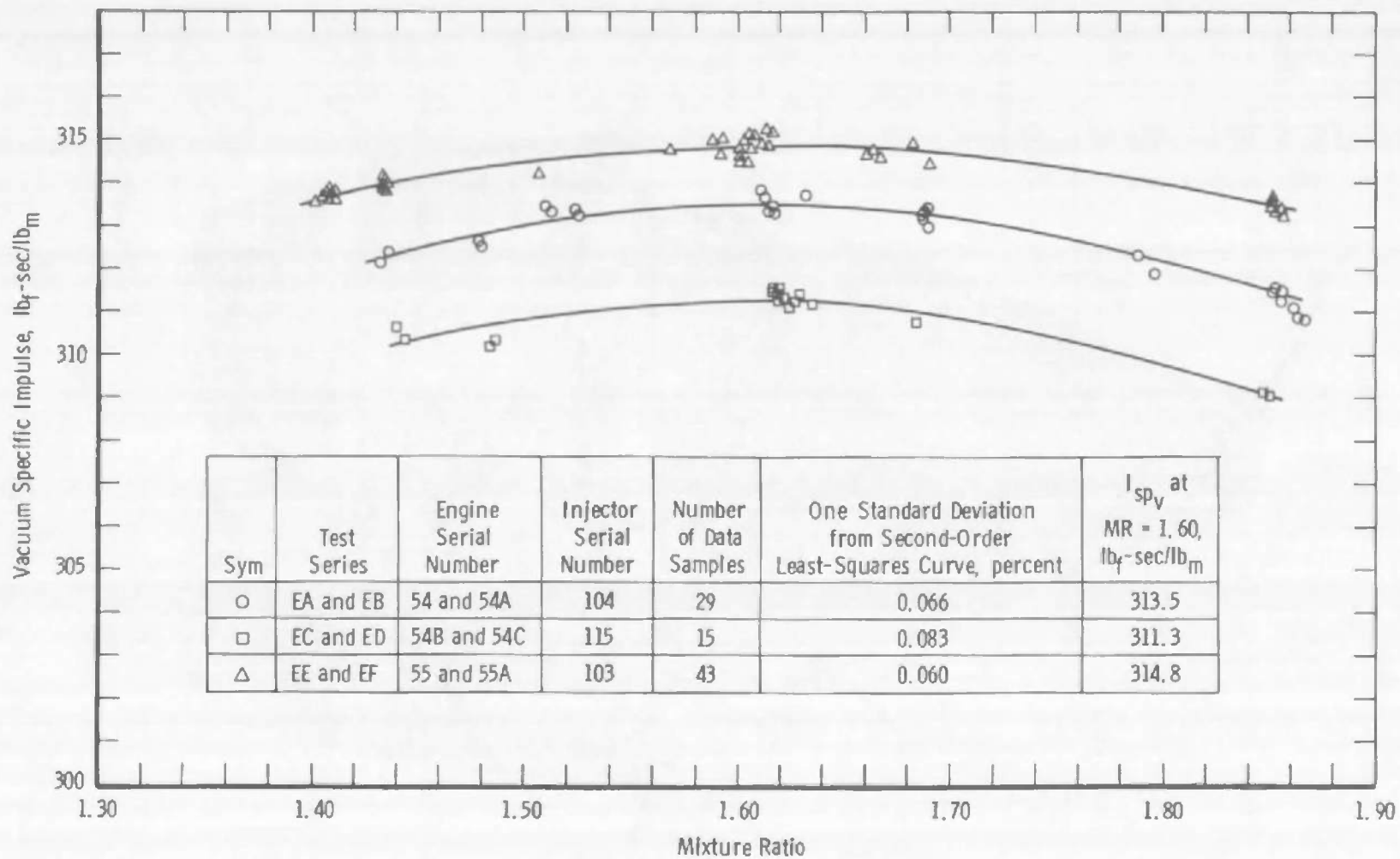


Fig. 15 Engine Performance at Nominal Chamber Pressure

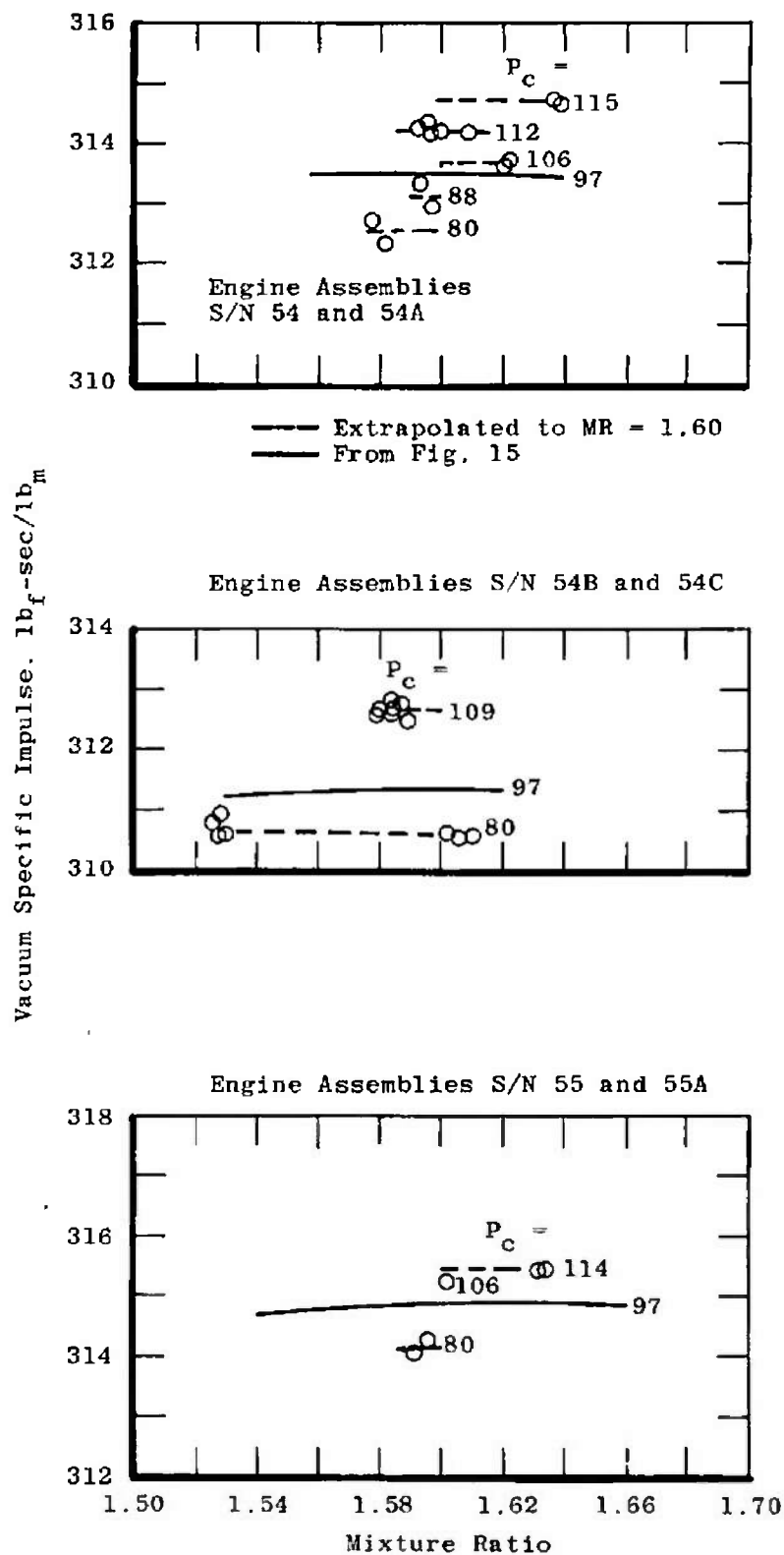


Fig. 16 Effects of Off-Design Chamber Pressure on Engine Performance

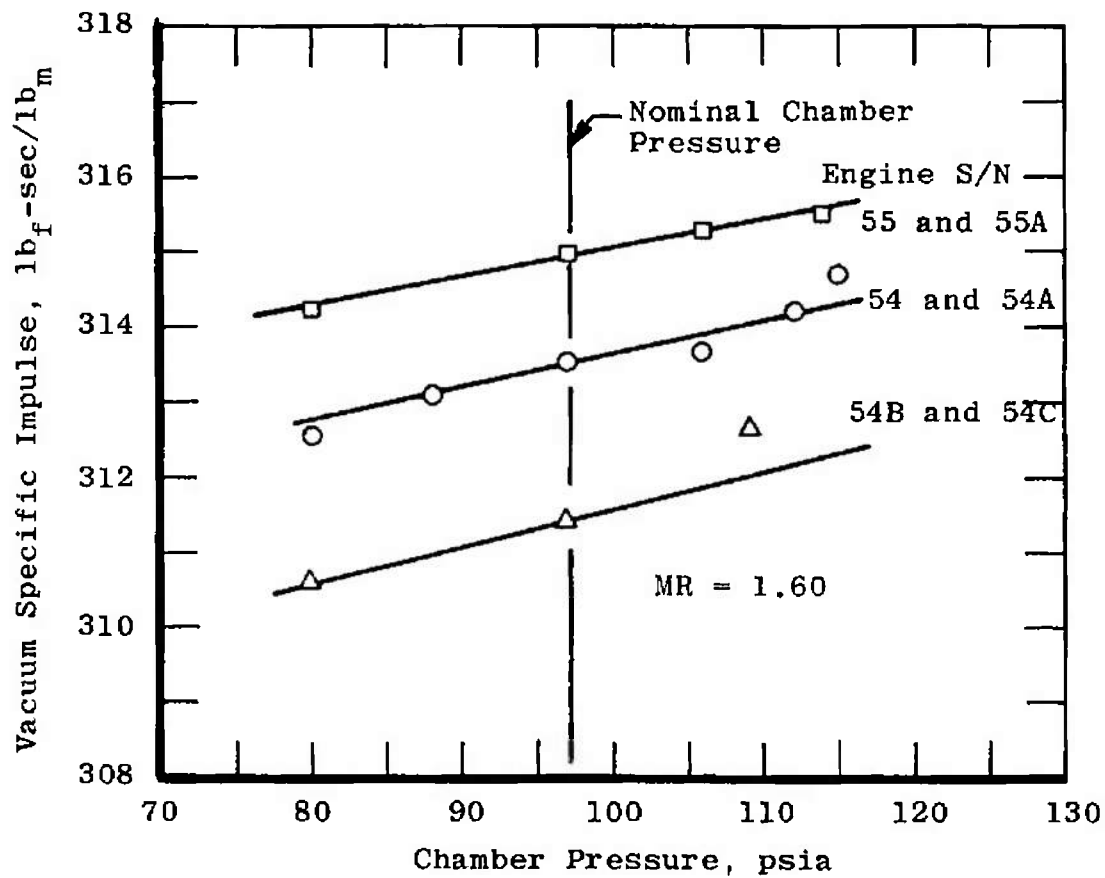


Fig. 17 Vacuum Specific Impulse-Chamber Pressure Relationship at Nominal Mixture Ratio

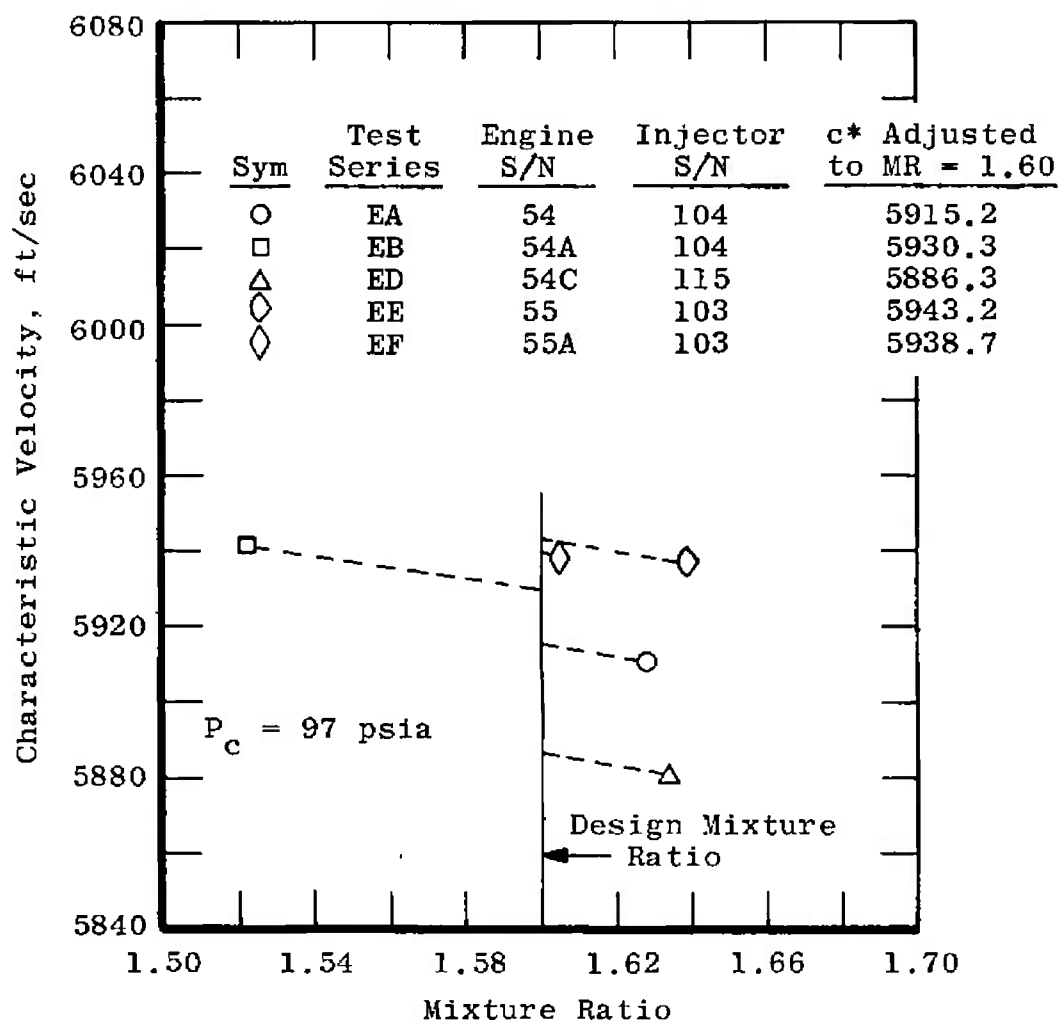
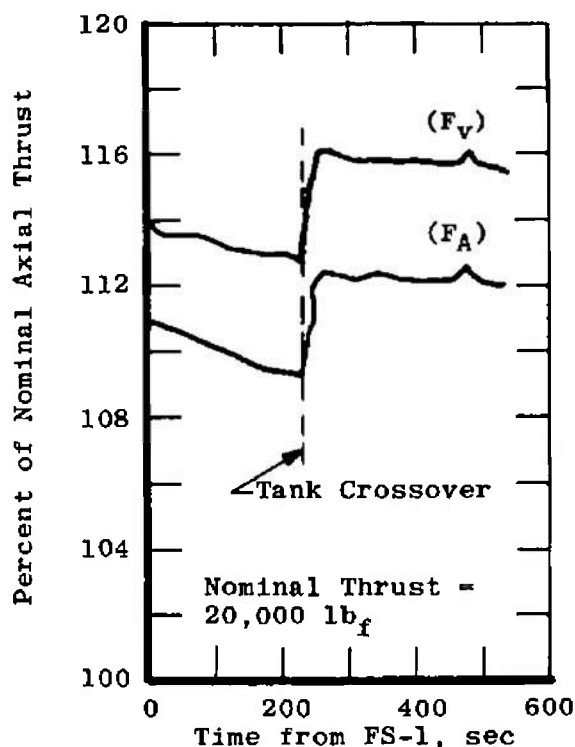
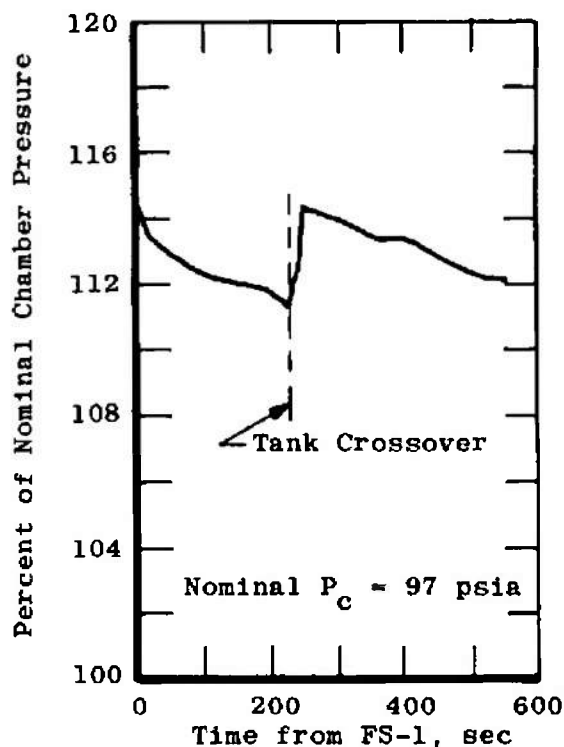


Fig. 18 Characteristic Velocity-Mixture Ratio Relationship

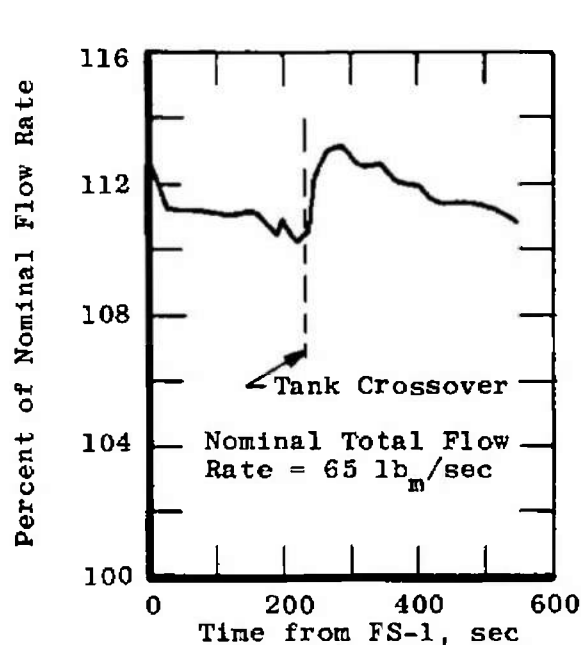
Test No. EC-06



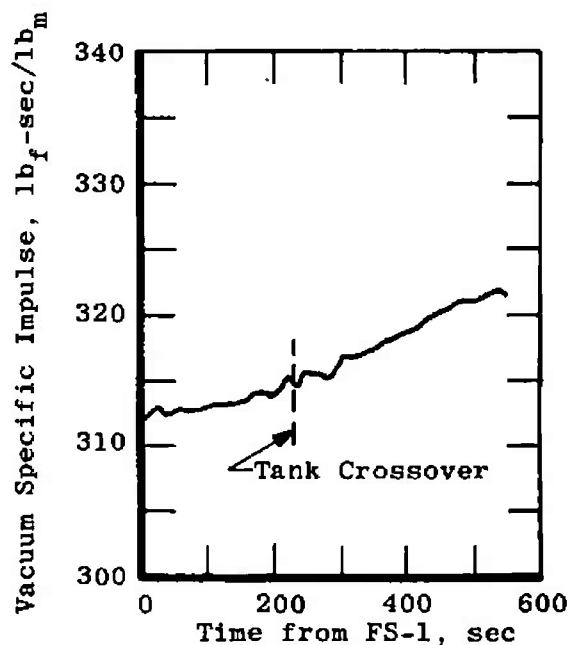
a. Axial Thrust



b. Chamber Pressure



c. Total Flow Rate



d. Vacuum Specific Impulse

Fig. 19 Effects of Axial Thrust Shift on Measured Engine Performance

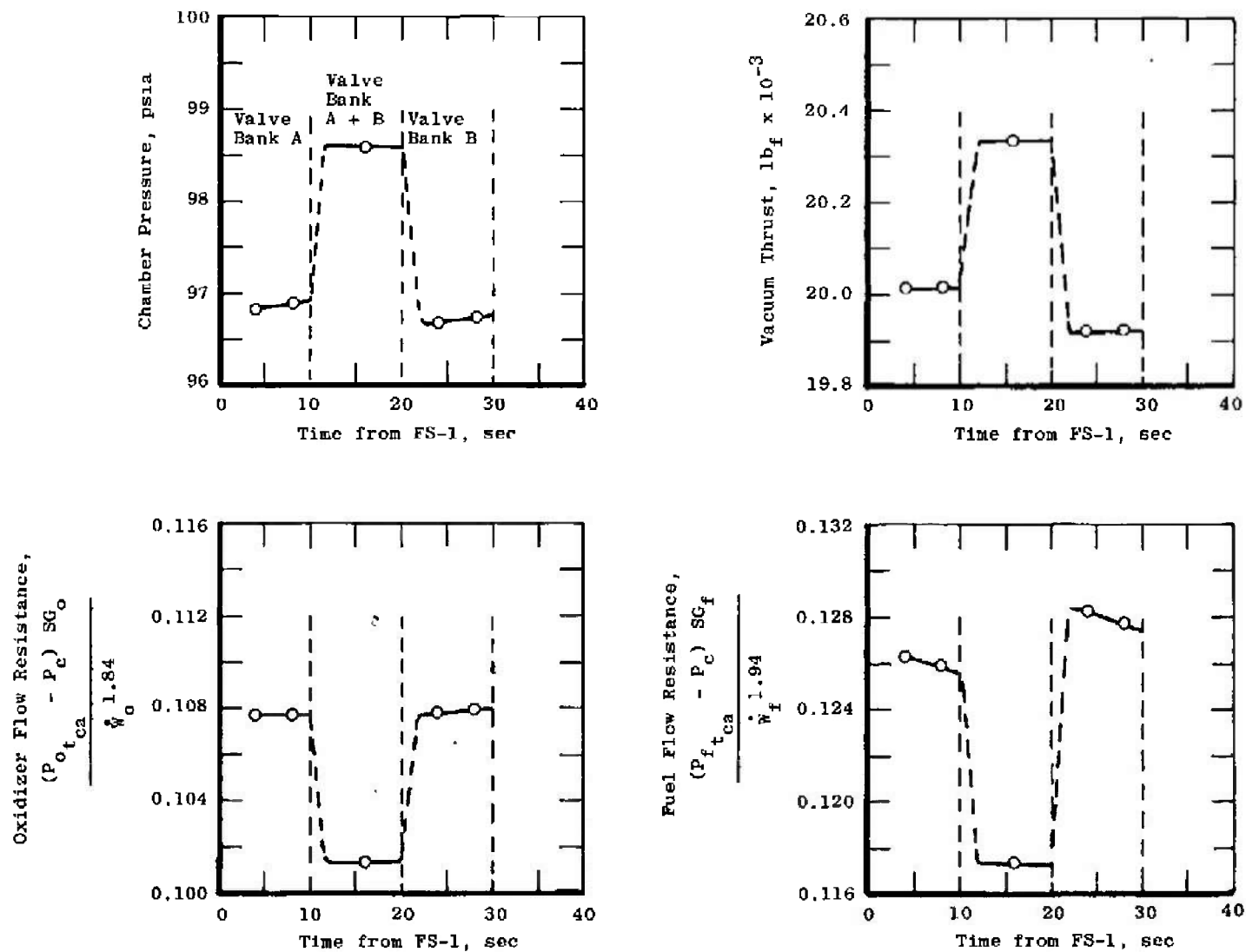


Fig. 20 Effect of Valve Bank Selections on Engine Operation

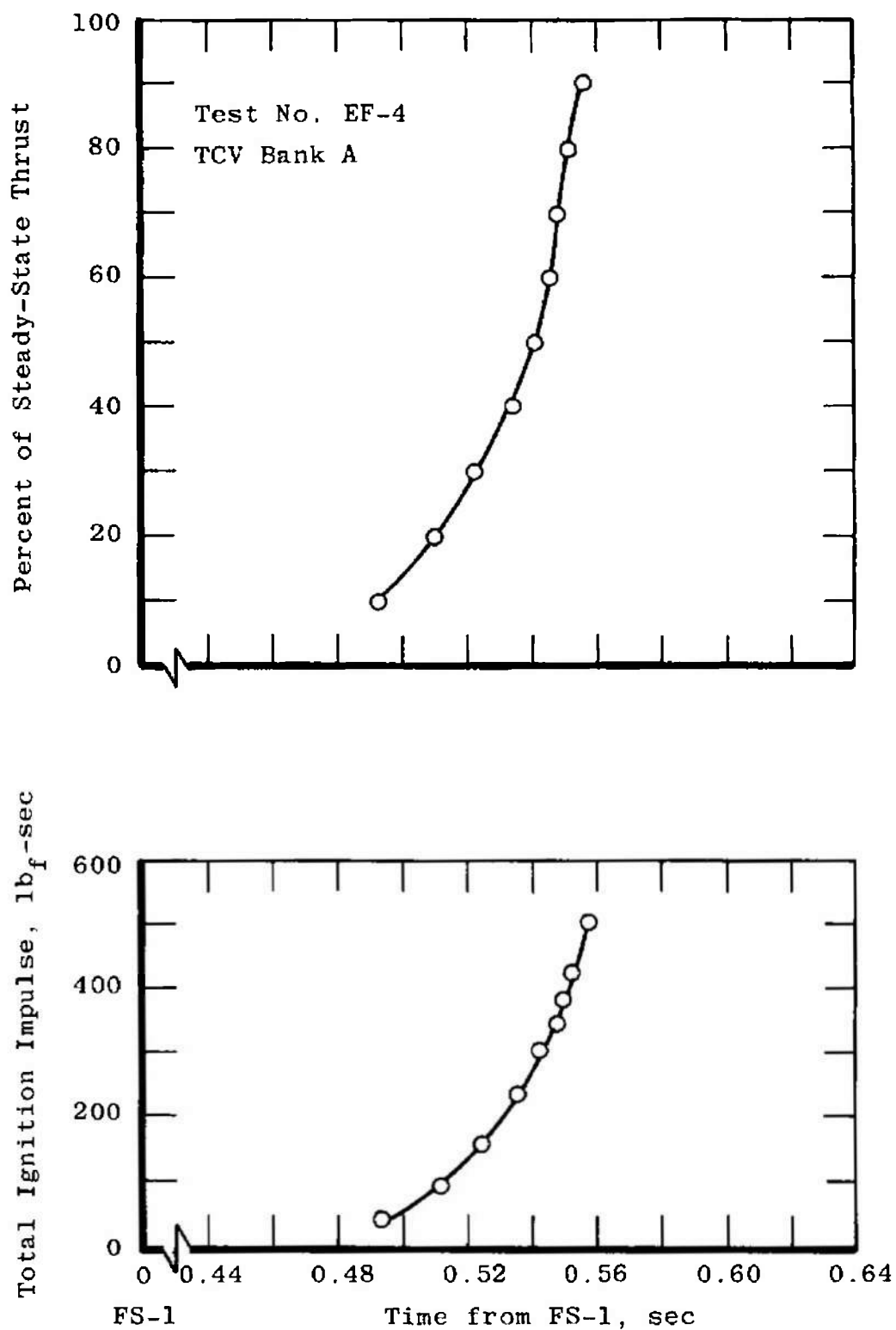


Fig. 21 Typical Ignition Transient

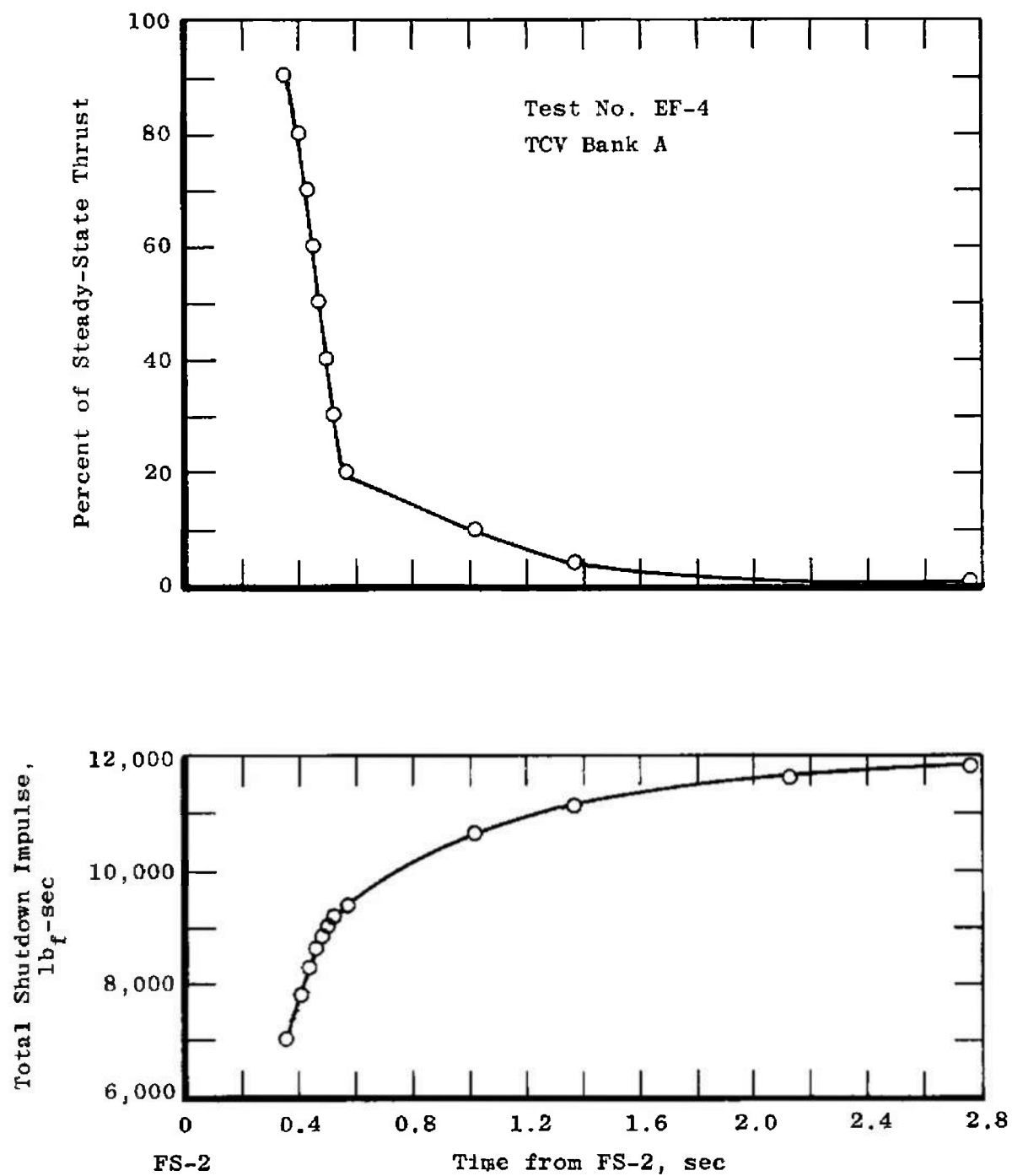


Fig. 22 Typical Shutdown Transient

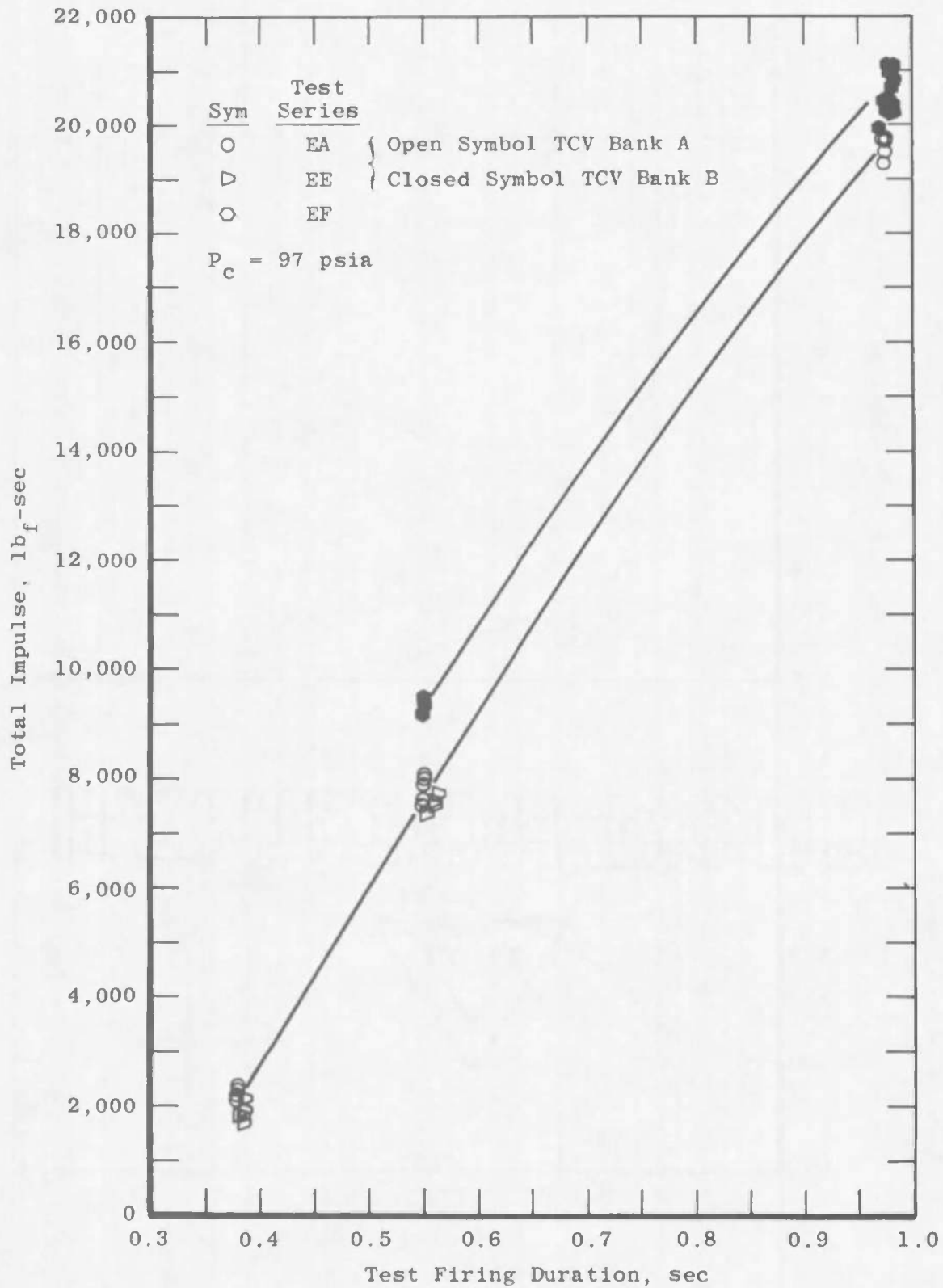


Fig. 23 Total Impulse Developed during Impulse Bit Firings

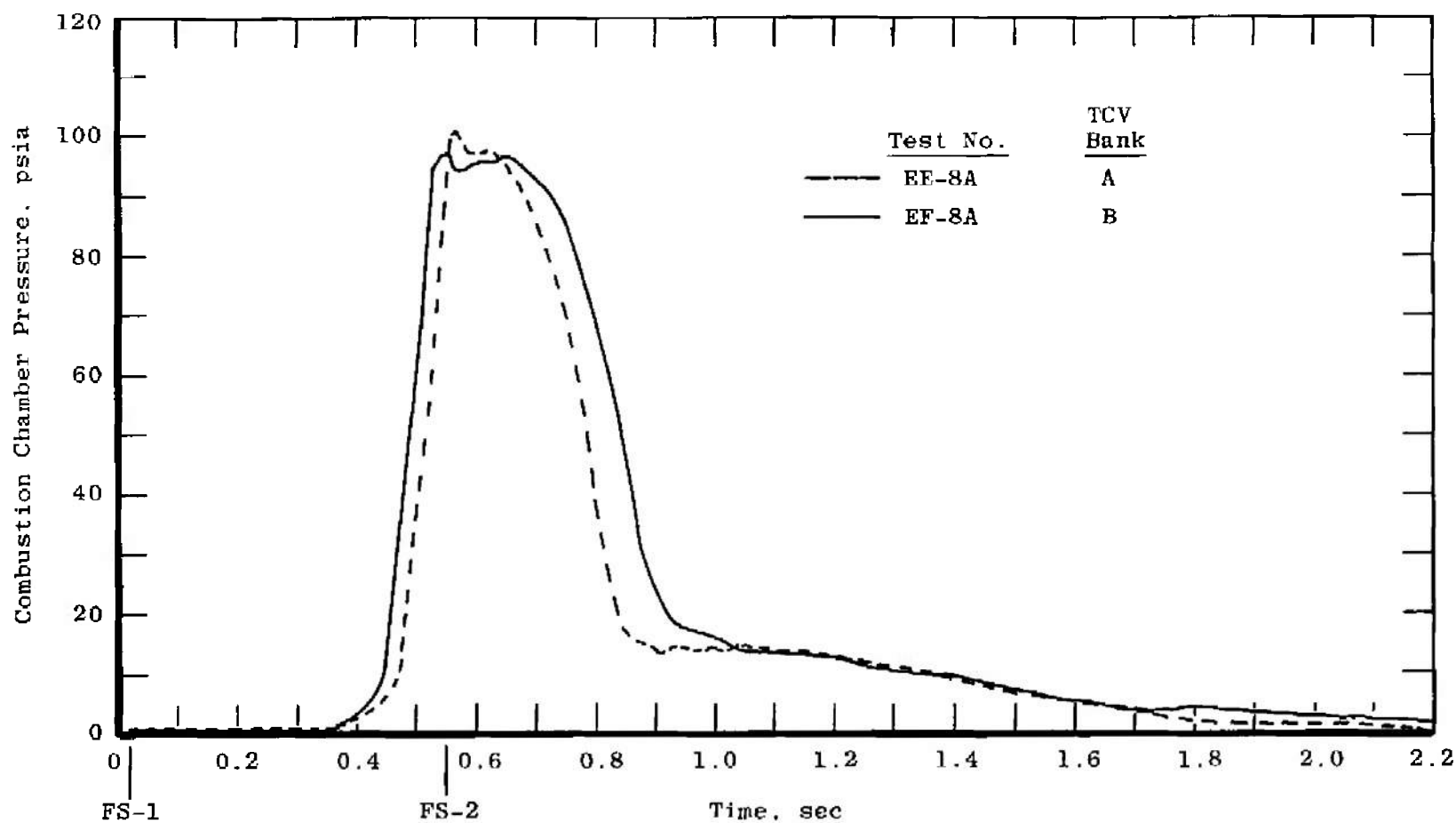
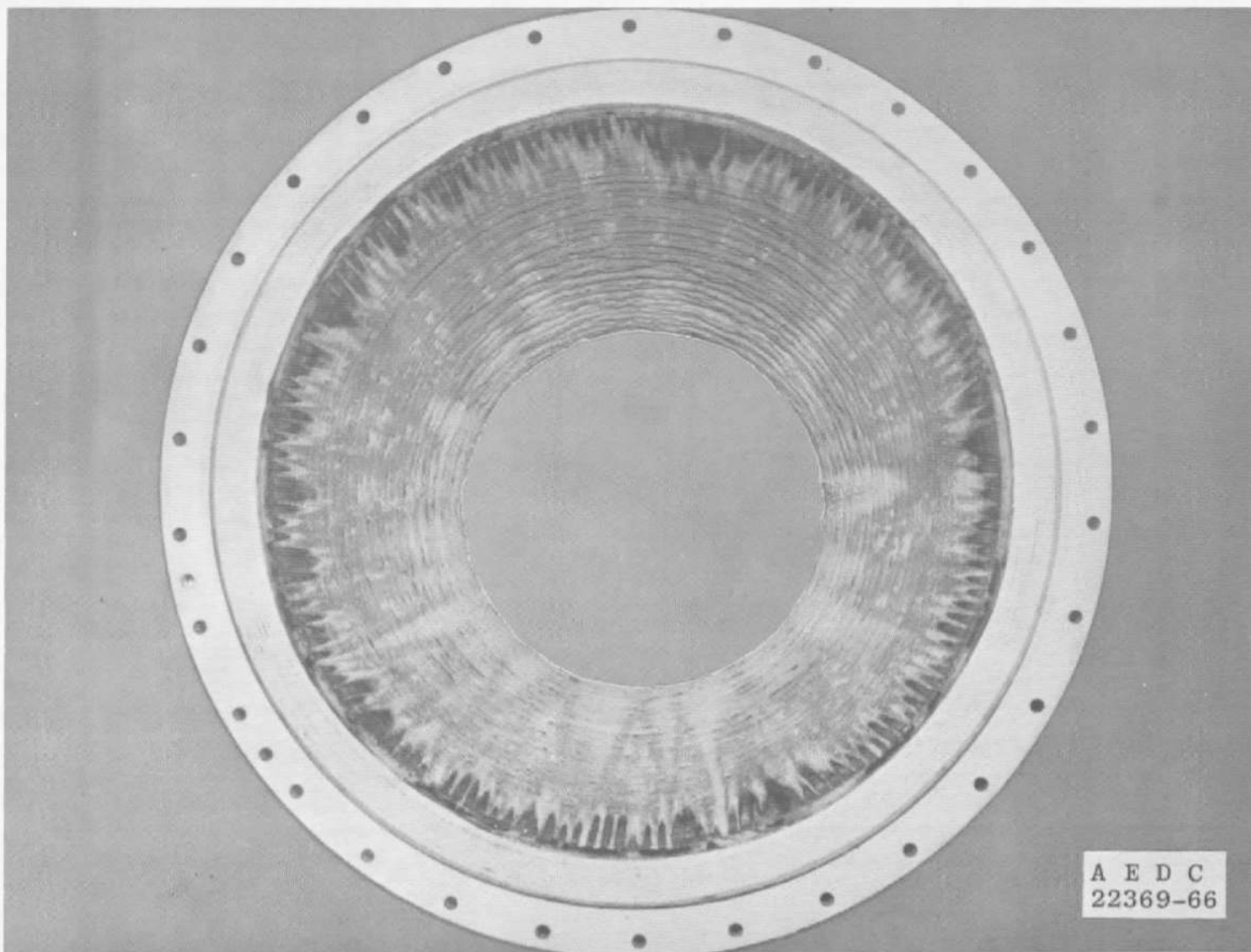
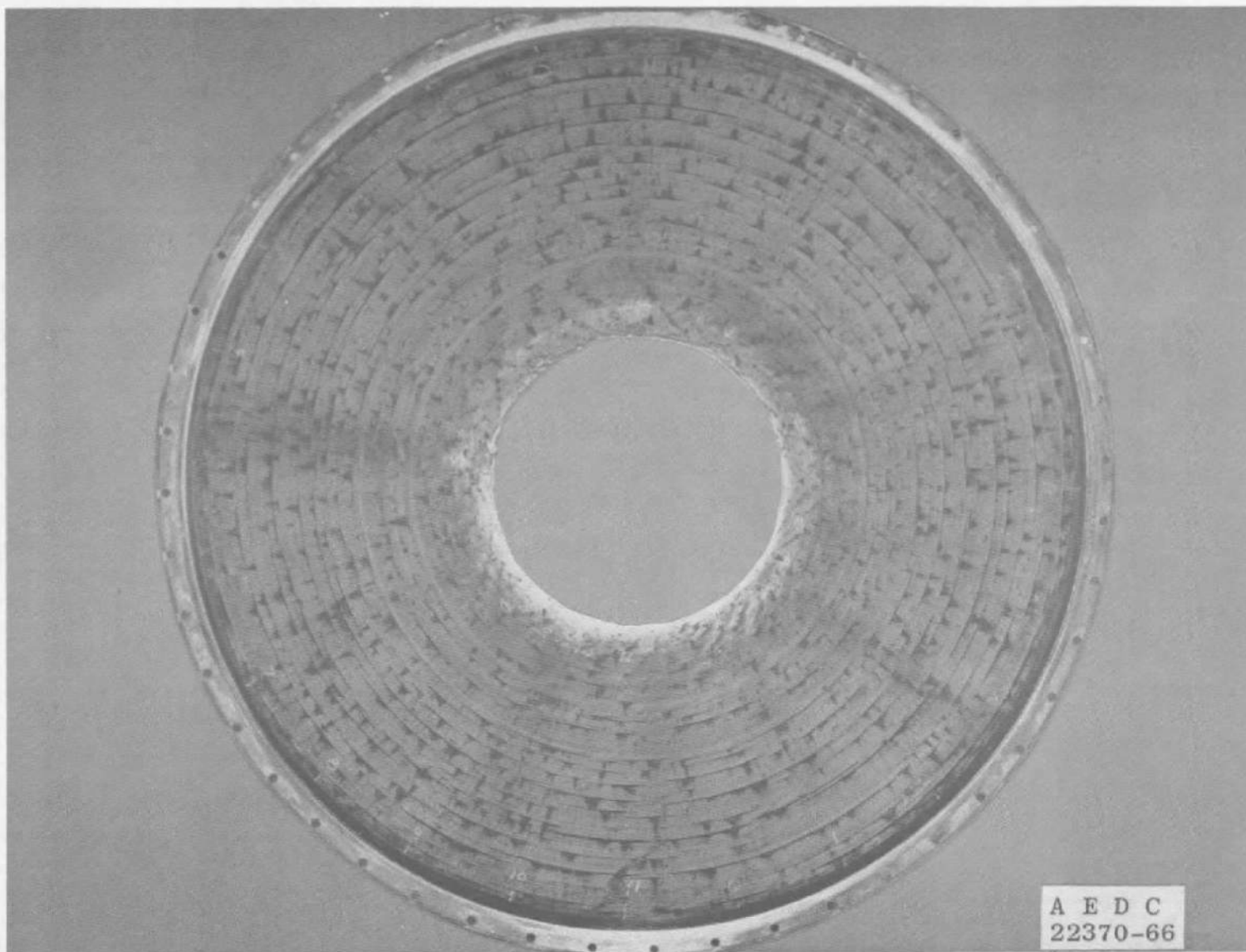


Fig. 24 Comparison of the Effect of TCV Bank Selection on Combustion Chamber Pressure Transient



a. View from Injector Mounting Flange
 Fig. 25 Typical Post-Fire Condition of Combustion Chamber



b. View from Nozzle Extension Mounting Flange

Fig. 25 Concluded

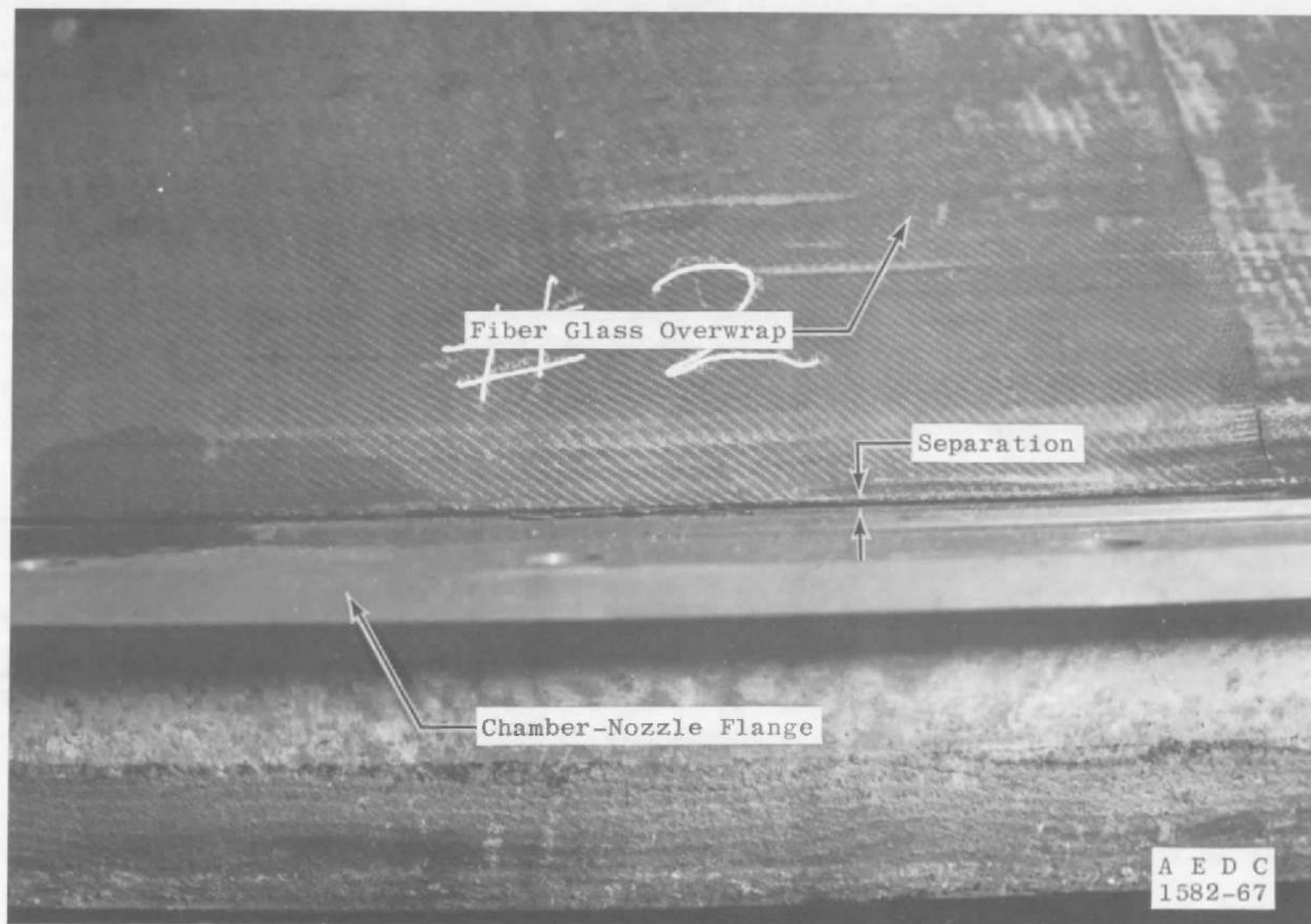


Fig. 26 Separation of Fiber Glass Overwrap from the Chamber-Nozzle Flange



Fig. 27 Nozzle Extension S/N 54 after 2250 sec of Firing Time

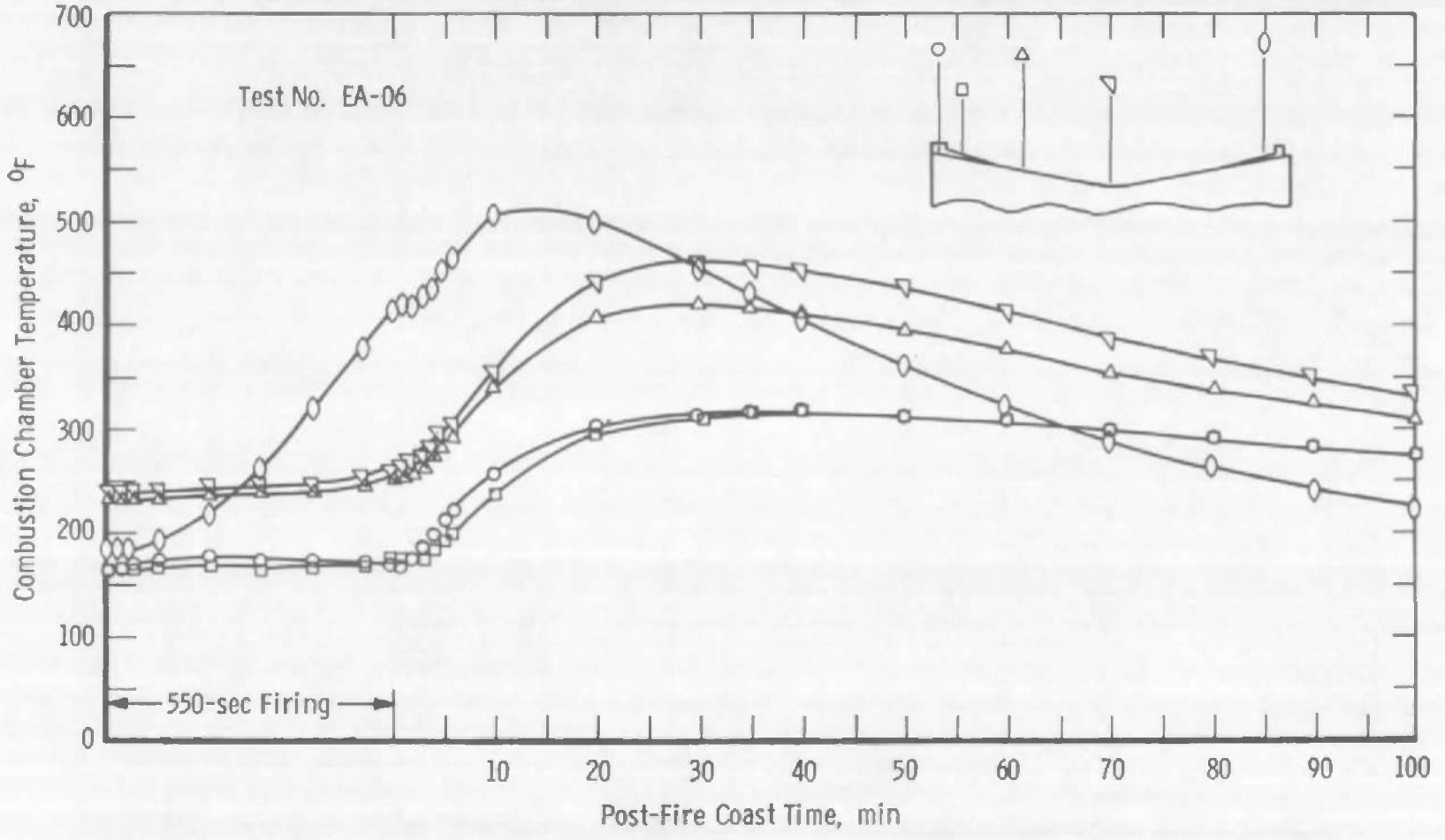


Fig. 28 Combustion Chamber Temperature History

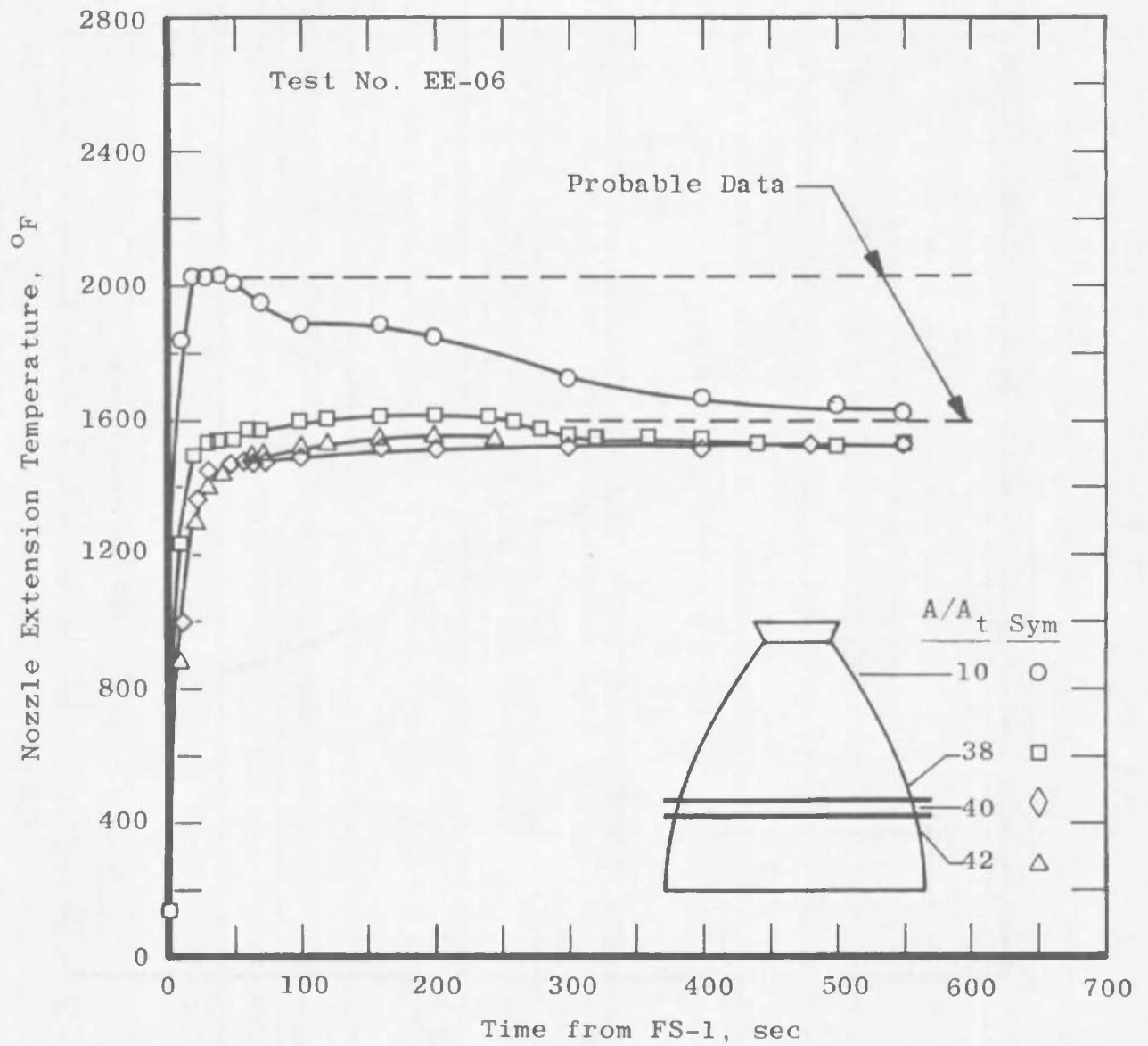


Fig. 29 Nozzle Extension Temperature History

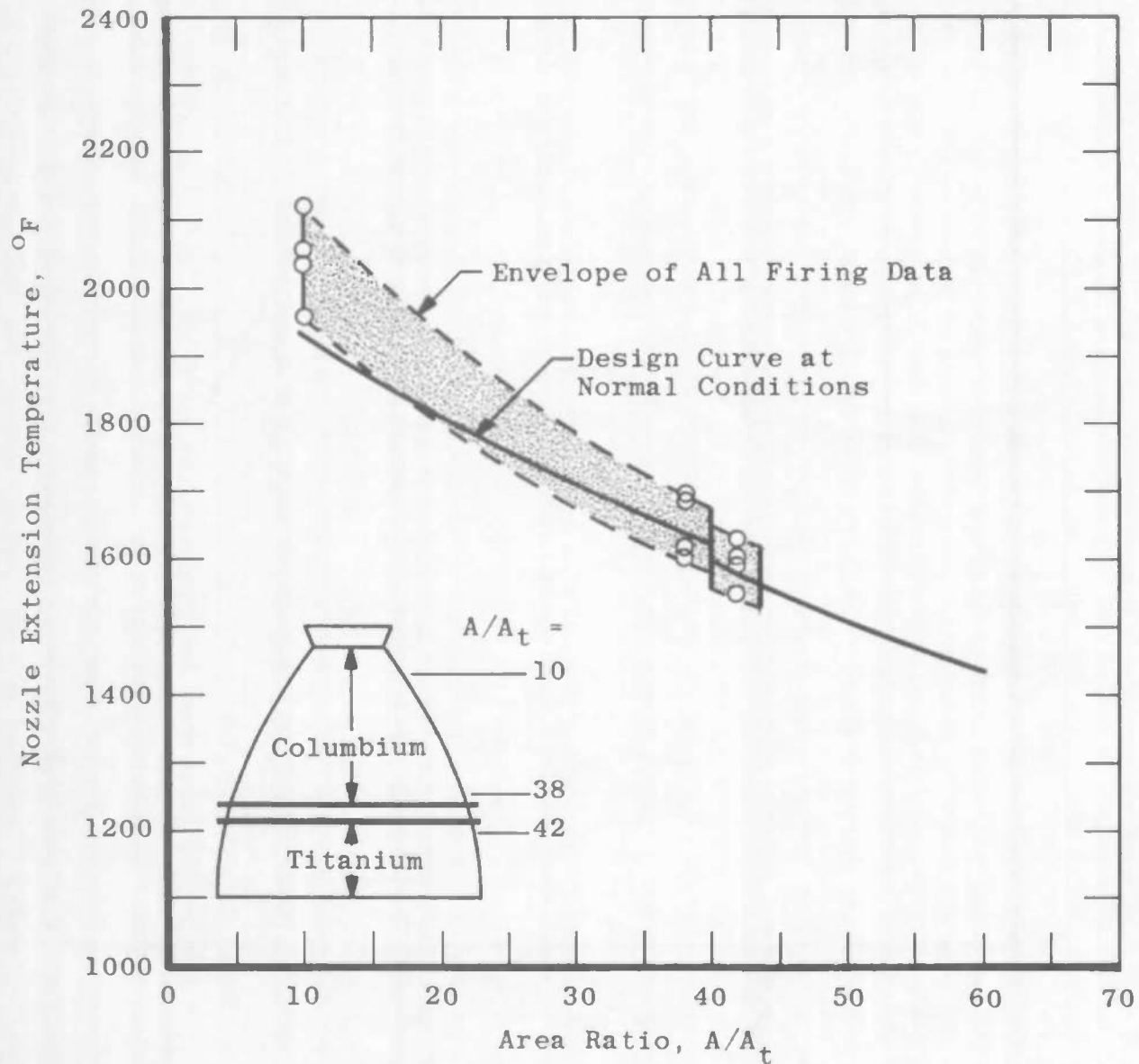
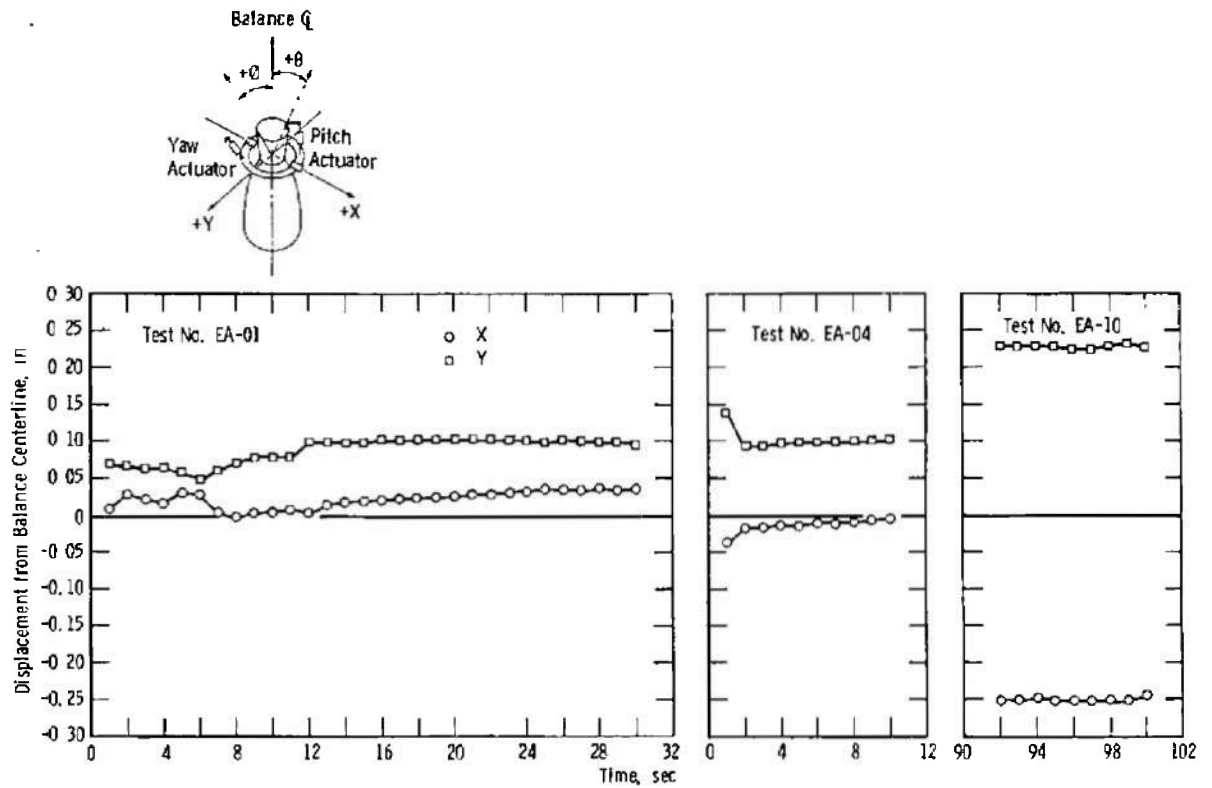
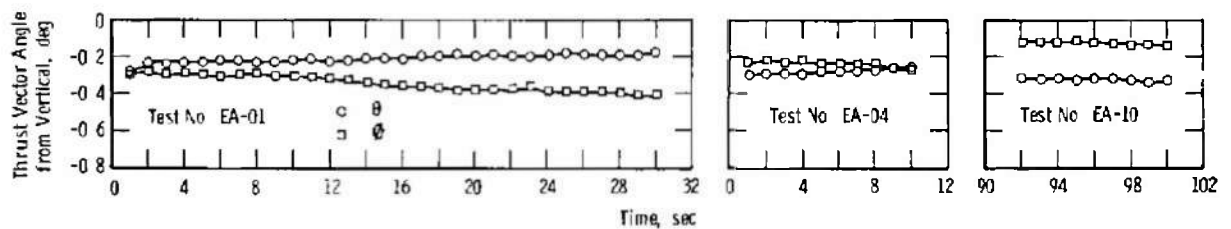


Fig. 30 Nozzle Extension Temperature Profile

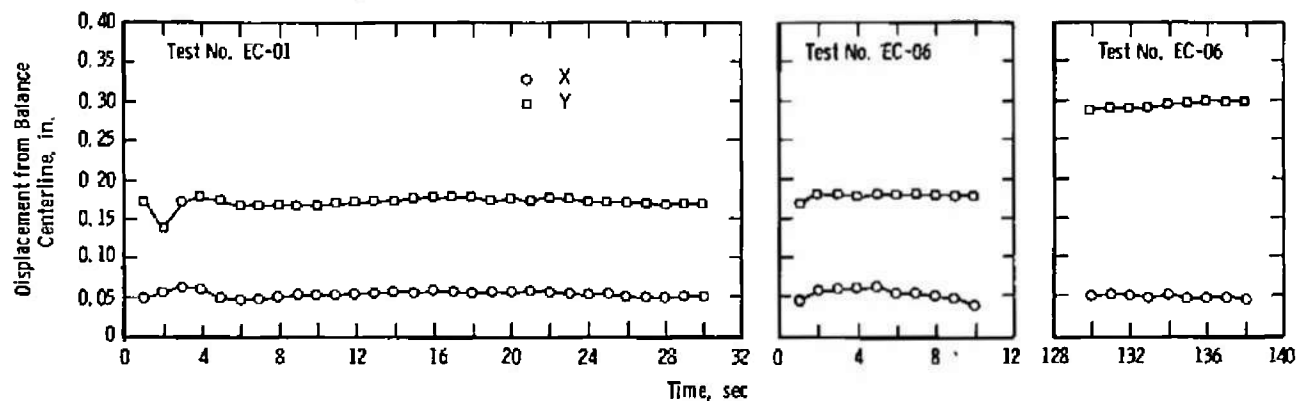
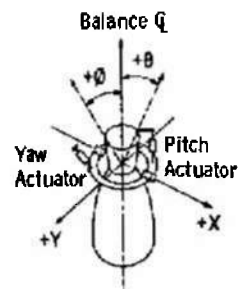


a. Variation of Thrust Vector Intercept Components in the Gimbal Plane

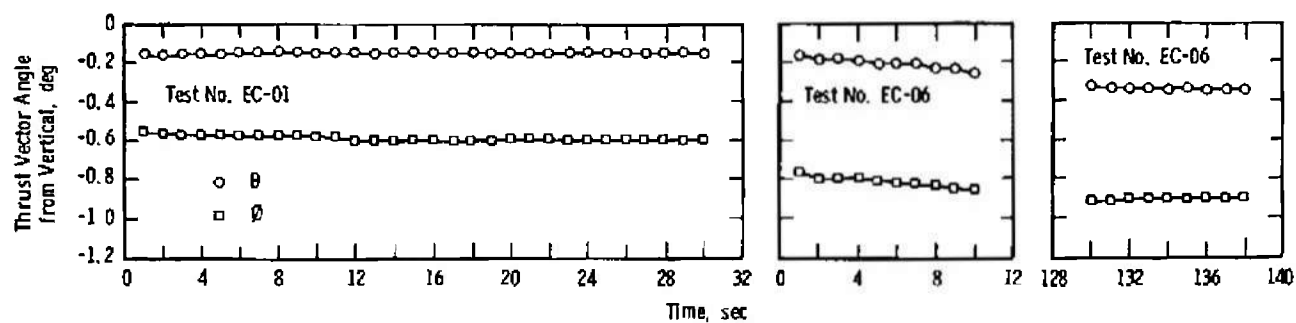


b. Angular Variation of Thrust Vector Components

Fig. 31 Thrust Vector Excursion of Engine S/N 54

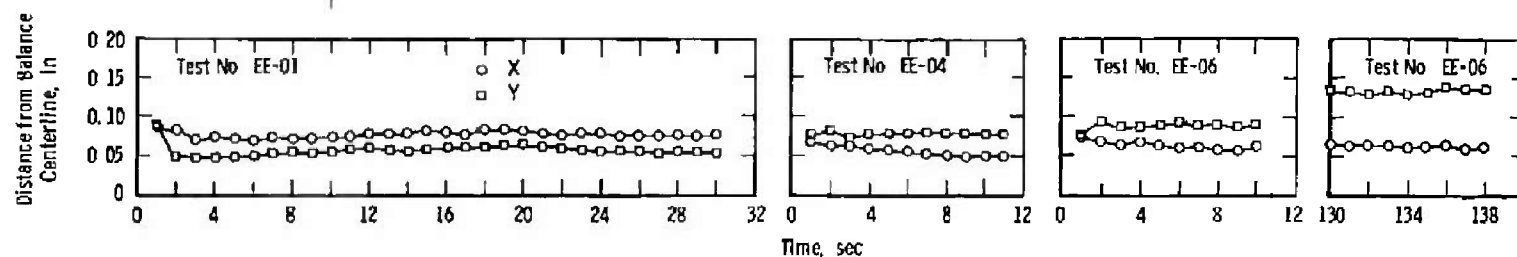
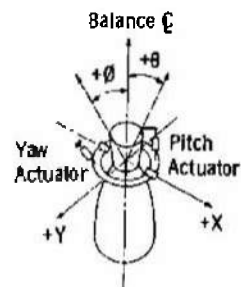


a. Variation of Thrust Vector Intercept Components in the Gimbal Plane

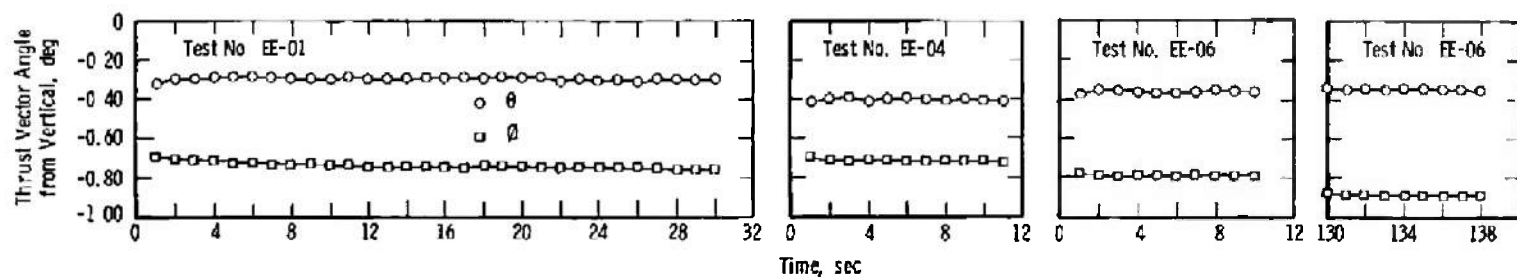


b. Angular Variation of Thrust Vector Components

Fig. 32 Thrust Vector Excursion of Engine S/N 54B



a. Variation of Thrust Vector Intercept Components in the Gimbal Plane



b. Angular Variation of Thrust Vector Components

Fig. 33 Thrust Vector Excursion of Engine S/N 55

TABLE I
ENGINE CONFIGURATIONS TESTED

Test Series	Engine S/N	Injector S/N	TCV S/N	Gimbal Actuator Pitch S/N	Gimbal Actuator Yaw S/N	Nozzle Extension S/N	Chamber S/N	Fuel Propellant Line S/N	Oxidizer Propellant Line S/N	Gimbal Ring S/N	Engine Interface Fuel Orifice Diameter, in.	Engine Interface Oxidizer Orifice Diameter, in.	TCV Fuel Orifice Diameter Upper Bank, in.	TCV Fuel Orifice Diameter Lower Bank, in.	TCV Oxidizer Orifice Diameter Upper Bank, in.	TCV Oxidizer Orifice Diameter Lower Bank, in.	F-3 Fixture Fuel Orifice Diameter, in.	F-3 Fixture Oxidizer Orifice Diameter, in.
EA	54	104	122	43	45	52	311	11	12	40	1.395	1.800	1.930	1.836	1.930	1.930	1.845	2.032
EB	54A	104	122	202	202	52	315	11	12	40	1.395	1.800	1.930	1.836	1.930	1.930	2.929	1.845
EC	54B	115	128	202	202	54	319	11	12	40	1.362	1.804	1.930	1.878	1.930	1.875	2.929	1.845
ED	54C	115	128	202	202	54	320	11	12	40	1.362	1.804	1.930	1.878	1.930	1.875	2.929	1.845
EE	55	103	122	201	201	52	318	18	13	41	1.381	1.728	1.732	1.640	1.930	1.930	2.929	1.845
EF	55A	103	122	201	201	54	324	18	13	41	1.352	1.728	1.732	1.640	1.930	1.930	2.929	1.845

All component serial numbers are composed of seven digits. The zeros in front of the significant numbers have been omitted for clarity, example: the injector S/N for test EA is 0000104.

TABLE II
PROPELLANT CONTAMINATION PARTICLE COUNTS

Test Series	Fuel and Oxidizer	Particles > 500 μ	Largest Particles	Fibers > 500 μ	Largest Fiber
EA	AZ-50 N ₂ O ₄	0	---	0	---
		2	700 by 100	0	---
EB	AZ-50 N ₂ O ₄	0	---	0	---
		0	---	1	500 by 20
EC	AZ-50 N ₂ O ₄	1	700 by 100	0	---
		0	---	0	---
ED	AZ-50 N ₂ O ₄	0	---	0	---
		0	---	0	---
EE	AZ-50 N ₂ O ₄	0	---	0	---
		1	700 by 480	0	---
EF	AZ-50 N ₂ O ₄	0	---	0	---
		56	1150 by 750	0	---
Aerojet Specification (Ref. 14)	AZ-50 N ₂ O ₄	0	---	---	1500 by 50

TABLE III
SUMMARY OF TEST FIRINGS

Test Number	Date	Firing Duration, sec	Number of Firings	Coast** Duration, min	TCV Bank	Engine S/N	Remarks	Test Objectives
EA-01	11-18-66	30.791	1	142	A, AB, B	54	+	Obtain Engine Qualification Performance Data at Various Chamber Pressures
EA-02		10.855	1	31	A		*	
EA-03		10.687	1	29			*	
EA-04		10.690	1	30			+	
EA-05		10.568	1	45			*	
EA-06		550.648	1	250			* Ruptured Burst Disk on Fuel Side	
EA-07		0.977	5	1-30				
EA-08		0.550	5	1-51				
EA-09		0.380	5	1-35				
EA-10		99.989	1	14	B		**	
EA-11		5.010	3	1-32			* Total Engine Firing Time	
EA-12		0.980	5	1-30			753.791 sec	
EB-01	11-30-66	30.773	1	113	A, AB, B	54A		Obtain Engine Qualification Performance Data at Various Mixture Ratios and at High Chamber Pressures
EB-02		10.517	1	31	B		*	
EB-03		10.861	1	30			*	
EB-04	12-1-66	10.602	1	30				
EB-05		10.457	1	32			*	
EB-06		551.241	1	269			*	
EB-07		0.980	5	1-48				
EB-08		0.550	5	1-44				
EB-09		0.365	5	1-45				
EB-10		99.099	1	138	A		*	
EB-11		4.990	3	1-33			* Total Engine Firing Time	
EB-12		0.980	5	1-30			753.084 sec	

+ Thrust Vector Data Obtained

* Engine Gimballed

**Where Two Numbers Occur in Coast Duration Column, First Number is Coast Period between Firing and Second Number is Coast Period after Last Firing in Series.

On First Firing of Every Test Series Valve Bank A Was Used for the First 10 sec of Firing, Banks A and B for Next 10 sec, and Bank B Alone for Last 10 sec.

TABLE III (Continued)

Test Number	Date	Firing Duration, sec	Number of Firings	Coast** Duration, min	TCV Bank	Engine S/N	Remarks	Test Objectives
EC-01	12-15-66	30.462	1	83	A, AB, B	54B	•	Obtain Engine Qualification Performance Data at High Chamber Pressure and Elevated Propellant Temperatures (110°F)
EC-02	↓	11.142	1	31	A	↓	•	
EC-03	↓	10.816	1	30	↓	↓	•	
EC-04	↓	11.191	1	31	↓	↓	+	
EC-05	↓	11.330	1	46	↓	↓	•	
EC-06	↓	550.530	1	381	↓	↓	•+	
EC-07	12-16-66	0.980	5	1-34	↓	↓		
EC-08	↓	0.555	5	1-35	↓	↓		
EC-09	↓	0.385	5	1-35	↓	↓		
EC-10	↓	99.945	1	135	B	↓		
EC-11	↓	4.830	3	1-30	↓	↓	* Total Engine *Firing Time 754.706 sec	
EC-12	↓	0.979	5	1-30	↓	↓		
ED-01	1-6-67	29.888	1	91	A, AB, B	54C		Obtain Engine Qualification Performance Data at Various Mixture Ratios and at Low Chamber Pressures
ED-02	↓	10.953	1	39	A	↓	•	
ED-03	↓	10.870	1	29	↓	↓	•	
ED-04	↓	11.324	1	29	↓	↓		
ED-05	↓	10.823	1	35	↓	↓	•	
ED-06	↓	550.860	1	488	↓	↓	•	
ED-07	↓	0.980	5	1-30	↓	↓		
ED-08	↓	0.555	5	1-33	↓	↓		
ED-09	↓	0.385	5	1-29	↓	↓		
ED-10	↓	99.985	1	60	B	↓		
ED-11	↓	4.860	3	1-30	↓	↓	* Total Engine *Firing Time 753.888 sec	
ED-12	↓	0.979	5	1-30	↓	↓		

+ Thrust Vector Data Obtained

*Engine Gimballed

**Where Two Numbers Occur in Coast Duration Column, First Number Is Coast Period between Firings and Second Number is Coast Period after Last Firing in Series.

On First Firing of Every Test Series Valve Bank A Was Used for the First 10 sec of Firing, Banks A and B for Next 10 sec, and Bank B Alone for Last 10 sec.

TABLE III (Concluded)

Test Number	Date	Firing Duration, sec	Number of Firings	Coast** Duration, min	TCV Bank	Engine S/N	Remarks	Test Objectives
EE-01	1-24-67	30.520	1	85	A, AB, B	55	+	Obtain Engine Qualification Performance Data at Various Chamber Pressures
EE-02	↓	10.760	1	30	A	↓	*	
EE-03	↓	10.540	1	30	↓	↓	*	
EE-04	↓	11.200	1	30	↓	↓	+	
EE-05	↓	10.200	1	60	↓	↓	*	
EE-06	1-25-67	552.150	1	305	↓	↓	*+	
EE-07	↓	0.980	5	1-30	B	↓	Instrumentation Malfunction Showed Low Sphere Pressure	
EE-08	↓	0.555	5	1-30	A	↓		
EE-09	↓	0.385	5	1-31	A	↓	↓	
EE-10	↓	99.880	1	1-29	B	↓	*+	
EE-11	↓	4.960	3	1-30	↓	↓	* Total Engine Firing Time 754.630 sec	
EE-12	↓	0.980	5	1-30	↓	↓		
EF-01	2-1-67	30.350	1	49	A, AB, B	55A	Propellants at 35°F	Obtain Engine Qualification Performance Data at Nominal Conditions with Cold Propellants (35°F)
EF-02	↓	10.660	1	30	A	↓	*	
EF-03	↓	10.940	1	30	↓	↓	* Pressure on Fuel Side Incorrectly Set	
EF-04	↓	10.480	1	30	↓	↓	↓	
EF-05	↓	10.770	1	30	↓	↓	*	
EF-06	↓	551.220	1	248	↓	↓	*	
EF-07	↓	0.980	5	1-42	B	↓	↓	
EF-08	↓	0.550	5	1-36	B	↓	↓	
EF-09	↓	0.380	5	1-30	A	↓	Propellants at 60°F	
EF-10	↓	100.120	1	60	↓	↓	*	
EF-11	↓	4.960	3	1-30	↓	↓	* Total Engine Firing Time 753.870 sec	
EF-12	↓	0.980	5	1-30	B	↓		

+ Thrust Vector Data Obtained

*Engine Gimballed

**Where Two Numbers Occur in Coast Duration Column, First Number is Coast Period between Firings and Second Number is Coast Period after Last Firing in Series.

On First Firing of Every Test Series Valve Bank A Was Used for the First 10 sec of Firing, Banks A and B for Next 10 sec, and Bank B Alone for Last 10 sec.

TABLE IV
SUMMARY OF ENGINE PERFORMANCE

Test No.	Engine S/N	Time for 2-sec Average	Propellant Pressures, psia				Flow Rates, lb _m /sec			MR	T _o , °F	T _f , °F	P _c , psia	F _v , lb _f	P _a , psia	A _{t calc} , in. ²	I _{spv} , lb _f -sec/lb _m	c*, ft/sec	C _{Fv}
			P _{ot}	P _{ol}	P _{it}	P _{fl}	W _o	W _f	W _t										
EA-01	54	8	157.7	161.1	171.8	165.1	39.8	24.4	64.2	1.63	59.3	66.5	97.1	20,135	0.073	121.4	313.8	5910	1.708
		16	159.7	160.7	171.3	164.5	40.2	25.0	65.2	1.61	59.3	66.6	98.9	20,456	0.073	121.2	313.8	5913	1.708
		28	159.0	160.7	168.3	164.8	39.4	24.4	63.8	1.61	59.3	66.6	97.0	20,012	0.072	121.1	313.3	5913	1.705
EA-02		9	203.7	203.5	211.7	207.6	47.0	28.7	75.7	1.64	60.2	66.9	114.6	23,807	0.075	121.2	314.7	5909	1.713
EA-03		9	180.6	181.7	189.1	186.5	43.3	26.6	69.9	1.62	60.4	66.9	106.0	21,981	0.073	121.1	313.7	5911	1.707
EA-04		9	133.4	139.8	144.4	145.3	35.5	22.3	57.8	1.59	60.5	67.0	88.1	18,124	0.071	120.7	313.3	5916	1.704
EA-05		9	110.2	121.5	121.9	126.9	31.9	20.2	52.1	1.58	60.7	67.0	79.6	16,300	0.065	120.5	312.7	5918	1.700
EA-10		8	164.9	166.0	174.6	163.8	40.5	24.0	64.5	1.69	65.0	69.3	98.5	20,187	0.068	120.2	312.8	5899	1.706
		24	165.6	165.8	174.7	163.6	40.6	24.0	64.6	1.69	65.1	69.3	98.3	20,200	0.070	120.3	313.0	5898	1.707
EB-01	54A	8	160.5	153.2	---	166.0	37.8	25.0	62.8	1.51	50.0	57.5	95.2	19,856	0.062	121.9	312.8	5943	1.694
		16	162.1	154.0	---	165.7	38.6	25.5	64.1	1.51	50.1	57.7	97.4	20,087	0.067	121.6	313.4	5943	1.700
		28	162.0	154.2	---	165.8	37.9	24.8	62.7	1.52	50.2	58.0	95.5	19,680	0.069	121.4	313.4	5942	1.697
EB-02		9	176.7	166.3	---	157.6	41.3	23.1	64.4	1.79	50.5	58.0	96.9	20,109	0.067	121.7	312.3	5890	1.706
EB-03		9	175.1	163.5	---	161.0	40.5	23.4	63.9	1.73	50.5	58.1	97.0	20,075	0.066	120.8	314.2	5905	1.712
EB-04		9	164.6	157.0	---	173.4	38.3	25.9	64.2	1.48	50.6	58.1	97.6	20,042	0.066	121.5	312.6	5947	1.691
EB-05		9	165.8	166.2	---	176.8	37.9	26.4	64.3	1.44	50.7	58.1	98.0	20,079	0.065	121.4	312.4	5951	1.689
EB-06		8	207.9	196.4	---	204.6	45.5	28.6	74.1	1.59	49.4	57.2	112.6	23,289	0.070	121.4	314.2	5932	1.704
		24	207.9	195.6	---	203.4	45.4	28.4	73.8	1.60	49.4	57.2	112.3	23,224	0.074	121.3	314.3	5931	1.705
EB-10		8	210.8	197.3	---	202.8	46.0	28.3	74.3	1.62	52.3	56.7	112.9	23,254	0.074	121.2	313.1	5926	1.700
		24	210.9	197.0	---	202.5	45.9	28.3	74.2	1.62	52.3	56.7	112.8	23,289	0.099	121.2	313.9	5927	1.704
EC-01	54B	8	178.8	165.0	164.9	167.6	39.6	24.6	64.2	1.61	106.5	110.0	96.7	20,064	0.077	122.1	312.7	5922	1.700
		16	177.0	164.6	164.9	167.3	40.0	25.0	65.0	1.60	107.2	111.8	98.2	20,371	0.074	122.0	313.1	5924	1.700
		28	177.0	164.9	165.0	167.3	39.3	24.5	63.8	1.60	108.0	111.8	96.5	19,961	0.072	121.7	313.0	5923	1.700
EC-02		9	213.9	197.9	196.8	198.6	45.2	27.8	73.0	1.62	107.9	111.3	109.9	22,749	0.070	122.1	311.7	5920	1.694
EC-03		9	208.6	193.3	197.2	199.1	44.1	27.8	71.9	1.59	108.1	111.1	108.9	22,514	0.068	121.7	312.9	5928	1.699
EC-04		9	207.9	192.7	196.8	198.7	44.1	27.7	71.8	1.59	108.2	111.3	108.7	22,437	0.068	121.7	312.5	5926	1.697
EC-05		9	208.3	192.9	196.7	199.0	44.0	27.9	71.9	1.58	108.1	111.3	108.8	22,462	0.068	121.7	312.5	5927	1.696
EC-06		8	208.9	196.2	198.1	202.4	44.6	28.2	72.8	1.58	108.5	105.6	110.2	22,778	0.076	121.8	312.7	5927	1.697
		24	209.4	196.1	197.1	201.0	44.6	28.0	72.6	1.59	108.5	105.6	109.9	22,738	0.074	121.7	313.1	5925	1.700

TABLE IV (Continued)

Test No.	Engine S/N	Time for 2-sec Average	Propellant Pressures, psia				Flow Rates, lb _m /sec			MR	T ₀ [*] , °F	T _f [*] , °F	P _c [*] , psia	F _v , lb _f	P _a [*] , psia	A _{tcalc} [*] , in. ²	I _{spv} [*] , lb _f -sec/lb _m	c [*] , ft/sec	C _{Fv}
			P ₀₁	P ₀₁	P _{f1}	P _{f1}	W ₀	W _f	W _t										
EC-10	54B	8	185.1	167.5	175.0	168.2	39.8	24.8	64.4	1.82	107.7	110.0	97.6	20,037	0.072	121.3	311.4	5921	1.692
		24	185.3	167.3	175.1	168.1	39.7	24.6	64.3	1.62	107.8	110.0	97.5	20,051	0.073	121.3	311.9	5921	1.695
ED-01		8	173.6	160.1	163.8	162.8	39.7	24.3	64.0	1.64	70.7	62.0	95.2	19,925	0.075	121.6	311.2	5880	1.703
		16	173.1	159.6	164.2	162.3	40.2	24.8	85.0	1.62	70.9	62.0	97.8	20,238	0.079	121.5	311.3	5883	1.702
		28	173.3	160.0	164.4	162.5	39.5	24.2	63.7	1.63	71.1	62.1	96.1	19,833	0.079	121.2	311.3	5882	1.703
ED-02		9	185.6	169.9	157.1	155.8	42.3	22.9	65.2	1.85	71.2	62.2	97.1	20,134	0.074	121.5	309.1	5830	1.706
ED-03		9	177.3	162.8	162.1	160.3	40.3	23.9	64.2	1.69	71.2	62.3	98.4	19,915	0.073	121.5	310.2	5870	1.700
ED-04		8	169.1	155.9	172.4	170.0	38.1	25.6	63.7	1.49	71.1	62.4	96.4	19,706	0.073	121.3	310.4	5902	1.692
ED-05		9	167.5	154.4	175.2	172.5	37.6	26.1	63.7	1.44	71.1	62.6	96.4	19,781	0.080	121.2	310.7	5906	1.692
ED-06		8	133.2	127.3	129.8	130.6	33.2	20.8	54.0	1.60	68.9	59.9	81.6	16,744	0.074	121.0	310.2	5886	1.696
		24	133.1	126.7	129.0	129.6	33.0	20.6	53.6	1.60	68.9	59.9	81.3	16,674	0.068	120.6	310.9	5886	1.700
ED-10		8	130.7	121.7	128.8	128.5	31.5	20.8	52.1	1.53	71.9	67.2	80.2	16,159	0.069	118.9	310.4	5897	1.694
		24	131.0	121.5	128.9	128.4	31.5	20.6	52.1	1.53	71.9	67.2	80.1	16,185	0.075	119.0	310.8	5897	1.695
EE-01	55	8	178.5	168.1	163.9	166.1	40.4	24.3	64.7	1.66	74.0	78.6	98.4	20,384	0.067	121.4	314.6	5932	1.707
		16	176.1	165.3	162.6	164.6	41.0	24.6	65.6	1.66	74.1	78.7	99.9	20,658	0.072	121.1	314.8	5932	1.707
		28	176.1	165.5	162.3	164.3	40.4	23.9	64.3	1.69	74.1	78.8	97.9	20,218	0.073	121.0	314.4	5926	1.707
EE-02		9	221.4	205.3	209.2	208.5	46.9	28.7	75.6	1.63	74.6	78.7	114.6	23,841	0.074	121.7	315.4	5938	1.709
EE-03		9	195.1	181.8	187.4	187.0	42.8	26.7	89.5	1.60	74.6	78.7	106.2	21,901	0.069	120.9	316.3	5943	1.707
EE-04		9	151.9	143.4	146.6	146.8	35.8	22.5	58.3	1.60	74.5	78.6	89.4	18,328	0.067	120.5	314.3	5944	1.701
EE-05		9	130.6	124.1	128.9	128.8	31.9	20.6	52.5	1.55	74.8	78.5	80.8	16,518	0.073	120.2	314.8	5951	1.703
EE-06		8	164.5	156.8	180.9	178.4	37.4	26.6	64.0	1.41	74.3	78.0	98.3	20,057	0.070	120.8	313.2	5966	1.689
		24	163.8	156.2	179.9	177.5	37.3	26.5	63.8	1.41	74.3	78.0	98.1	20,007	0.068	120.6	313.6	5966	1.691
EE-10		8	163.9	159.4	179.8	179.4	37.9	26.4	64.3	1.44	80.5	79.0	99.4	20,151	0.072	119.8	313.6	5984	1.692
		24	164.0	159.2	180.2	179.2	37.9	26.4	64.3	1.44	80.5	79.0	99.4	20,166	0.074	119.8	313.9	5964	1.693

TABLE IV (Concluded)

Test No.	Engine S/N	Time for 2-sec Average	Propellant Pressures, psia				Flow Rates, lb _m /sec			MR	T ₀ , °F	T _f , °F	P _c , psia	F _v , lb _f	P _a , psia	A _{tcalc} , in. ²	I _{spv} , lb _f sec/lb _m	c*, ft/sec	C _{Fv}
			P _{0t}	P _{0l}	P _{f_t}	P _{f_l}	Ḡ ₀	Ḡ _f	Ḡ _t										
EF-01	55A	8	167.1	158.4	163.6	164.1	39.1	24.4	63.5	1.60	31.0	32.6	96.9	20,018	0.075	121.1	315.0	5938	1.707
		16	167.3	157.8	163.4	163.9	39.6	24.9	64.5	1.59	31.0	32.6	98.6	20,336	0.077	120.9	315.0	5940	1.706
		28	167.8	158.1	163.4	163.9	39.0	24.2	63.2	1.61	31.1	32.7	96.7	19,922	0.077	120.7	314.9	5937	1.707
FF-02		9	167.4	157.7	163.0	163.3	39.0	24.3	63.3	1.60	31.1	32.6	96.7	19,891	0.070	120.7	314.5	5938	1.704
EF-04		9	167.6	157.0	162.2	162.3	38.9	24.2	63.1	1.61	31.1	32.6	96.8	19,864	0.071	120.4	314.8	5938	1.706
EF-05		9	167.6	156.7	162.2	162.2	38.8	24.3	63.1	1.60	31.2	32.5	96.7	19,844	0.075	120.4	314.6	5939	1.704
EF-06		8	167.7	161.0	167.4	169.3	39.4	25.1	64.5	1.57	32.6	33.0	99.0	20,315	0.074	120.4	314.8	5944	1.704
		24	168.1	160.3	164.1	165.4	39.4	24.6	64.0	1.61	32.6	33.0	98.3	20,168	0.073	120.2	315.2	5938	1.708
EF-10		8	173.0	165.5	153.9	152.6	41.3	22.3	63.6	1.86	55.3	54.9	96.9	19,917	0.085	120.0	313.1	5880	1.713
		24	172.9	165.2	154.2	152.4	41.3	22.3	63.6	1.86	55.3	54.9	96.7	19,931	0.082	120.2	313.5	5882	1.715

TABLE V
SUMMARY OF IGNITION TRANSIENT IMPULSE DATA

Test No.	Engine S/N	Thrust Chamber Valve Bank	Chamber Pressure, psia	Time from FS-1 to 90 percent of Steady-State Thrust, sec	Impulse from FS-1 to 90 percent of Steady-State Thrust, lb _f -sec
EA-01	54	*	87	0.533	465
02	↓	A	115	0.517	377
03	↓	↓	108	0.526	416
04	↓	↓	87	0.548	498
05	↓	↓	80	Did Not Reach 80 percent	
06	↓	↓	85	0.545	574
10	↓	B	97	0.536	884
11A	↓	↓	87	0.587	1783
11B	↓	↓	87	0.523	748
11C	↓	↓	87	0.512	548
EB-01	54A	*	97	0.542	315
02	↓	B	97	0.555	436
03	↓	↓	97	0.552	519
04	↓	↓	97	0.552	538
05	↓	↓	98	0.577	785
08	↓	↓	112	0.580	927
10	↓	A	112	0.502	404
11A	↓	↓	112	0.516	788
11B	↓	↓	112	0.481	349
11C	↓	↓	112	0.490	388
EC-01	54B	*	97	0.581	700
02	↓	A	110	0.540	831
03	↓	↓	110	0.545	952
04	↓	↓	109	0.559	1039
05	↓	↓	109	0.585	1203
08	↓	↓	110	0.577	1328
10	↓	B	98	0.521	1043
11A	↓	↓	117	0.518	1347
11B	↓	↓	117	0.515	1124
11C	↓	↓	117	0.507	1048
ED-01	54C	*	97	0.557	451
02	↓	A	97	0.547	529
03	↓	↓	97	0.550	600
04	↓	↓	97	0.556	652
05	↓	↓	86	0.567	712
08	↓	↓	84	Did Not Reach 90 percent	
10	↓	B	80	↓	↓
11A	↓	↓	80	↓	↓
11B	↓	↓	80	↓	↓
11C	↓	↓	80	↓	↓
EE-01	55	*	100	0.813	1301
02	↓	A	115	0.529	428
03	↓	↓	105	0.541	470
04	↓	↓	90	0.580	883
05	↓	↓	80	Did Not Reach 90 percent	
08	↓	↓	98	0.572	1030
10	↓	B	100	0.496	670
11A	↓	↓	100	0.498	977
11B	↓	↓	100	0.489	744
11C	↓	↓	100	0.484	698
EF-01	55A	*	97	0.531	799
02	↓	A	97	0.551	428
03	↓	↓	97	0.553	438
04	↓	↓	97	0.557	503
05	↓	↓	97	0.588	598
06	↓	↓	100	0.589	614
10	↓	↓	97	0.538	400
11A	↓	↓	97	0.533	551
11B	↓	↓	97	0.512	388
11C	↓	↓	97	0.513	376

*Valve Bank A 10 sec, A and B Next 10 sec, B Remaining 10 sec

TABLE VI
SUMMARY OF SHUTDOWN TRANSIENT IMPULSE DATA

Test No.	Engine S/N	Thrust Chamber Valve Bank	Chamber Pressure, psia	Time from FS-2 to CR, sec	Impulse from FS-2 to CR, lbf-sec
EA-01	54	*	97	4.610	10,917
02	↓	A	115	2.730	11,116
03			106	2.690	10,567
04		↓	87	2.670	9,306
05			80	2.650	8,619
06		↓	95	2.670	10,108
10		B	97	2.490	10,747
11A		↓	97	3.490	10,223
11B			97	2.490	10,112
11C	↓	↓	97	2.610	10,079
EB-01	54A	*	97	2.910	9,936
02	↓	B	97	3.930	10,040
03		↓	97	4.710	10,150
04			97	4.110	10,300
05		↓	98	3.710	10,234
06			112	2.850	11,914
10		A	112	2.010	12,100
11A		↓	112	2.010	10,615
11B			112	1.910	10,597
11C	↓	↓	112	1.930	10,540
EC-01	54B	*	97	2.310	10,174
02	↓	A	110	2.290	11,502
03		↓	110	2.530	11,361
04			109	2.070	11,500
05		↓	109	2.310	11,508
06		B	110	1.730	11,653
10			98	2.210	10,283
11A		↓	117	2.910	13,067
11B			117	2.550	12,999
11C	↓	↓	117	2.010	12,947
ED-01	54C	*	97	2.870	10,313
02	↓	A	97	3.870	10,611
03		↓	97	3.590	10,529
04			97	3.610	10,534
05		↓	96	2.970	10,580
06			84	2.630	9,359
10		B	80	2.510	8,938
11A		↓	80	4.990	8,638
11B			80	2.910	8,556
11C	↓	↓	80	3.710	8,525
EE-01	55	*	100	2.610	11,192
02	↓	A	115	5.050	12,687
03		↓	105	2.590	11,566
04			90	2.510	10,088
05		↓	80	2.410	9,239
06			98	2.330	11,083
10		B	100	2.590	10,695
11A		↓	100	2.230	10,311
11B			100	2.090	10,150
11C	↓	↓	100	2.150	10,170
EF-01	55A	*	97	3.490	10,622
02	↓	A	97	4.850	11,750
03		↓	97	3.650	11,698
04			97	3.770	11,876
05		↓	97	3.810	11,749
06			100	3.490	12,226
10		B	98	3.010	11,137
11A		↓	97	2.770	10,583
11B			97	2.770	10,583
11C	↓	↓	97	3.130	10,536

*Valve Bank A 10 sec, A and B Next 10 sec, B Remaining 10 sec

TABLE VII
MINIMUM IMPULSE BIT SUMMARY

Test No.	Engine S/N	Thrust Chamber Valve Bank	Chamber Pressure, psia	Test Duration, sec	Impulse, lbf-sec
EA-07A	54	A	97	0.976	19,271
07B	↓	↓	97	0.977	19,485
07C	↓	↓	97	0.978	19,737
07D	↓	↓	98	0.978	19,754
07E	↓	↓	98	0.977	19,743
08A	↓	↓	95	0.550	7,575
08B	↓	↓	95	0.550	8,037
08C	↓	↓	95	0.560	7,444
08D	↓	↓	95	0.550	7,935
08E	↓	↓	95	0.550	7,892
09A	↓	↓	28	0.380	2,365
09B	↓	↓	25	0.380	2,233
09C	↓	↓	27	0.380	2,167
09D	↓	↓	25	0.385	2,200
09E	↓	↓	20	0.385	2,050
12A	↓	B	97	0.980	18,450
12B	↓	↓	97	0.980	18,728
12C	↓	↓	97	0.975	18,876
12D	↓	↓	97	0.975	18,955
12E	↓	↓	97	0.975	18,876
EB-07A	54A	B	115	0.980	21,169
07B	↓	↓	113	0.980	21,826
07C	↓	↓	113	0.980	22,002
07D	↓	↓	113	0.980	21,927
07E	↓	↓	112	0.980	21,867
08A	↓	↓	105	0.550	7,412
08B	↓	↓	105	0.550	7,706
08C	↓	↓	105	0.550	7,678
08D	↓	↓	105	0.550	7,734
08E	↓	↓	105	0.550	7,639
09A	↓	↓	20	0.385	2,079
09B	↓	↓	18	0.385	1,717
09C	↓	↓	23	0.385	1,669
09D	↓	↓	17	0.385	1,608
09E	↓	↓	22	0.385	1,693

Table VII Continued

Test No.	Engine S/N	Thrust Chamber Valve Bank	Chamber Pressure, psia	Test Duration, sec	Impulse, lbf-sec
EB-12A	54A	A	110	0.990	20,629
12B	↓	↓	112	0.980	21,257
12C	↓	↓	112	0.980	21,265
12D	↓	↓	112	0.990	21,296
12E	↓	↓	112	0.980	21,166
EC-07A	54B	A	112	0.980	21,442
07B	↓	↓	113	0.980	21,735
07C	↓	↓	112	0.980	21,700
07D	↓	↓	112	0.980	21,687
07E	↓	↓	112	0.980	21,637
08A	↓	↓	107	0.560	8,551
08B	↓	↓	107	0.553	8,312
08C	↓	↓	107	0.556	8,268
08D	↓	↓	107	0.556	8,236
08E	↓	↓	107	0.560	8,191
09A	↓	↓	34	0.385	2,575
09B	↓	↓	32	0.385	2,453
09C	↓	↓	32	0.385	2,452
09D	↓	↓	32	0.385	2,471
09E	↓	↓	32	0.385	2,415
12A	↓	B	117	0.979	23,725
12B	↓	↓	117	0.980	24,218
12C	↓	↓	118	0.978	24,213
12D	↓	↓	118	0.980	24,214
12E	↓	↓	118	0.975	24,214
ED-07A	54C	A	82	0.980	15,728
07B	↓	↓	82	0.985	15,838
07C	↓	↓	82	0.980	15,950
07D	↓	↓	82	0.980	15,912
07E	↓	↓	82	0.980	15,796
08A	↓	↓	76	0.555	6,043
08B	↓	↓	80	0.555	5,732
08C	↓	↓	74	0.555	5,702
08D	↓	↓	74	0.555	5,622
08E	↓	↓	75	0.555	5,589

Table VII Continued

Test No.	Engine S/N	Thrust Chamber Valve Bank	Chamber Pressure, psia	Test Duration, sec	Impulse, lbf-sec
ED-09A	54C	A	16	0.390	1,638
09B		↓	17	0.385	1,548
09C			17	0.380	1,594
09D			18	0.385	1,534
09E			14	0.390	1,488
12A		B	82	0.982	16,092
12B		↓	83	0.979	16,236
12C			83	0.980	16,360
12D			84	0.979	16,400
12E			84	0.979	16,420
EE-07A	55	B	100	0.980	20,668
07B		↓	100	0.980	20,727
07C			100	0.980	20,896
07D			102	0.980	20,930
07E			102	0.980	20,898
08A		A	100	0.550	7,330
08B		↓	97	0.565	7,706
08C			97	0.555	7,602
08D			96	0.555	7,554
08E			97	0.555	7,616
09A		↓	22	0.385	2,183
09B			20	0.385	1,856
09C			22	0.380	1,789
09D			24	0.385	1,911
09E			20	0.385	1,740
12A		B	98	0.980	19,543
12B		↓	99	0.980	20,214
12C			100	0.980	20,312
12D			100	0.980	20,315
12E			100	0.980	20,390

Table VII Concluded

Test No.	Engine S/N	Thrust Chamber Valve Bank	Chamber Pressure, psia	Test Duration, sec	Impulse, lbf-sec
EF-07A	55A	B	97	0.980	20,475
07B			98	0.980	20,828
07C			98	0.980	21,039
07D			98	0.980	21,105
07E			98	0.980	21,106
08A			95	0.550	9,133
08B			95	0.550	9,448
08C			95	0.550	9,410
08D			95	0.550	9,393
08E			95	0.550	9,469
09A		A	16	0.380	1,886
09B			16	0.385	1,716
09C			15	0.380	1,652
09D			15	0.390	1,752
09E			16	0.385	1,603
12A		B	97	0.970	19,921
12B			97	0.975	20,281
12C			97	0.975	20,289
12D			97	0.975	20,380
12E			97	0.975	20,413

APPENDIX III

PROPELLANT FLOWMETER AND WEIGH SCALE CALIBRATIONS

GENERAL

An in-place flowmeter calibration system was installed in the J-3 test cell so that accurate propellant flow rates could be measured. With this system, flowmeters are calibrated in the line configuration and at the same temperatures, pressures, and propellant flow rates that exist during engine firing.

In-Place Calibration in Propellant

The flowmeter calibration system is represented schematically in Fig. III-1. The flowmeter is calibrated by recording its total flow indication during a given time period while the flow was accumulated in the weigh tank mounted on the platform scales. A cavitating venturi installed in the line gave the same system pressure drop as the engine.

The following procedures were used for all flowmeter calibrations: Propellant flow was established from the pressurized F-3 sump tank to the J-3 test cell storage tank. After steady-state flow was established, the diverter valve was actuated so that propellant flow to the weigh tank occurred for a 60-sec time period. At the end of this time, the diverter valve was again actuated so that flow to the weigh tank was stopped and flow to the J-3 storage tank occurred. Flow was then terminated. The weigh scale reading represented the total accumulated propellant weight, and total flowmeter signal counts were obtained from electronic counters. These flowmeter counts represented the flowmeter output from the time the signal was given to divert the flow to the weigh tank (Signal 1, Fig. III-2) until the time the signal was given to divert the flow to the storage tank (Signal 2, Fig. III-2). These total counts were corrected for diverter valve transients using an oscillograph record of the flowmeter output and diverter valve position. Figure III-2 shows graphically how these corrections were made. A flowmeter constant with the units of lb-water/cycle was determined using the corrected flowmeter counts, total propellant weight, and propellant specific gravity. Propellant specific gravity was determined in the chemical laboratory using a sample obtained from the F-3 sump tanks.

Weigh Scale Calibration

The accumulated propellant weight was obtained from a load cell installed in the linkage of a beam scale. The load cell was in-place

calibrated by applying deadweights to the scale platform and obtaining a sensitivity factor for the load cell. Weights were applied in increments up to a total of 3200 lb to determine the linearity and repeatability of the system. The effect on indicated weight of various gas pressures in the weigh tank was also established, because flows into the weigh tank were made with tank vents closed to prevent loss of weight by venting propellant vapors.

The weights used to calibrate the weigh scale were calibrated by the Engineering Support Facility at AEDC, and the calibration is traceable to the National Bureau of Standards. Weight corrections for local gravity and air buoyancy were made.

DISCUSSION

Oxidizer Flowmeter In-Place Calibrations

Six oxidizer flowmeter calibrations (Fig. III-3) were made during Phase V testing using flowmeter S/N I-26669. Each calibration consisted of approximately seven data points, except for the first calibration which was the certification consisting of 28 data points. The resulting flowmeter constants for each calibration with the standard deviation (1σ) from the mean are listed below. These flowmeter constants were used to calculate the oxidizer flow rates for the test series indicated:

Test Series	Average Propellant Temperature, °F	K, $\text{lb}_m - \text{H}_2\text{O}/\text{cycle}$	1σ , percent
EA	67	0.07354	0.099
EB	52	0.07368	0.077
EC	108	0.07355	0.163
ED	73	0.07374	0.047
EE	78	0.07360	0.137
EF	43	$1.42 \times 10^{-6} (\text{cps} - 450) + 0.07385$	0.079*

*One-sigma deviation from equation of mean line.

The one-sigma deviation from the mean for all data was ± 0.100 percent.

Fuel Flowmeter In-Place Calibration

Six fuel flowmeter calibrations (Fig. III-4) were conducted during Phase V testing. The first four calibrations were with flowmeter S/N I-28040, and the last two calibrations with flowmeter S/N I-27559. Each calibration consisted of approximately seven data points, except for the first and fifth which were certification calibrations consisting of 21 and 14 data points, respectively. The resulting flowmeter constants were used to calculate the fuel flow rates for the corresponding test series indicated in the tabulation below:

Test Series	Average Propellant Temperature, °F	K, $\text{lb}_m - \text{H}_2\text{O}/\text{cycle}$	1 σ , percent
EA	68	$6.4 \times 10^{-7} (\text{cps}-800) + 0.06962$	0.160*
EB	63	$7.1 \times 10^{-7} (\text{cps}-800) + 0.06966$	0.077*
EC	111	$6.0 \times 10^{-7} (\text{cps}-800) + 0.06957$	0.219*
ED	63	$9.5 \times 10^{-7} (\text{cps}-800) + 0.06979$	0.137*
EE	73	0.07467	0.085
EF	45	0.07454	0.059

*One-sigma deviation from equation of mean line.

The one-sigma deviation from the mean for all data was ± 0.139 percent.

Overall System Error

The overall error of the in-place propellant calibration system was determined by considering the error of the individual components in conjunction with the precision of the flowmeter constants. The errors of the individual components and overall system errors are listed below:

Component	Error Oxidizer (N_2O_4) System 1 σ , percent	Error Fuel (AZ-50) System 1 σ , percent
Deadweights	± 0.001	± 0.001
Weigh scale and load cell system	± 0.099	± 0.096
Flowmeter	± 0.100	± 0.139
Overall System	± 0.141	± 0.169

SUMMARY OF RESULTS

1. The overall error of the oxidizer in-place flowmeter calibration system is ± 0.141 percent (1σ).
2. The overall error of the fuel in-place flowmeter calibration system is ± 0.169 percent (1σ).

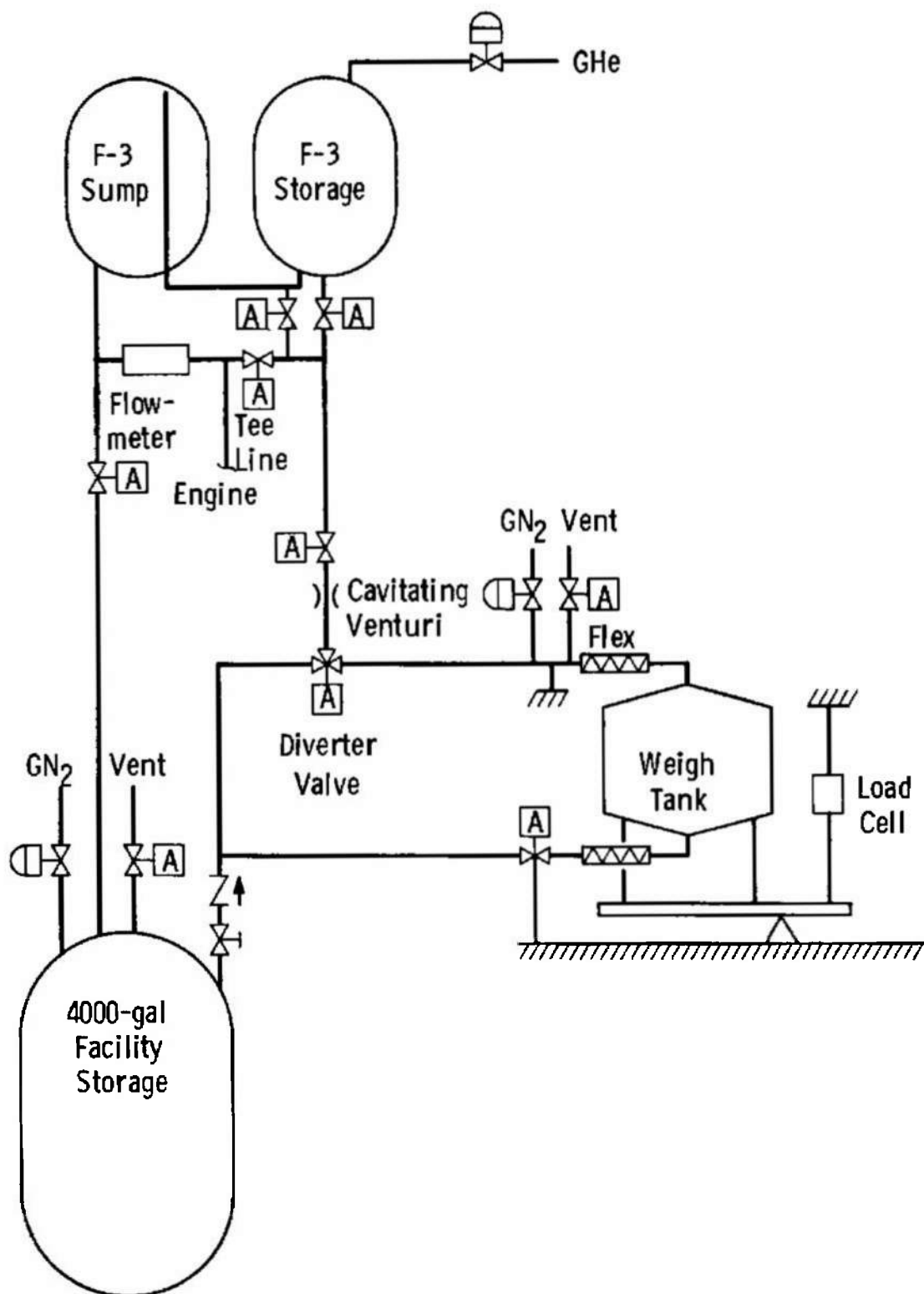


Fig. III-1 Schematic Diagram of J-3 In-Place Flowmeter Calibration System

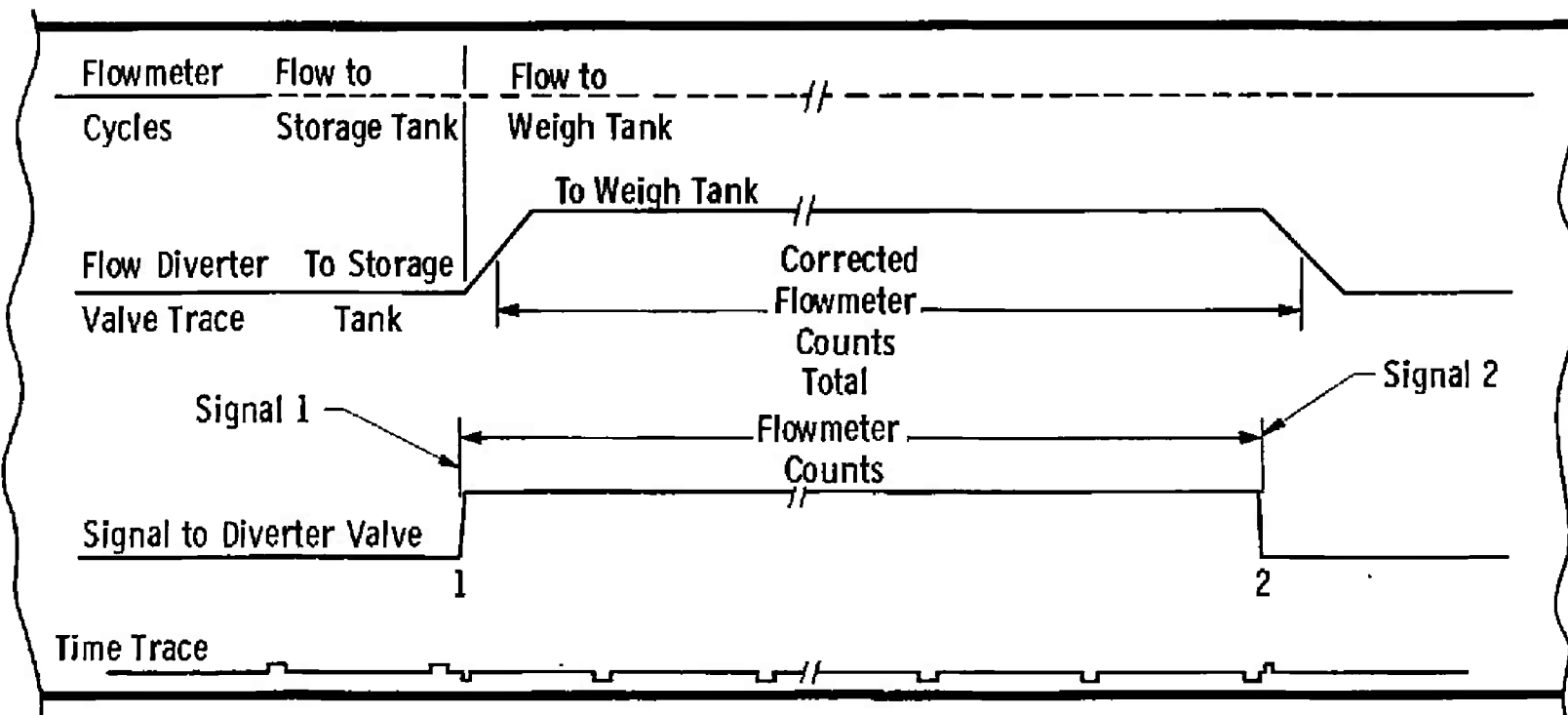


Fig. III-2 Typical Oscillograph Data for In-Place Flowmeter Calibration System

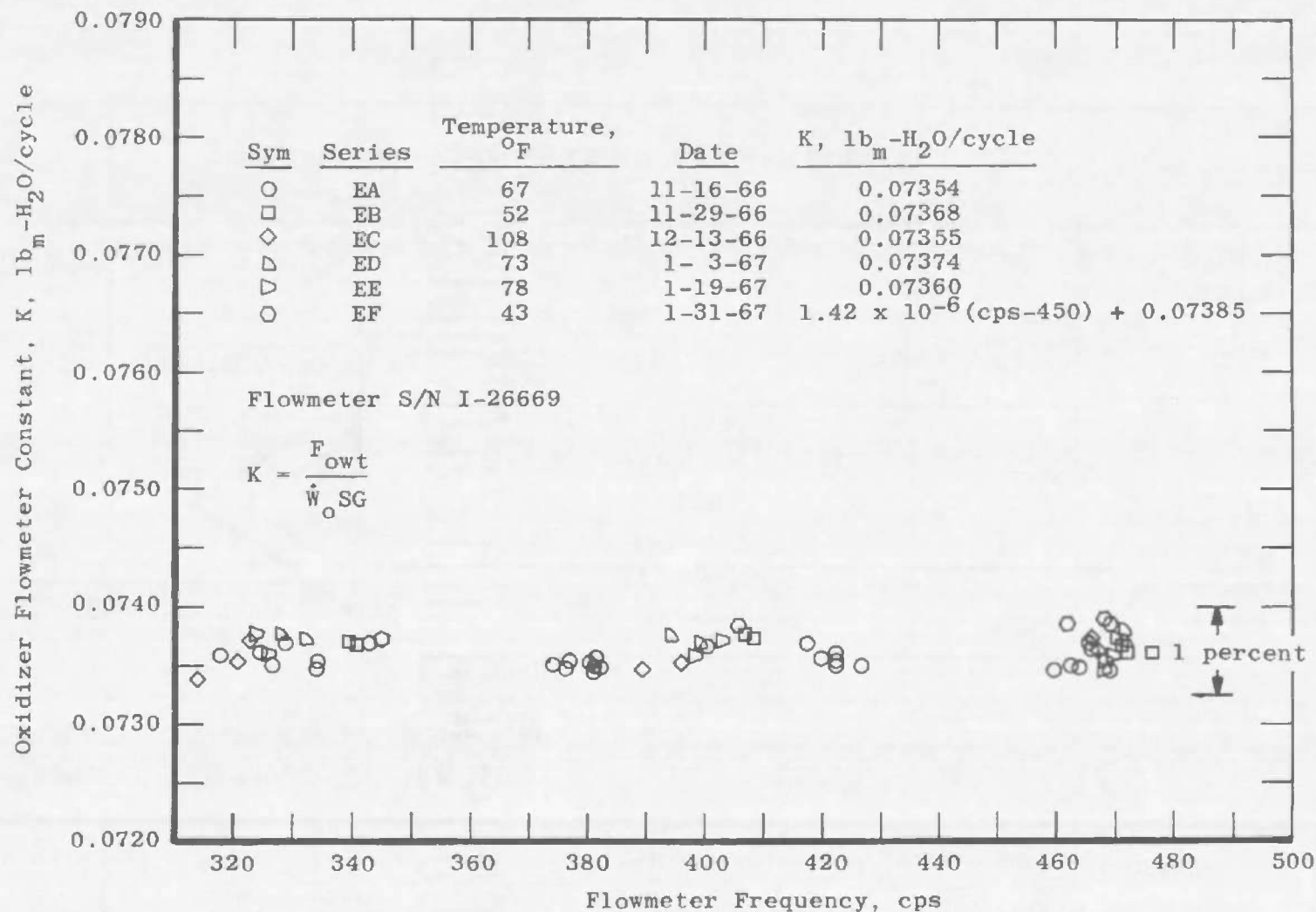


Fig. III-3 Oxidizer Flowmeter Calibrations

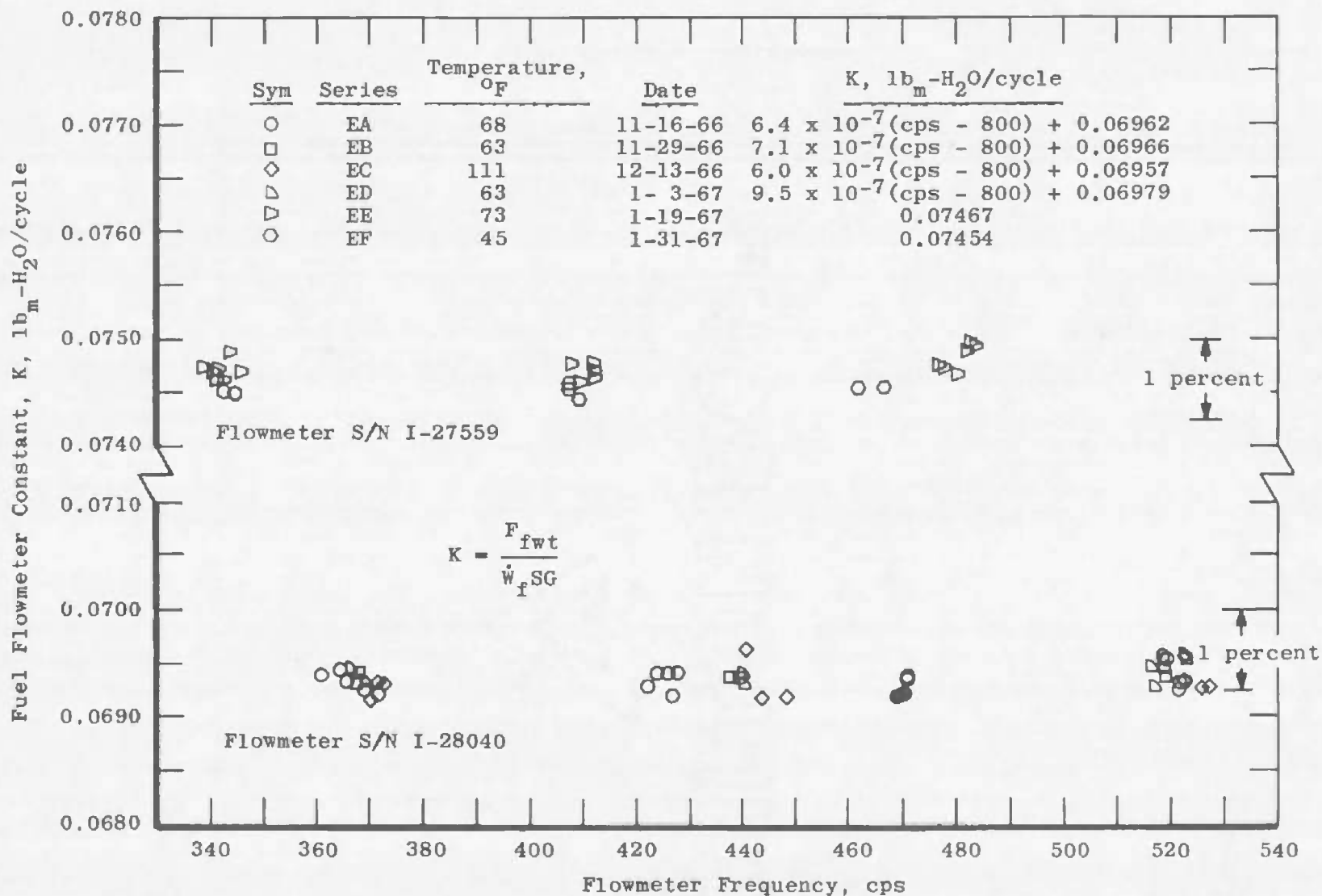


Fig. III-4 Fuel Flowmeter Calibrations

UNCLASSIFIED

Security Classification

DOCUMENT CONTROL DATA - R&D

(Security classification of title, body of abstract and indexing annotation must be entered when the overall report is classified)

1 ORIGINATING ACTIVITY (Corporate author) Arnold Engineering Development Center ARO, Inc., Operating Contractor Arnold Air Force Station, Tennessee		2a REPORT SECURITY CLASSIFICATION UNCLASSIFIED	
		2b GROUP N/A	
3 REPORT TITLE QUALIFICATION TESTS OF THE APOLLO BLOCK II SERVICE MODULE ENGINE (AJ10-137)			
4 DESCRIPTIVE NOTES (Type of report and inclusive dates) N/A			
5 AUTHOR(S) (Last name, first name, initial) Gall, E. S., McIlveen, M. W., and Berg, A. L., ARO, Inc.			
6 REPORT DATE May 1967	7a TOTAL NO. OF PAGES 102	7b. NO OF REFS 16	
8a CONTRACT OR GRANT NO. AF40(600)-1200 b. System 921E/9158 c. d.	9a ORIGINATOR'S REPORT NUMBER(S) AEDC-TR-67-63		
		9b. OTHER REPORT NO(S) (Any other numbers that may be assigned this report) N/A	
10 AVAILABILITY/LIMITATION NOTICES This document is subject to special export controls and each transmittal to foreign governments or foreign nationals may be made only with prior approval of National Aeronautics and Space Administration (EP-2).			
11 SUPPLEMENTARY NOTES Available in DDC.		12. SPONSORING MILITARY ACTIVITY National Aeronautics and Space Administration, Manned Spacecraft Center, Houston, Texas	
13 ABSTRACT High altitude qualification tests of an Apollo Block II Service Module engine were conducted to establish the performance characteristics and engine durability. Test hardware consisted of an Aerojet-General Corporation liquid-propellant rocket engine (AJ10-137) and a North American Aviation ground test replica of the Apollo Service Module propellant system. Seventy-two firings with an accumulated duration of 4524 sec were conducted on six engine assemblies at pressure altitudes of approximately 115,000 ft. Engine performance characteristics and engine durability were determined at various chamber pressures, mixture ratios, and propellant temperatures. The vacuum specific impulse obtained from the engine assemblies tested was dependent on the injector used, although all injectors were of identical design within limits of quality control. The average repeatability of I_{spv} data for a particular injector was ± 0.07 percent (1 σ); however, the deviation from the average I_{spv} (313.2 lbf-sec/lb _m) for all injectors was ± 0.57 percent (1 σ). Chamber durability was excellent except during one test series when the fiber glass overwrap separated from the chamber-nozzle flange. The thrust chamber valve had excessive leakage past the ball seals on several occasions during these tests. (AFR-310-2 Statement-2)			

This document has been approved for public release
its distribution is unlimited. *Per A.F. Little*
dated 27 June 1973

DD FORM 1473
1 JAN 64

UNCLASSIFIED

Security Classification

14 KEY WORDS	LINK A		LINK B		LINK C	
	ROLE	WT	ROLE	WT	ROLE	WT
APOLLO service module engine qualification tests altitude testing performance characteristics rocket engines liquid propellants <i>16-3</i> <i>1. Project Apollo Block II</i> <i>2. Rocket Motors - - AJ 10-13 7.</i> <i>3. Service Modules - Performance</i> <i>4. Rocket Motors - Performance</i> <i>16-3</i>						

INSTRUCTIONS

1. **ORIGINATING ACTIVITY:** Enter the name and address of the contractor, subcontractor, grantee, Department of Defense activity or other organization (corporate author) issuing the report.

2a. **REPORT SECURITY CLASSIFICATION:** Enter the overall security classification of the report. Indicate whether "Restricted Data" is included. Marking is to be in accordance with appropriate security regulations.

2b. **GROUP:** Automatic downgrading is specified in DoD Directive 5200.10 and Armed Forces Industrial Manual. Enter the group number. Also, when applicable, show that optional markings have been used for Group 3 and Group 4 as authorized.

3. **REPORT TITLE:** Enter the complete report title in all capital letters. Titles in all cases should be unclassified. If a meaningful title cannot be selected without classification, show title classification in all capitals in parenthesis immediately following the title.

4. **DESCRIPTIVE NOTES:** If appropriate, enter the type of report, e.g., interim, progress, summary, annual, or final. Give the inclusive dates when a specific reporting period is covered.

5. **AUTHOR(S):** Enter the name(s) of author(s) as shown on or in the report. Enter last name, first name, middle initial. If military, show rank and branch of service. The name of the principal author is an absolute minimum requirement.

6. **REPORT DATE:** Enter the date of the report as day, month, year; or month, year. If more than one date appears on the report, use date of publication.

7a. **TOTAL NUMBER OF PAGES:** The total page count should follow normal pagination procedures, i.e., enter the number of pages containing information.

7b. **NUMBER OF REFERENCES:** Enter the total number of references cited in the report.

8a. **CONTRACT OR GRANT NUMBER:** If appropriate, enter the applicable number of the contract or grant under which the report was written.

8b, 8c, & 8d. **PROJECT NUMBER:** Enter the appropriate military department identification, such as project number, subproject number, system numbers, task number, etc.

9a. **ORIGINATOR'S REPORT NUMBER(S):** Enter the official report number by which the document will be identified and controlled by the originating activity. This number must be unique to this report.

9b. **OTHER REPORT NUMBER(S):** If the report has been assigned any other report numbers (either by the originator or by the sponsor), also enter this number(s).

10. **AVAILABILITY/LIMITATION NOTICES:** Enter any limitations on further dissemination of the report, other than those imposed by security classification, using standard statements such as:

- (1) "Qualified requesters may obtain copies of this report from DDC."
- (2) "Foreign announcement and dissemination of this report by DDC is not authorized."
- (3) "U. S. Government agencies may obtain copies of this report directly from DDC. Other qualified DDC users shall request through _____."
- (4) "U. S. military agencies may obtain copies of this report directly from DDC. Other qualified users shall request through _____."
- (5) "All distribution of this report is controlled. Qualified DDC users shall request through _____."

If the report has been furnished to the Office of Technical Services, Department of Commerce, for sale to the public, indicate this fact and enter the price, if known.

11. **SUPPLEMENTARY NOTES:** Use for additional explanatory notes.

12. **SPONSORING MILITARY ACTIVITY:** Enter the name of the departmental project office or laboratory sponsoring (paying for) the research and development. Include address.

13. **ABSTRACT:** Enter an abstract giving a brief and factual summary of the document indicative of the report, even though it may also appear elsewhere in the body of the technical report. If additional space is required, a continuation sheet shall be attached.

It is highly desirable that the abstract of classified reports be unclassified. Each paragraph of the abstract shall end with an indication of the military security classification of the information in the paragraph, represented as (TS), (S), (C), or (U).

There is no limitation on the length of the abstract. However, the suggested length is from 150 to 225 words.

14. **KEY WORDS:** Key words are technically meaningful terms or short phrases that characterize a report and may be used as index entries for cataloging the report. Key words must be selected so that no security classification is required. Identifiers, such as equipment model designation, trade name, military project code name, geographic location, may be used as key words but will be followed by an indication of technical context. The assignment of links, rules, and weights is optional.